NASA

Technical Memorandum 86154

PHYSICS OF NONMAGNETIC RELATIVISTIC THERMAL PLASMAS

Charles Dermer

JULY 1984

National Aeronautics and
Space Administration

Goddard Space Flight Center
Greenbelt, Maryland 20771

UNIVERSITY OF CALIFORNIA

SAN DIEGO

Physics of Nonmagnetic Relativistic Thermal Plasmas

A dissertation submitted in partial satisfaction of the

requirements for the degree Doctor of Philosophy

in Physics

by

Charles Dennison Dermer

Committee in charge:

Professor Robert J. Gould, Chairman
Professor James. R. Arnold
Professor Harding E. Smith, Jr.
Professor Nguyen-Huu Xuong
Professor David Y. Wong

1984

The dissertation of Charles Dennison Dermer is approved,

and it is acceptable in quality and form for

publication on microfilm:

Chairman

University of California, San Diego

1984

Preceding Page Blank

TABLE OF CONTENTS

Page

LIST OF FIGURES AND TABLES

ACKNOWLEDGMENTS

I thank my advisor, Bob Gould, for his counsel and instruction during my residence at UCSD. I express my gratitude to both him and Richard Lingenfelter for helping reveal to me the beauty and austerity of physics, and the excitement of astrophysics. Hugh Hudson's asides were always witty and illuminating, and I have enjoyed many talks with him, as well as innumerable talks on all sorts of subjects with Scott Frasier, whose friendship I value. I also acknowledge discussions with Larry Peterson, Eldon Whipple, and Greg Jung, and I wish to thank Wayne Stein for the memorable course he taught in extragalactic astrophysics.

The kindness and generosity of my family, the Dermers and the Schicks, is a continuous source of strength. Ann Bataller's secretarial work was invaluable, and the final draft of this dissertation has been typed by Annetta Whiteman. This work is supported by NASA through grant NGR 05-005-004.

VITA

[redacted]

1977 - B.S. Harvey Mudd College, Claremont, California

1977-1978 - Teaching Assistant in Physics, Dartmouth College, Hanover, New Hampshire

1979 - M.A. Dartmouth College, Hanover, New Hampshire

1978-1979 - Regents Fellow, University of California, San Diego

1980 - M.S. University of California, San Diego

1979-1984 - Research Assistant in Physics, University of California, San Diego

PUBLICATIONS

"Ultrasound Attenuation in Solid CD_4," F. A. Stahl, R. P. Wolf, and C. D. Dermer, Jr. 1979, J. Phys. Chem. Solids, 40, 191.

"Temperature Derivative of the Electronic Work Function of Copper at Low Temperatures," J. U. Free, C. D. Dermer, and P. B. Pipes. 1979, Phys. Rev., B19, 631.

"The Production Spectrum of a Relativistic Maxwell-Boltzmann Gas," Charles D. Dermer. 1984, Ap. J., 280, 328.

FIELDS OF STUDY

Major Field: Physics

Studies in Experimental Low Temperature Physics
Professors R. P. Wolf and F. A. Stahl

Studies in Experimental Low Temperature Physics
Professors P. B. Pipes and J. U. Free

Studies in Cosmology and High Energy Astrophysics
Professor Robert J. Gould

ABSTRACT OF THE DISSERTATION

Physics of Nonmagnetic Relativistic Thermal Plasmas

by

Charles Dennison Dermer

Doctor of Philosophy in Physics

University of California, San Diego, 1984

Professor Robert J. Gould, Chairman

A detailed treatment of the kinematics of relativistic systems of particles and photons is presented. In the case of a relativistic Maxwell-Boltzmann distribution of particles, the reaction rate and luminosity are written as single integrals over the invariant cross section, and the production spectrum is written as a double integral over the cross section differential in the energy of the produced particles (or photons) in the center-of-momentum system of two colliding particles. The result is valid for all temperatures and for the general case when the plasma contains different mass particles.

The results are applied to the calculation of the annihilation spectrum of a thermal electron-positron plasma, confirming previous numerical and analytic results. Relativistic thermal electron-ion and electron-electron bremsstrahlung are calculated exactly to lowest order, and relativistic thermal electron-positron

bremsstrahlung is calculated in an approximate way, by interpolating between the modified Bethe-Heitler formula and the exact lowest order electron-electron bremsstrahlung spectrum. An approximate treatment of relativistic Comptonization is developed.

The question of thermalization of a relativistic plasma is considered. A formula for the energy loss or exchange rate from the interaction of two relativistic Maxwell-Boltzmann plasmas at different temperatures is derived. It is concluded that at temperatures greater than about 1 MeV, full thermalization of an electron-proton plasma is not possible because of the dominance of bremsstrahlung losses.

Application to a stable, uniform, nonmagnetic relativistic thermal plasma is made. Approximate expressions for dominant rates, taking account of the effects of Comptonization, are used to model the system at extreme relativistic temperatures and at subrelativistic temperatures in the limit of large optical depth. Equilibrium pair densities, critical temperatures, and emergent spectra are calculated. Comparison is made with other studies.

I. INTRODUCTION

The existence of relativistic plasmas is supposed to account for many astrophysical observations made during the past two decades. These observations include gamma ray bursts, jet structures observed near some extragalactic radio sources or stars (SS433), and the central energy sources of active galactic nuclei and quasi-stellar objects including, perhaps, the center of our own galaxy. One might also include indirect observations relating to that epoch of the early universe when nucleosynthesis and neutrino decoupling were occurring, according to standard cosmology. In order to characterize the physical conditions relating to such observations, a systematic study of relativistic gases is required.

A relativistic plasma, or gas, is a system of particles and photons in which the average particle and photon energy is sufficiently great that particle-creating reactions occur and influence the observed properties of the gas. The created particles are produced at the expense of excess kinetic energy in collisions between two particles in the plasma, or as a result of particle production through photon-particle or photon-photon interactions. Since the produced particles may in turn participate in particle-creating reactions, the description of the system requires a self-consistent treatment which is, in general, nonlinear.

The aim of this work is to examine, by means of theoretical

analysis of relativistic particle gases, processes in relativistic plasmas. In particular, investigation is made of processes occurring in the "transrelativistic" regime where the average particle kinetic energy is of the same magnitude as the particle rest mass energy. Because cross sections for particle or photon production can be extremely complicated in this regime, asymptotic forms may not be used and a simplified, general treatment is essential. Of course, the results must properly approach limiting forms in the nonrelativistic and extreme relativistic limits.

Conditions of thermal equilibrium cannot be assumed in the study of relativistic gases. Indeed, the predominance of certain energy-loss processes can prevent the formation of a thermal distribution of the particle momenta (Gould 1982a; Stepney 1983), as we shall examine in more detail later. The term relativistic gas will be used interchangeably with the term relativistic plasma; though the system will be in a state consisting of independent charged particles, the possibility of collective modes of excitation will not be treated in this study, as we consider a nonmagnetic system.

The examination of the properties of a relativistic gas begins with an elaboration of the various processes that contribute to the behavior of the gas. The processes which are most important depend on the nature of the problem under consideration. It is then essential to calculate energy loss rates and time scales in order to

determine whether the particles of the gas can be thermalized, as the form of the particle distribution function defines particle production and annihilation rates and photon spectral emissivities.

It will then prove useful in a self-consistent analysis of the nonmagnetic relativistic plasma to consider ranges of system parameters such as optical depth, proton number density, and temperature, where expressions for rates assume convenient analytic forms. In addition, an exact treatment of the Comptonization of internally generated photons by a relativistic particle plasma is a formidable task, so approximate techniques are necessary. These results can be compared to a gross numerical simulation.

The plan of this dissertation is as follows: A theoretical formalism is developed in Chapter II for the calculation of rate processes and timescales in relativistic gases. A general formula for the production spectrum from an isotropic relativistic Maxwell-Boltzmann gas is derived, and a treatment of the Compton power and Compton scattered spectrum is developed. Timescales for reaction and energy loss processes are also examined. Application of the formalism is made in Chapter III, including the calculation of annihilation spectra and bremsstrahlung from a relativistic Maxwell-Boltzmann plasma, calculations of absorption and opacity, and a compilation of invariant cross sections useful for the analysis of problems in high energy astrophysics.

Physical applications of the preceding results are developed in Chapter IV. A uniform nonmagnetic relativistic plasma is analyzed in various temperature and optical depth regimes, asymptotic expressions for the dominant rates are derived, and an approximate treatment of Comptonization is developed. Discussion of the principle features of this system follows, including comparison with other work. Results and conclusions are set forth in Chapter V.

II. THEORETICAL TREATMENT OF PROCESSES IN A RELATIVISTIC PLASMA

A. Introduction

Historically, the theory of the relativistic gas begins with the derivation of the relativistic generalizations of equilibrium particle distribution functions (Jüttner 1911a, b; 1928). Later developments include generalizations of kinetic equations for relativistic gases. Early results are summarized in a monograph by Synge (1957), and details of the kinetic theory of relativistic gases may be found in the book by de Groot, van Leeuwen, and van Weert (1980).

In this chapter, expressions for rate processes and the spectral emissivity are derived for isotropic relativistic particle gases. The results are specialized to the case of a relativistic Maxwell-Boltzmann (MB) distribution. Considerable simplification of the production spectrum of a MB gas is achieved in this case. Expressions for reaction and energy-loss timescales are also presented. Finally, a formalism is developed for calculating the Compton power and approximate Compton scattered spectra for a gas containing photons and electrons.

B. Relativistic Kinematics

Consider a relativistic gas of particles. The relativistic reaction rate r is defined as the number of collisions per unit time per unit volume and is an invariant quantity. The reaction rate for

two interacting distributions of particles is given by

$$r = (1 + \delta_{12})^{-1} \int \cdots \int \beta_r \cdot (1 - \underset{\sim}{\beta}_1 \cdot \underset{\sim}{\beta}_2) \, d\sigma \, dn_1 \, dn_2 \qquad (1)$$

(Landau and Lifshitz 1962; Gould 1971). In this expression, completely general, the integration extends over all momenta of the interacting distributions of particles. The number of particles per unit interval of momentum in the observer's system of reference (LS), or the spectral density, is denoted by dn_i for particles of the type i. The factor $(1 + \delta_{12})^{-1}$ corrects for double counting if the particles are identical (self-interacting) and $d\sigma$ is the invariant cross section.

The speed of light c is set equal to 1 in equation (1) and the momentum $\underset{\sim}{p}_i$, energy E_i, and mass m_i are written in energy units throughout. In this case $\underset{\sim}{\beta}_i = \underset{\sim}{p}_i / E_i$ and β_r, the invariant relative velocity, is defined as

$$\beta_r = \left[\frac{(\pi_i \cdot \pi_2)^2 - m_1^2 m_2^2}{(\pi_1 \cdot \pi_2)^2} \right]^{1/2} , \qquad (2)$$

where the four-momentum of particle i is given by $\pi_i = (E_i, p_i)$ and the metric is (+, -, -, -). The variable β_r represents the absolute value of the velocity of one particle in the frame of reference in which the other particle is at rest. The factor $(1 - \underset{\sim}{\beta}_1 \cdot \underset{\sim}{\beta}_2)$ accounts for relativistic changes in time and particle density in transforming from one reference frame to another.

In the general case of two distinct nonisotropic interacting gases, equation (1) is a 6-fold integral and admits no simplification. Assuming, however, that the interacting gases are isotropic, equation (1) may be written as an integration over three quantities necessary to uniquely characterize a collision between two different particles. These are conventionally taken to be the momenta p_1 and p_2, and θ, the angle between the direction of the two momenta in the LS. Thus, $\cos\theta = \underset{\sim}{p}_1 \cdot \underset{\sim}{p}_2 / p_1 p_2$. In terms of these variables,

$$r = \frac{8\pi^2 A_1 A_2}{1+\delta_{12}} \int_0^\infty dp_1\, p_1^2\, f_1(p_1) \int_0^\infty dp_2\, p_2^2\, f_2(p_2) \int_{-1}^{1} d(\cos\theta) \times [\sigma(p_1, p_2, \cos\theta) \cdot (1 - \beta_1 \beta_2 \cos\theta) \cdot \beta_r(p_1, p_2, \cos\theta)] . \tag{3}$$

The functions $f_i(p_i)$ describe the momentum distributions of the interacting particles and are related to dn_i and the normalization coefficient A_i through the expression

$$n_i = \int dn_i = 4\pi A_i \int_0^\infty dp_i\, p_i^2\, f_i(p_i) \; ; \tag{4}$$

n_i is the volume density of particles of the type i.

Ordinarily, equation (3) is used to calculate reaction rates as it stands. It is reasonable to suppose that equation (3) can be simplified by a judicious choice of variables. In particular, one

such variable should be the argument of the invariant cross section. In this case, the integration over this variable can be performed last, and the generally complicated dependence of the cross section can be avoided as long as possible.

To this end, it is convenient to choose the invariant Lorentz factor γ_r associated with the relative velocity β_r, defined in equation (2), as this variable. In terms of p_1, p_2, and θ,

$$\gamma_r = (1 - \beta_r^2)^{-1/2} = \frac{\pi_1 \cdot \pi_2}{m_1 m_2} = \frac{E_1 E_2 - p_1 p_2 \cos\theta}{m_1 m_2} \quad . \tag{5}$$

For the other two variables, introduce γ_c and the angle ω, where γ_c is defined as the Lorentz factor corresponding to the velocity of the center-of-momentum of the two interacting particles with respect to the LS. It can be written as

$$\gamma_c = \frac{E_1 + E_2}{[(s(\gamma_r)]^{1/2}} \quad , \tag{6}$$

in terms of the invariant quantity

$$s = (\pi_1 + \pi_2)^2 = m_1^2 + m_2^2 + 2m_1 m_2 \gamma_r \quad , \tag{7}$$

which describes the strength of the collision between the two particles. The variable γ_c is a natural extension of the center-of-momentum variable used in nonrelativistic studies of rate processes.

The angle ω is defined through the relation

$$\sin \omega = \frac{p_1 p_2 \sin \theta}{m_1 m_2 \beta_r \gamma_r \beta_c \gamma_c} \quad . \tag{8}$$

The significance of ω is as follows: If we transform to the center-of-momentum system (CM) of the two colliding particles and call the transformed momentum of particle 1 p_1', then ω represents the angle p_1' makes with respect to the direction of transformation from the LS to the CM (see Figures 1a and 1b).

The Jacobian J for the transformation from the variables p_1, p_2, $\cos\theta$ to γ_r, γ_c, $\cos\omega$ is found to be

$$J\begin{pmatrix} p_1, p_2, \cos\theta \\ \gamma_r, \gamma_c, \cos\omega \end{pmatrix} = \frac{E_1 E_2 m_1^2 m_2^2 \beta_r \gamma_r \beta_c \gamma_c}{p_1^2 p_2^2} \quad . \tag{9}$$

Changing to this new set of variables in equation (3), it is convenient to rewrite equation (3) in a general fashion so as to incorporate expressions for different rate processes. Letting $P(y)$ stand for a rate process of the relativistic gas for the parameter value(s) y associated with the weighting $\rho(y; \gamma_r, \gamma_c, u)$, and defining $u = \cos\omega$, then

$$P(y) = \frac{8\pi^2 A_1 A_2 m_1^3 m_2^3}{1+\delta_{12}} \int_1^\infty d\gamma_r (\gamma_r^2 - 1) \int_1^\infty d\gamma_c (\gamma_c^2 - 1)^{1/2}$$
$$\times \int_{-1}^{1} du\, f_1[p_1(\gamma_r, \gamma_c, u)]\, f_2[p_2(\gamma_r, \gamma_c, u)]\, \rho(y; \gamma_r, \gamma_c, u) \quad . \tag{10}$$

Figure 1. Kinematic quantities associated with relativistic transformations. Transformation from the LS to the CM is effected by a Lorentz transformation by momentum $\underset{\sim}{p}_c$ defined in terms of the momenta $|\underset{\sim}{p}_1|$ and $|\underset{\sim}{p}_2|$ of the interacting particles and the angle θ between them. Transformation to the C-system is effected by an additional counterclockwise rotation of the axes by an angle ω. The terms $\underset{\sim}{p}$, $\underset{\sim}{p}'$ and $\underset{\sim}{p}^*$ represent the momentum of a produced particle as seen in the three frames of reference. The coordinate system employed in the three frames (illustrated only in the C-system) consists of specifying the absolute value of $\underset{\sim}{p}$, the cosine of the angle ψ that $\underset{\sim}{p}$ makes with the z-axis, and the angle ϕ between the x-axis and the projection of the momentum $\underset{\sim}{p}$ on the x-y plane.

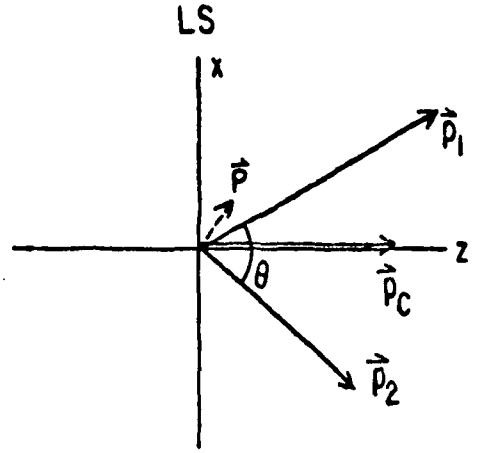
LS
x
$\vec{p}_1$
$\vec{p}$
z
θ
$\vec{p}_c$
$\vec{p}_2$

(a)

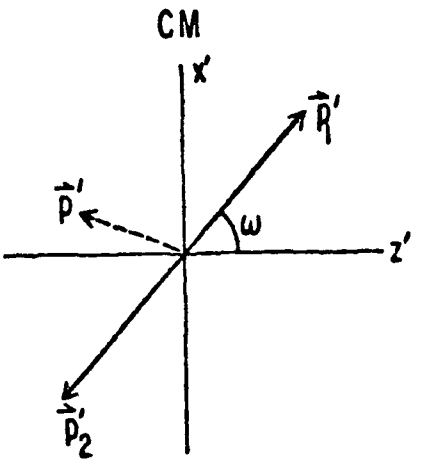
CM
x'
$\vec{p}_1'$
$\vec{p}'$
ω
z'
$\vec{p}_2'$

(b)

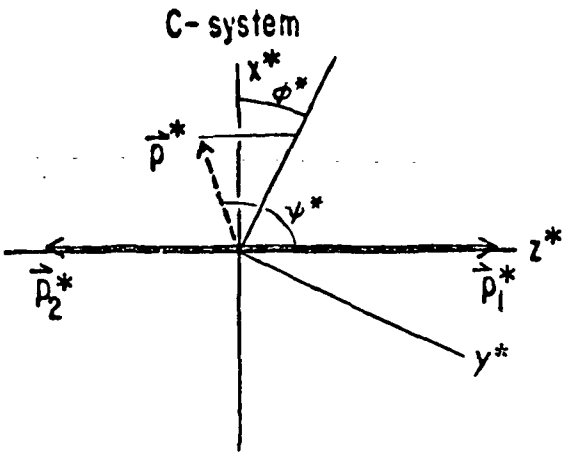
C- system
x*
φ*
$\vec{p}^*$
ψ*
z*
$\vec{p}_2^*$
$\vec{p}_1^*$
y*

(c)

For example, $P(y) = r$, the reaction rate, when $\rho(y; \gamma_r, \gamma_c, u) = \sigma(\gamma_r)$. The luminosity ℓ is the total energy produced in particles or photons per unit volume per unit time as measured in the LS. If the energy liberated per interaction as recorded in the LS is denoted by $\epsilon(\gamma_r, \gamma_c, u)$, then $P(y) = \ell$ when $\rho(y; \gamma_r, \gamma_c, u) = \sigma(\gamma_r)\epsilon(\gamma_r, \gamma_c, u)$. In like manner, the production spectrum $S(E)$ (number of photons produced per unit volume per unit time per unit energy interval dE) is $P(y) = S(E)$ when $\rho(y; \gamma_r, \gamma_c, u) = d\sigma(E; \gamma_r, \gamma_c, u)/dE$. This last quantity is the cross section differential in the LS energy of the produced particles or photons in an interaction characterized by the reaction parameters γ_r, γ_c, and u.

These rate processes are closely related to one another, and consistency of results requires that the following relationships hold for the reaction rate r, the luminosity ℓ, and the production spectrum $S(E)$:

$$r = \int_{m_j}^{\infty} dE\, S(E) \tag{11}$$

and

$$\ell = \int_{m_j}^{\infty} dE\, E\, S(E) \ , \tag{12}$$

where m_j is the rest mass of the particle produced in collisions between particles in the gas ($m_j = 0$ if photon production is

considered).

We now specialize to the case of collisions in a particle plasma described by a relativistic MB distribution in order to derive an expression for the reaction rate. The MB distribution for relativistic particles of the type i is

$$f_i(p_i) = \exp\left[-b(p_i^2 + m_i^2)^{1/2}\right], \tag{13}$$

defining $b = 1/k_B T$ and noting from relation (4) that

$$A_i = \frac{n_i \mu_i}{4\pi m_i^3 K_2(\mu_i)}, \tag{14}$$

where $\mu_i = bm_i$ and $K_\nu(x)$ is the modified Bessel function of order ν (Synge 1957). Assuming that both interacting gases have MB form at the same temperature, equation (6) implies that

$$f_1(p_1) f_2(p_2) = \exp\left\{-b\gamma_c [s(\gamma_r)]^{1/2}\right\}. \tag{15}$$

Substituting equation (15) into equation (10) for the case of the reaction rate gives

$$r = \frac{n_1 n_2 \mu_1 \mu_2}{(1+\delta_{12}) K_2(\mu_1) K_2(\mu_2)} \int_1^\infty d\gamma_r \frac{(\gamma_r^2 - 1) K_1\{b[s(\gamma_r)]^{1/2}\}}{\{b[s(\gamma_r)]^{1/2}\}} \sigma(\gamma_r), \tag{16}$$

agreeing with the result of Weaver (1976).

C. Secondary Particle Production Kinematics

The preceding considerations show how the reaction rate and luminosity are related to the spectral emissivity. In order to derive the spectral emissivity, it is necessary to calculate the LS cross section differential in energy of the produced particles or photons for an arbitrary collision between two particles. In terms of the variables γ_r, γ_c, and u, it is clear that all particle reactions characterized by the value γ_r are kinematically equivalent in the C-system, the reference frame rotated so that the directions of the incident particles are along the z^*-axis of the C-system (see Figure 1c). It is then only a matter of performing the appropriate Lorentz transformation from the C-system to the LS, defined in terms of $u = \cos \omega$ and γ_c, to get the cross section differential in the LS energy of the produced particles or photons.

The appropriate transformation consists of two successive Lorentz transformations: a clockwise rotation of the coordinate axes of the C-system by an angle ω followed by a boost of the CM by velocity $-\beta_c$ along the x' axis. The equations of transformation are easily derived, and it will be useful for later work to display the relevant coordinate transformation equations. Quantities in the C-system are labelled by asterisks. Define a coordinate system in the LS and C-system by the variables $(p, \cos\psi, \phi)$ and $(p^*, \cos\psi^*, \phi^*)$, respectively, as illustrated in Figure 1. A

produced particle whose energy is E^*, momentum is p^*, and production angles are $\cos\psi^*$ and ϕ^* has energy

$$E = \gamma_c [E^* + \beta_c (p^* \cos\psi^* \cos\omega - p^* \sin\psi^* \cos\phi^* \sin\omega)] \qquad (17)$$

in the LS. The reverse transformations are given by

$$E^* = \gamma_c (E - \beta_c p \cos\psi), \quad \text{and} \qquad (18a)$$

$$p^* \cos\psi^* = \gamma_c (p \cos\psi - \beta_c E) \cos\omega + p \sin\psi \cos\phi \sin\omega. \qquad (18b)$$

To determine the cross section differential in energy in the LS, it is best to use invariant production cross sections, as the question of the Jacobian of the transformation is thereby avoided. The Lorentz invariant cross section for the production of particle j in the reaction $1 + 2 \rightarrow j + X$ is given by

$$E^* \frac{d^3\sigma_j^*}{dp^{*3}} = \frac{d^3\sigma_j^*}{p^* dE^* d(\cos\psi^*) d\phi^*} = F_j^*(E^*, p^{*3}; \gamma_r); \qquad (19)$$

X represents all final state particles other than those of the type j. The invariant cross section F_j^* represents the probability that the produced particle j will be deposited in the phase space volume d^3p^*/E^* in a collision characterized by the reaction strength s, or equivalently, γ_r, since the two are linearly related through equation (7) (Berger 1975). Asterisks in the definition of the Lorentz invariant cross section in equation (19) serve to remind that F_j^* is

most conveniently written in C-system quantities, and in fact experimental results are usually presented in just this coordinate system, though the LS and CM representations are completely equivalent.

The invariant cross section is normalized through the relation

$$\langle \xi(\gamma_r) \rangle \sigma_{TOT}(\gamma_r) = \int \frac{d^3 \underset{\sim}{p}^*}{E^*} F_j^*(E^*, \underset{\sim}{p}^{*3}; \gamma_r) \ , \qquad (20)$$

with the integral extending over all momenta. In this expression $\langle \xi_j(\gamma_r) \rangle$ is the average multiplicity of the produced particle j and $\sigma_{TOT}(\gamma_r)$ is the total cross section of the reaction 1+2 characterized by the collision strength γ_r, though other conventions are possible (Likhoded and Shlyapnikov 1978).

The energy spectrum in any frame related by a coordinate transformation, whether it be a rotation or boost or some combination of the two, is given by

$$\frac{d\sigma(E; \gamma_r, \gamma_c, u)}{dE} = (E^2 - m_j^2)^{1/2} \int d\phi \int d(\cos\psi) F_j^*(E^*, \psi^*; \gamma_r) \ , \qquad (21)$$

with E^* and ψ^* written in terms of E, ψ, and ϕ according to the transformation equations (18). Azimuthal symmetry in the production of j has been assumed in equation (21), and the limits of integration over $\cos\psi$ and ϕ remain to be specified.

Define $\xi = E_M^*(\gamma_r)$ as the maximum possible energy that the produced particle j can carry off in a reaction characterized by the value γ_r. Relativistic mechanics can be used to explicitly

evaluate this quantity, giving $\xi = (s - \overline{m}_X^2 + m_j^2)/2s^{1/2}$, where $\overline{m}_X$ is the smallest possible value of the mass of all remaining particles so that the reaction $1+2 \rightarrow j+X$ may proceed. The limits of integration are then implied by the transformation equations (18). For fixed energy E, $\cos\psi$ extends from $\cos\psi_M = (\gamma_c E - \xi)/\beta_c \gamma_c p$ to $\cos\psi = 1$. The integration is over all ϕ as equation (18a) is independent of ϕ (Taylor et al. 1976; Tan and Ng 1981).

Employing the preceding considerations with equations (19) and (21), the following identity may be written:

$$\frac{d\sigma(E;\gamma_r,\gamma_c,u)}{dE} = p\int_0^{2\pi} d\phi \int_{\cos\psi_M}^{1} d(\cos\psi) \int_{m_j}^{\xi} dE_0^* \frac{\delta(E^* - E_0^*)}{2\pi p_0^*} \cdot \frac{d^2\sigma_j^*(E_0^*, \cos\psi^*; \gamma_r)}{dE_0^* \, d(\cos\psi^*)} , \tag{22}$$

with E^* and $\cos\psi^*$ given by equation (18). For the problem of the production spectrum $S(E)$ of a relativistic isotropic MB gas, equations (10), (15), and (22) give

$$S(E) = \frac{1}{2} \frac{n_1 n_2 \mu_1 \mu_2}{(1+\delta_{12}) K_2(\mu_1) K_2(\mu_2)} \int_1^{\infty} d\gamma_r (\gamma_r^2 - 1) \int_1^{\infty} d\gamma_c (\gamma_c^2 - 1)^{1/2} \cdot \exp\{-b\gamma_c [s(\gamma_r)]^{1/2}\}$$

$$\times \left[\frac{p}{2\pi} \int_{m_j}^{\xi} \frac{dE_0^*}{p_0^*} \int_{-1}^{1} du \int_{0}^{2\pi} d\phi \int_{\cos\psi_M}^{1} d(\cos\psi)\, \delta(E^* - E_0^*) \right.$$

$$\left. \cdot \frac{d^2\sigma_j^*(E_0^*, \cos\psi^*; \gamma_r)}{dE_0^*\, d(\cos\psi^*)} \right] . \qquad (23)$$

Call the term in brackets I. Performing the integral over $\cos\psi$ using equation (18a) in the delta function and equation (18b) for $\cos\psi^*$, one finds that

$$I = \frac{1}{2\pi\beta_c\gamma_c} \int_{\gamma_c(E-\beta_c p)}^{\xi} \frac{dE_0^*}{p_0^*} \int_{-1}^{1} du \int_{0}^{2\pi} d\phi$$

$$\cdot \frac{d^2\sigma_j^*[E_0^*, \cos\psi^* = \eta u + (1-\eta^2)^{1/2}(1-u^2)^{1/2}\cos\phi; \gamma_r]}{dE_0^*\, d\cos\psi^*} , \qquad (24)$$

where η is defined as $(E - \gamma_c E_0^*)/\beta_c\gamma_c p_0^*$ and is bound by the limits -1 and 1 due to the previously established limits on $\cos\psi$.

The last two integrals in equation (24) represent an integration over all solid angles in $u - \phi$ space. Identifying $\cos\theta_1$ with η, we may substitute $\cos\chi$ for $\cos\theta_1\cos\omega + \sin\theta_1\sin\omega\cos\phi$ using a standard trigonometric identity. The limits of integration remain as before -- over all solid angles -- but now over an integrand possessing azimuthal symmetry. The expression becomes

$$I = \frac{1}{\beta_c \gamma_c} \int_{m_j}^{\xi} \frac{dE_0^*}{p_0^*} \int_{-1}^{1} d(\cos\chi) \frac{d^2\sigma_j^*(E_0^*, \cos\chi; \gamma_r)}{dE_0^* \, d(\cos\chi)} \quad . \tag{25}$$

The last integral in equation (25) is just the production cross section integrated over the angle χ (or equivalently, ψ^*) in the C-system and will be denoted as $d\sigma^*(E_0^*; \gamma_r)/dE_0^*$. (This result reflects the uniformity in $\cos\omega$ of the phase space factor in equation (10) and the independence of the product MB distribution, equation (15), of $\cos\omega$.)

The production spectrum (23) becomes, reversing the order of integration over E_0^* and γ_c,

$$S(E) = \frac{1}{2} \frac{n_1 n_2 \mu_1 \mu_2}{(1+\delta_{12}) K_2(\mu_1) K_2(\mu_2)} \int_1^{\infty} d\gamma_r (\gamma_r^2 - 1)$$

$$\cdot \int_{m_j}^{\xi} \frac{dE_0^*}{p_0^*} \frac{d\sigma^*(E_0^*; \gamma_r)}{dE_0^*} \int_{\gamma_c^-}^{\gamma_c^+} d\gamma_c \, e^{-b\gamma_c [s(\gamma_r)]^{1/2}} \quad . \tag{26}$$

The limits of integration are implies by a consideration of those values of γ_c which contribute for fixed values of E_0^* and E. For material particles, $\gamma_c^{\pm} = (EE_0^* \pm pp_0^*)/m_j^2$, whereas for photon production the limits are $\gamma_c^- = (E^2 + E_0^{*2})/2EE_0^*$ and $\gamma_c^+ \to \infty$ (with, of course, $m_j = 0$ and $p_0^* = E_0^*$ in the integration over E_0^*).

Using these limits, the integral over γ_c is trivially performed and equation (26) gives the general formula for the

calculation of the production spectrum of particles or photons from interactions in a MB gas at all temperatures, from the nonrelativistic to the extreme relativistic limits. It is written in terms of the cross section differential of the produced particles (or photons) in the C-system of the collision. As most cross sections are calculated or measured in terms of these variables, equation (26) is a convenient formula for analysis. Clearly no further simplification can be made without referring to a specific problem. Applications of equation (26) will be deferred to the next chapter.

From equation (26), the reaction rate and luminosity can be derived through relations (11) and (12). It is straightforward to integrate the production spectrum (26) over energy to recover the reaction rate (16). To obtain a corresponding expression for the luminosity, define

$$\epsilon^*(\gamma_r)\,\sigma(\gamma_r) = \int_{m_j}^{\xi} dE_0^*\, E_0^*\, \frac{d\sigma^*(E_0^*;\gamma_r)}{dE_0^*} \tag{27}$$

as the average energy, weighted by the cross section, of particles or photons released in the CM of a collision characterized by the reaction strength γ_r. Then the luminosity is

$$\ell = \frac{n_1 n_2 \mu_1 \mu_2}{(1+\delta_{12})K_2(\mu_1)K_2(\mu_2)} \int_1^{\infty} d\gamma_r \, \frac{(\gamma_r^2-1)K_2\{b[s(\gamma_r)]^{1/2}\}}{\{b[s(\gamma_r)]^{1/2}\}} \epsilon^*(\gamma_r)\,\sigma(\gamma_r) \ . \tag{28}$$

D. Annihilation and Energy Loss Timescales

The derivations of equation (26), the spectral emissivity, as well as the expressions for the reaction rate and luminosity, equations (16) and (28), are performed under the assumption that the particles are described by an isotropic energy distribution of MB form. This assumption considerably simplifies the results. Whether, or under what conditions, this assumption is warranted will be the concern of this section.

It should be remarked at this point that under many conditions of astrophysical interest, the state of complete thermodynamic equilibrium, in which the photons are of Bose-Einstein form and the electrons and positrons possess a Fermi-Dirac distribution at zero chemical potential, cannot be achieved. Yet the particles can be thermalized, that is obtain MB form (which is just the Fermi-Dirac distribution with large negative chemical potential). The establishment of a thermal distribution of particles requires that elastic scattering processes dominate over inelastic processes. The processes that drive a gas composed of electrons, positrons, and ions to thermal form are the elastic Coulomb scattering processes, namely Møller scattering between two electrons or two positrons, Bhabha scattering between an electron and a positron, and Rutherford and Mott scattering between ions and an ion and electron (or positron), respectively. Bremsstrahlung or synchrotron emission

are typical energy loss mechanisms that can prevent the establishment of a thermal distribution.

There is a considerable literature dealing with the thermalization of particles at subrelativistic temperatures. Basic results can be found in Spitzer's book (1962). A systematic study of the thermalization of particles in a relativistic gas has only recently been considered. Gould (1981b) treats the thermalization rates of a highly relativistic particle in the presence of a MB gas at temperatures greater than 0.5 MeV. Since the high energy particle is in the tail of the Maxwellian of the relativistic gas, which is in fact that portion of the distribution function requiring longest to relax, the timescales for energy loss accurately represent the time of a particle gas to relax to thermal form.

In subsequent papers (Gould 1982a, b, c), comparisons of the earlier results are made with the energy loss timescales due to various inelastic processes in relativistic electron and nucleonic gases, and it is shown under what conditions a thermal distribution can and cannot be obtained. In particular, above a certain temperature, a relativistic electron gas cannot be thermalized because of the predominance of bremsstrahlung losses. Moreover, a sufficiently strong magnetic field can prevent thermalization through synchrotron energy losses at even lower temperatures.

The approach to be taken here is somewhat different. First,

a general expression for the reaction rate of a single test particle in the presence of a MB gas will be derived. This result will provide, for example, the timescale for annihilation of a positron in an electron gas, or the timescale for an energy loss process in which a large amount of energy is lost in a single collision as occurs, for instance, in pair production through particle-particle collision. Second, an exact expression for the energy loss of a test particle in the presence of a relativistic MB gas is derived. Then the timescale for energy exchange between two MB gases will be determined. This result is a generalization of an expression derived by Stepney (1983), and is valid for two interacting MB gases at any two temperatures.

Suppose a particle of momentum p_2^o interacts with the particles of a relativistic gas described by the momentum distribution $f_1(p_1)$. The reaction rate is given from equation (10) by

$$r = \frac{8\pi^2 A_1 A_2 m_1^3 m_2^3}{1+\delta_{12}} \int_1^\infty d\gamma_r (\gamma_r^2-1) \int_1^\infty d\gamma_c (\gamma_c^2-1)^{1/2} \int_{-1}^1 du\, f_1(p_1) f_2(p_2)\, \sigma(\gamma_r) . \tag{29}$$

Since the reaction rate is the number of collisions per unit volume per unit time, the average time for the particle of momentum p_2^o to survive between collisions is $T_r = (r/n_2)^{-1}$, where n_2 is the density (to be normalized to unity) of the particle of momentum p_2^o, and is closely associated with the absorption coefficient, as will become clear in Chapter III.

The distribution function of particles of the type 1 is now taken to be of MB form, given by equation (13), with normalization coefficient (14). The momentum distribution function of the particle of momentum p_2^o is a delta function. Incorporating the phase space factor, it is convenient to take the distribution function as

$$f_2(p_2) = \frac{1}{4\pi p_2^2} \delta(p_2 - p_2^o) \quad . \tag{30}$$

From the normalization condition (4), $A_2 = n_2 = 1$.

The reaction rate (29) for an individual test particle becomes

$$r_t = \frac{n_1 b_1 m_1 m_2^3}{2K_2(b_1 m_1)} \frac{1}{p_2^o E_2^o} \int_1^\infty d\gamma_r (\gamma_r^2 - 1)\, \sigma(\gamma_r) \int_1^\infty d\gamma_c (\gamma_c^2 - 1)^{1/2}$$

$$\cdot \int_{-1}^{1} du\, e^{-b_1 E_1}\, \delta(E_2 - E_2^o) \quad , \tag{31}$$

where $b_1 = 1/k_B T_1$ refers to the inverse temperature of particle distribution 1 and the delta function has been converted to energy variables. From a consideration of equations (5), (6), and (7), it is possible to express E_1 and E_2 in terms of the variables γ_r, γ_c, and u. The relations are

$$E_1 = \frac{m_1(m_2 \gamma_r + m_1)\gamma_c}{s^{1/2}} + \frac{m_1 m_2 \beta_r \gamma_r \beta_c \gamma_c}{s^{1/2}}\, u \quad , \quad \text{and} \tag{32a}$$

$$E_2 = \frac{m_2(m_1\gamma_r + m_2)\gamma_c}{s^{1/2}} - \frac{m_1 m_2 \beta_r \gamma_r \beta_c \gamma_c}{s^{1/2}} u \ . \qquad (32b)$$

Performing the delta function over u and determining what the conditions $-1 \le u \le 1$ implies for the limits on γ_c, we find that, after integrating over γ_c, the reaction rate r_t is

$$r_t = \frac{n_1}{2K_2(\mu_1')} \frac{1}{\beta_2 \gamma_2^2} \int_1^\infty d\gamma_r \beta_r \gamma_r \sigma(\gamma_r)$$

$$\times \left[e^{-\mu_1' \gamma_2 \gamma_r} \left(e^{\mu_1' \beta_2 \gamma_2 \beta_r \gamma_r} - e^{-\mu_1' \beta_2 \gamma_2 \beta_r \gamma_r} \right) \right] , \qquad (33)$$

where $\mu_i' = b_i m_i$, $m_2\gamma_2 = E_2^o$, and $m_2 \gamma_2 \beta_2 = p_2^o$.

Equation (33) gives the formula for the annihilation or reaction rate of a single test particle of momentum p_2^o and mass m_2 in the presence of an isotropic MB gas of particles of mass m_1 at temperature $1/b_1$. To be consistent with earlier results, it should reduce to equation (16) when integrated over a MB distribution of particles of type 2, also at temperature $1/b_1$. To determine the reaction rate of two interacting MB gases at different temperatures, note that

$$e^{-b_2 E_2^o} = \int_0^\infty dp_2 (4\pi p_2^2) \, e^{-b_2 E_2} \, f_2(p_2) \qquad (34)$$

where $f_2(p_2)$ is given by equation (30) and the normalization coefficient is now given by expression (14). Multiplying equation (33) by

$(4\pi p_2^{o2})\exp(-b_2 E_2^o)$ and integrating over dp_2^o according to equation (34), the reaction rate is

$$r = \frac{n_1 n_2 \mu_2'}{2(1+\delta_{12})K_2(\mu_1')K_2(\mu_2')} \int_1^\infty d\gamma_r \, \beta_r \, \gamma_r \, \sigma(\gamma_r) \times \left\{ \int_1^\infty d\gamma_2 \, e^{-(\mu_2' + \mu_1' \gamma_r)\gamma_2} \left[e^{\mu_1' \beta_r \gamma_r \beta_2 \gamma_2} - e^{-\mu_1' \beta_r \gamma_r \beta_2 \gamma_2} \right] \right\} . \quad (35)$$

The remainder of the derivation is similar to the treatment of Weaver (1976). Defining $ch\theta_1 = (\mu_2' + \mu_1' \gamma_r)/z^{1/2}$ and $ch\theta_2 = \gamma_2$, with $z = \mu_1'^2 + \mu_2'^2 + 2\mu_1' \mu_2' \gamma_r$, gives Weaver's result for the reaction rate of two interacting MB gases at different temperatures, namely

$$r = \frac{n_1 n_2 \mu_1' \mu_2'}{(1+\delta_{12})K_2(\mu_1')K_2(\mu_2')} \int_1^\infty d\gamma_r \frac{(\gamma_r^2 - 1)\sigma(\gamma_r) K_1(z^{1/2})}{z^{1/2}} . \quad (36)$$

If the gases are at the same temperatures, $\mu_1' = \mu_1$, $\mu_2' = \mu_2$, $z^{1/2} = bs^{1/2}$, and equation (16) is recovered.

To determine the thermalization and energy loss timescales for various processes in a relativistic gas, consider the expression for the change in the LS energy of a particle before and after a collision. The average energy change can be defined as

$$\langle \Delta E \rangle = \frac{1}{\sigma(\gamma_r)} \int d^3\underset{\sim}{p}^* \left(\frac{d^3\sigma^*}{d\underset{\sim}{p}^{*3}} \right) \Delta E \,, \tag{37}$$

where $d^3\underset{\sim}{p}^* = p^{*2}\, dp^*\, d\cos\psi^*\, d\phi^*$, employing the coordinate system illustrated in Figure 1. The cross section for scattering into the phase volume $d^3\underset{\sim}{p}^*$ is given by $(d^3\sigma^*/d^3\underset{\sim}{p}^*)$ and ΔE is defined as the change in the LS particle energy as the result of being scattered into the phase volume $d^3\underset{\sim}{p}^*$ in the C-system. From equation (17), the energy change is just

$$\Delta E = \gamma_c (E^* - E_i^*) + \beta_c \gamma_c [(p^* \cos\psi^* - p_i^*)\cos\omega - p^* \sin\psi^* \cos\phi^* \sin\omega], \tag{38}$$

where p_i^* and E_i^* refer to the particle momentum and energy prior to scattering. The value of p_i^* is in fact given by

$$p_i^*(\gamma_r) = (m_1 m_2 \beta_r \gamma_r)/[s(\gamma_r)]^{1/2} \,. \tag{39}$$

The momentum and energy of the particle after scattering are denoted by p^* and E^*, respectively.

The timescale for energy loss by a system, whether it be a gas or a test particle, is defined as $T_\ell^{-1} = \ell / e_k$, where e_k is the kinetic energy density of the system. If the system loses energy by inelastic scattering through the production of particles or photons, then ℓ has been determined for the case of two MB gases at the same temperature, namely equation (28). If the scattering is

elastic, or if the energy exchange rate of two MB gases at different temperatures is being considered, it will be necessary to proceed differently.

Consider first a test particle that loses LS energy through collisions with particles of an isotropic MB gas. If the test particle has momentum p_2, its momentum distribution is described by equation (30), and the rate of change of the LS energy of the test particle is given through equations (10) and (38), after integrating over the delta function, as

$$\ell_t = \frac{1}{2}\frac{n_1 n_2 m_2^2 \mu_1' e^{b_1 E_2^o}}{m_1 K_2(\mu_1') p_2^o E_2^o} \int_1^\infty d\gamma_r \beta_r \gamma_r s^{1/2} \int_{m_j}^{\xi} dE^* \int_1^2 d\cos\psi^* \left(\frac{d^2\sigma^*}{dE^* d\cos\psi^*}\right)$$
$$\times \int_{\gamma_c^-}^{\gamma_c^+} d\gamma_c \gamma_c e^{-b_1 s^{1/2}\gamma_c} \left\{(E^* - E^*_{i,2}) + \beta_c \left[(p^* \cos\psi^* + p_i^*)\left(\frac{\gamma_c E^*_{i,2} - E_2^o}{\beta_c \gamma_c p_i^*}\right)\right]\right\}. \tag{40}$$

The subscript "t" again refers to the case of a test particle, and the maximum and minimum values of the cosine of the scattering angle in the C-system, $\cos\psi^*$, are denoted by 1 and 2, respectively, and $\gamma_c^{\pm} = (E_2^o E^*_{i,2} \pm p_2^o p^*_{i,2})/m_2^2$. The quantity $E^*_{i,2} = (p_i^{*2} + m_2^2)^{1/2}$ and is the energy of the test particle in the CM, noting, from equations (32b) and (39), that $E_2 = \gamma_c(E^*_{i,2} - \beta_c p_i^* u)$.

Specializing to energy changes of the test particle due to elastic scattering, equation (40) gives

$$\ell_{t,el} = -\frac{1}{2}\frac{n_1 n_2 e^{b_1 E_2^o}}{K_2(\mu_1')\, p_2^o E_2^o}\int_1^\infty d\gamma_r \beta_r \gamma_r \int_1^2 d(\cos\psi^*)(1+\cos\psi^*)\left(\frac{d\sigma^*}{d\cos\psi^*}\right)$$

$$\times\left[\Omega^-(E_2^o p_i^{*2} + m_2^2 E_{i,2}^*/b_1 s^{1/2}) - \Omega^+ p_2^o p_i^* E_{i,2}^*\right], \qquad (41)$$

where $\Omega^\pm = \exp(-b_1 s^{1/2}\gamma_c^-) \pm \exp(-b_1 s^{1/2}\gamma_c^+)$. The kinetic energy density e_k for the test particle is just $(E_2^o - m_2)/n_2$.

A simpler expression for the rate of change of LS energy can be derived by considering the interactions between two isotropic relativistic MB gases at different temperatures. The instantaneous LS energy loss rate of one of the gases, due to scattering from particles in the other gas, is given through equations (10) and (37) as

$$\ell_{MB} = \frac{1}{2}\frac{n_1 n_2 \mu_1' \mu_2'}{(1+\delta_{12})K_2(\mu_1')K_2(\mu_2')}\int_1^\infty d\gamma_r(\gamma_r^2-1)\int_{m_j}^\xi dE^* \int_1^2 d(\cos\psi^*)$$

$$\times\left(\frac{d^2\sigma^*(E^*,\cos\psi^*;\gamma_r)}{dE^*\, d\cos\psi^*}\right)$$

$$\times\int_1^\infty d\gamma_c(\gamma_c^2-1)^{1/2}\int_{-1}^1 du\, e^{-b_1E_1 - b_2E_2}\left[\gamma_c(E_i^* - E^*)\right. \qquad (42)$$

$$\left. + \beta_c\gamma_c(p_i^* - p^*\cos\psi^*)u\right] .$$

The Kronecker delta function accounts for the self-interacting case, and azimuthal symmetry is assumed in the scattering process.

Equation (42) can be simplified by recalling the definitions of E_1 and E_2 from equations (32) and employing the following substitutions: $\gamma_c = \mathrm{ch}\,\theta_1$; $(m_2\gamma_r + m_1)/s^{1/2} = \mathrm{ch}\,\theta_2$; $(m_1\gamma_r + m_2)/s^{1/2} = \mathrm{ch}\,\theta_2'$. It is then necessary to calculate a pair of two-fold integrals along the lines suggested for the calculation of the integral in equation (35). These are

$$I_1 = \int_0^\infty d\theta_1\, \mathrm{ch}\,\theta_1\, \mathrm{sh}^2\theta_1 \int_{-1}^{1} du\, e^{-\Xi} e^{-\Lambda u} \quad , \quad \text{and} \tag{43a}$$

$$I_2 = \int_0^\infty d\theta_1\, \mathrm{sh}^3\theta_1 \int_{-1}^{1} du\, u\, e^{-\Xi} e^{-\Lambda u} \quad , \tag{43b}$$

where $\Xi = \mathrm{ch}\theta_1(\mu_1'\,\mathrm{ch}\theta_2 - \mu_2'\,\mathrm{ch}\theta_2')$ and $\Lambda = \mathrm{sh}\theta_1(\mu_1'\,\mathrm{sh}\theta_2 - \mu_2'\,\mathrm{sh}\theta_2')$. Identifying $-\Xi \pm \Lambda$ with $-z^{1/2}\mathrm{ch}(\theta_1 \mp B)$, one finds that $\mathrm{sh}B = z^{-1/2}(\mu_1'\,\mathrm{sh}\theta_2 - \mu_2'\,\mathrm{sh}\theta_2')$. Using the integral representation for the Bessel functions and the recursion relation $K_{\nu+1}(x) - K_{\nu-1}(x) = 2\nu K_\nu(x)/x$ (Abramowitz and Stegun 1965), one obtains $I_1 = 2\mathrm{ch}B K_2(z^{1/2})/z^{1/2}$ and $I_2 = -2\mathrm{sh}B K_2(z^{1/2})/z^{1/2}$. Equation (42) becomes

$$\ell_{MB} = \frac{n_1 n_2 \mu_1'\mu_2'}{(1+\delta_{12})K_2(\mu_1')K_2(\mu_2')} \int_1^\infty d\gamma_r\,(\gamma_r^2-1)\frac{K_2(z^{1/2})}{z^{1/2}} \int_{m_j}^{\xi} dE^* \int_1^2 d(\cos\psi^*)$$

$$\times \left(\frac{d^2\sigma^*}{dE^*\, d\cos\psi^*}\right) [(E_i^* - E^*)\,\mathrm{ch}\,B - (p_i^* - p^*\cos\psi^*)\,\mathrm{sh}\,B] \,. \tag{44}$$

The hyperbolic functions are given explicitly by

$$\text{sh } B = m_1 m_2 \beta_r \gamma_r (b_1 - b_2)/(zs)^{1/2} \quad , \quad \text{and} \tag{45a}$$

$$\text{ch } B = (zs)^{-1/2}[(b_1 m_1^2 + b_2 m_2^2)^2 + 2\gamma_r m_1 m_2 (b_1 b_2 m_1^2 + b_1 b_2 m_2^2 + b_1^2 m_1^2 + b_2^2 m_2^2) + \gamma_r^2 m_1^2 m_2^2 (b_1 + b_2)^2]^{1/2} \quad . \tag{45b}$$

Though equation (44) is still rather complicated, it reduces in a number of cases. For example, if the scattering is elastic, $d^2\sigma^*/dE^* \, d\cos\psi^* \rightarrow \delta[E^* - E_i^*(\gamma_r)](d\sigma^*/d\cos\psi^*)$, and we recover the formula derived by Stepney (1983), namely

$$\ell_{MB} = \frac{m_1 m_2 n_1 n_2 \mu_1'^2 \mu_2'^2 (k_B T_1 - k_B T_2)}{(1+\delta_{12}) K_2(\mu_1') K_2(\mu_2')} \int_1^\infty d\gamma_t \, \frac{(\gamma_r^2 - 1)^2 K_2(z^{1/2})}{z \cdot s}$$

$$\times \int_1^2 d(\cos\psi^*) \left(\frac{d\sigma^*}{d\cos\psi^*}\right) (1 - \cos\psi^*) \quad . \tag{46}$$

If the gases are at the same temperature, then shB = 0 and chB = 1. Therefore

$$\ell_{MB} = \frac{n_1 n_2 \mu_1 \mu_2}{(1+\delta_{12}) K_2(\mu_1) K_2(\mu_2)} \int_1^\infty d\gamma_r \, \frac{(\gamma_r^2 - 1) K_2(bs^{1/2})}{bs^{1/2}} \int_{m_j}^{\xi} dE^* \left(\frac{d\sigma^*}{dE^*}\right)(E_i^* - E^*). \tag{47}$$

The second integral is simply $\epsilon^*(\gamma_r)\,\sigma(\gamma_r)$, defined in equation (27), because $E_i^* - E^* = E_0^*$, where E_0^* is the average energy of a

secondary created in an inelastic collision, so equation (47) properly reduces to the LS energy density loss rate -- the luminosity -- due to particle collisions of one isotropic MB gas with a second at the same temperature. The kinetic energy density of a relativistic MB gas is given by

$$e_k = 4\pi A \int_0^\infty dp\, p^2 (E - m) e^{-bE} = nm \left[\frac{3}{\mu} + \frac{K_1(\mu)}{K_2(\mu)} - 1 \right] \qquad (48)$$

which, with equation (44), permits the calculations of the energy loss timescales.

Calculations of the various timescales will be performed in the following chapter. Note that the energy loss timescales computed through equations (44) and (48) refer to the average energy loss for the entire distribution function whereas, in fact, one portion of the distribution may fall out of thermal form more rapidly than another. In this sense, Gould's treatment cited earlier is more accurate since it considers that portion of the distribution that would be first to fall out of equilibrium or last to be thermalized. This treatment does however have the advantage of applying to all temperatures, and particularly the important transrelativistic regime.

E. Compton Scattering

The process known as Compton scattering, in which a photon is scattered by an electron, is of considerable astrophysical

importance. Felten and Morrison (1966) calculate the diffuse X- and γ-ray background emission from the "inverse" Compton scattering of ambient low energy photons by the high energy cosmic ray electrons. Inverse Compton scattering is also proposed to explain the hard X-ray spectrum of Cygnus X-1 in a two-temperature accretion disk model (Shapiro, Lightman, and Eardley 1976). Numerical studies of the Comptonization of low energy photons by a cloud of relativistic electrons have been used to model emission from X-ray sources (Pozdnyakov, Sobol', and Syunyaev 1978; Sunyaev and Titarchuk 1980).

Jones (1965) derives an expression for the rate of change of energy of an electron Compton scattered by a monoenergetic photon gas, and applies the results to the energy loss rate from a Planckian distribution of photons. The exact spectrum of Compton scattered photons for an isotropic monoenergetic photon source is also calculated by Jones (1968); the complexity of the exact result renders it effectively useless except for the purpose of verifying limiting forms. Approximate expressions for the Compton power and the Compton scattered spectra in the Thomson and the extreme Klein-Nishina limit can be found in the review by Blumenthal and Gould (1970).

The purpose of this section is to briefly treat the Compton power in the regime appropriate to the problem of Compton scattering between a relativistic electron gas and an internally produced

photon source. The scattering oftentimes takes place intermediate to the Thomson and Klein-Nishina limits. Results will be applied to energy and momentum exchange rates between a relativistic photon and electron gas for the purpose, for example, of calculating the Compton-driven radiation forces which have been suggested as the mechanism for driving the jets observed in the vicinity of some galactic nuclei. Later uses of the formalism will be for the calculation of the average energy increase of a photon per Compton scattering due to an isotropic MB electron gas, in the manner of Lightman and Band (1981). An approximate Compton scattered spectrum can be calculated for such systems.

The formalism used in Sections B and C to derive equation (26) for calculating production spectra from interacting gases of particles can be modified to a photon-electron system. The boost transformation is now to the rest frame of the electron rather than to the CM of the two particles. Letting γ be the Lorentz factor of the electron in the LS and θ the angle between the photon and electron momenta in the LS, define

$$x = \gamma k (1 - \beta \cos \theta) , \tag{49}$$

where k is the photon energy measured in units of the electron rest mass. The quantity x is the dimensionless photon energy in the CM. If $x \ll 1$, we are in the Thomson limit, whereas if $x \gg 1$, the scattering is in the Klein-Nishina limit.

From equation (21), the spectrum of Compton scattered photons with energy E (also measured in units of the mass of the electron) due to a scattering characterized by the reaction parameters x, γ, and k is

$$\frac{d\sigma(E; x, \gamma, k)}{dE} = E \int_0^{2\pi} d\phi \int_{(\cos\psi)_{min}}^{1} d(\cos\psi)\, F_c^*(E^*, \cos\psi^*, x), \quad (50)$$

where E^* and $\cos\psi^*$ are given in terms of E, γ, and $\cos\psi$ through equations (18). The invariant Compton cross section is

$$F_c^*(E^*, \cos\psi^*, x) = (r_e^2/2)\frac{1}{E^*}\left(\frac{E^*}{x}\right)^2\left(\frac{x}{E^*} + \frac{E^*}{x} - 1 + \cos^2\psi^*\right) \times \delta\left[E^* - \frac{x}{1 + x(1 - \cos\psi^*)}\right] \quad (51)$$

(Jauch and Rohrlich 1976), where r_e is the classical radius of the electron.

Following procedures similar to those leading to equation (26), the Compton scattered spectrum becomes, after integrating over $\cos\phi$ in the delta function,

$$\frac{d\sigma(E; x, \gamma, k)}{dE} = \frac{r_e^2}{\theta\gamma x^2} \int_{\frac{x}{1+2x}}^{x} \frac{dE^*}{E^*} \frac{\left(\frac{E^*}{x} + \frac{x}{E^*} - 1 + z^2\right)}{[D^2 - (z - C)^2]^{1/2}}, \quad (52)$$

defining $z = 1/x + 1 - 1/E^*$, $C = uv$, and $D = (1-u^2)^{1/2}(1-v^2)^{1/2}$,

with $u = (k - \gamma x)/\beta\gamma x$ and $v = (E - \gamma E^*)/\beta\gamma E^*$. Integration of equation (52) is complicated by the appearance of E^* in v, but has been accomplished, with an additional integration over x from $\gamma k(1 - \beta)$ to $\gamma k(1 + \beta)$, corresponding to an isotropic monoenergetic photon distribution, in the paper by Jones (1968) just cited.

Now define

$$\langle E^n \sigma \rangle = \int_0^\infty dE\, E^n \frac{d\sigma(E; x, \gamma, k)}{dE} \tag{53}$$

as the n^{th} moment of the scattered spectrum. Thus, $\langle E^o \sigma \rangle = \sigma_C(x)$ is the exact Compton cross section, $\langle E^1 \sigma \rangle / \langle E^o \sigma \rangle$ defines the average energy of Compton scattered photons in a scattering process characterized by x, γ, and k, and so on. Substituting $d\sigma/dE$ from equation (52) into equation (53), and using the relation $E = \gamma E^*(1 + \beta v)$, we have

$$\langle E^n \sigma \rangle = \frac{r_e^2}{x^2} \int_{x/1+2x}^{x} dE^* (\gamma E^*)^n \left(\frac{E^*}{x} + \frac{x}{E^*} - 1 + z^2 \right) \int_{v^-(E^*)}^{v^+(E^*)} dv \frac{(1+\beta v)^n}{R} , \tag{54}$$

where $R = [(1 - u^2 - z^2) + 2vuz - v^2]^{1/2}$. The limits are given by $v^{\pm} = uz \mp (1 - u^2)^{1/2}(1 - z^2)^{1/2}$ from a consideration of the scattering process. Defining

$$I_i = \int_{v^-}^{v^+} \frac{dv\, v^i}{R} , \tag{55}$$

straightforward integration gives $I_0 = \pi$, $I_1 = uz\pi$, $I_2 = [3u^2z^2 + (1 - u^2 - z^2)]\pi/2$, etc. For $n = 0$, one obtains the Compton cross section

$$\langle E^0\sigma\rangle = \sigma_C(x) = \frac{\pi r_e^2}{x^2}\left[4 + \frac{2x^2(x+1)}{(1+2x)^2} + \frac{x^2 - 2x - 2}{x}\ell n\,(1+2x)\right]$$

$$\longrightarrow \begin{cases} \sigma_T\left(1 - 2x + \frac{26}{5}x^2 + \cdots\right), & x \ll 1, \text{ and} \\ \frac{\pi r_e^2}{x}\left[\ell n(2x) + 1/2\right], & x \gg 1, \end{cases} \tag{56}$$

reducing to the appropriate limiting values (Heitler 1954). The Thomson cross section $\sigma_T = 8\pi r_e^2/3$.

The first moment, the average scattered photon energy, is given through

$$\langle E\rangle = \langle E^1\sigma\rangle/\sigma_C(x) = [1 - \Gamma(x)]\left(\frac{\gamma x - k}{x}\right) + k\Gamma(x) \tag{57}$$

using the relation $k = \gamma x(1 + \beta u)$. The function $\Gamma(x)$ in equation (57) is defined as

$$\Gamma(x) = \frac{\pi r_e^2}{\sigma_C(x)}\left\{\frac{1}{3x^2}\left[\frac{8x^2 - 5x - 6}{1+2x} - \frac{x}{(1+2x)^3}\right] + \frac{\ell n\,(1+2x)}{x^3}\right\} \tag{58}$$

and has the limiting forms

$$\Gamma(x) \longrightarrow \begin{cases} 1 - x, & x \ll 1, \text{ and} \\ 4/3\,\ell n\,2x, & x \gg 1. \end{cases} \tag{59}$$

Since the initial photon energy is just k, the change in the photon energy due to Compton scattering is

$$\Delta E = \langle E \rangle - k = [1 - \Gamma(x)] \cdot (\gamma x - kx - k)/x \ . \qquad (60)$$

The integration over the variable x appropriate to an isotropic distribution of photons in order to determine the exact electron energy loss rate can be evaluated (Jones 1965). For the present purposes, it will be more useful to consider approximations based on the behavior of functions related to $\Gamma(x)$. The appropriate functions, namely $\sigma_C(x)/\sigma_T$, $\sigma_C(x)[1 - \Gamma(x)]/\sigma_T$, and $\sigma_C(x) \cdot \Gamma(x)/\sigma_T$ are shown in Figure 2.

The energy exchange rate due to Compton scattering between a photon and an electron gas is given by equations (10) and (60) as

$$\ell_{ph\text{-}el} = \frac{1}{2} \int dn_{ph}(\underset{\sim}{k}) \int dn_{el}(\underset{\sim}{p}) \int d(\cos\theta) \cdot \Delta E \cdot (1 - \beta \cos\theta) \cdot \sigma_C(x)$$

$$= 8\pi^2 m^3 A_{ph} A_{el} \int_0^\infty dk\, f_{ph}(k) \int_1^\infty d\gamma\ f_{el}(\gamma) \int_{\gamma k(1-\beta)}^{\gamma k(1+\beta)} dx\, \sigma_C(x)$$

$$\cdot [1 - \Gamma(x)](\gamma x - k - kx) \ , \qquad (61)$$

where the last expression applies to isotropic photon and electron gases. Equation (61) properly reduces when the scattering is in the Thomson and Klein-Nishina limits (Blumenthal and Gould 1970). From Figure 2, one sees that for x between about 0.05 and 300, $\sigma_C(x)[1 - \Gamma(x)]/\sigma_T$ is equal to about 0.07, within a factor of 2.

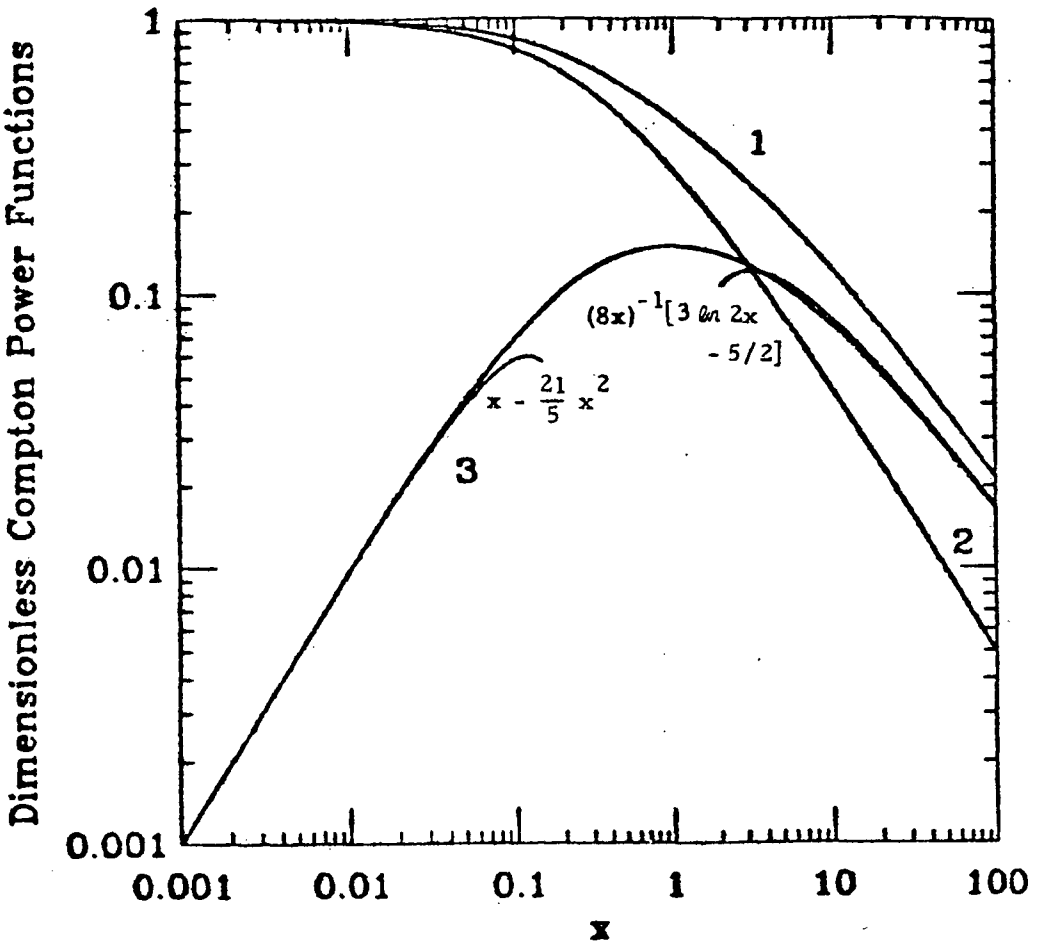

Figure 2. Associated Compton power functions. The dimensionless functions $\sigma_C(x)/\sigma_T$ (label 1), $\sigma_C(x)\cdot\Gamma(x)/\sigma_T$ (label 2), and $\sigma_C(x)\,[1 - \Gamma(x)]/\sigma_T$ (label 3) are graphed along with some approximating formulas. Functions are defined in the text.

Therefore the energy exchange rate is given approximately by

$$\ell_{\text{ph-el}} \approx 0.07\,\sigma_T \int dn_{\text{ph}}(\underset{\sim}{k}) \int dn_{\text{el}}(\underset{\sim}{p})(\beta^2\gamma - k)$$

$$= 0.07\,\sigma_T \left[n_{\text{ph}} \langle \beta^2\gamma \rangle - n_{\text{el}} \langle k \rangle\right] , \qquad (62)$$

the last expression referring to an isotropic distribution of photons and electrons. Here $\langle k \rangle$ is the average photon energy of the photon gas and $\langle \beta^2\gamma \rangle$ is the weighted value of $\beta^2\gamma$ over an isotropic electron distribution.

Equation (62) is adequate for calculating the energy exchange rate between a relativistic electron gas and a gas of photons with energy comparable to the rest mass energy of the electron. For example, given an electron MB plasma at about 0.5 MeV, the relative number of electrons with $\gamma \geqslant 10$ is insignificant ($\approx 0.35\%$). All photons with energies between about 25 keV and 8 MeV are covered in this approximation, and the Compton energy exchange rate is then approximately given by equation (62).

For $x \ll 1$, an expansion of equations (56) and (60) gives $x \cdot \sigma_C(x) \cdot \Delta E = \sigma_T(-1 + 21x/5) \cdot [x^2(k - \gamma) + kx]$. A calculation of the energy exchange rate gives

$$\ell_{\text{ph-el}} = \sigma_T \int dn_{\text{ph}}(\underset{\sim}{k}) \int dn_{\text{el}}(\underset{\sim}{p}) \left\{ k \left(\frac{4}{3}\beta^2\gamma^2\right) + k^2 \left[\gamma - \frac{16}{15}\beta^2\gamma + \frac{42}{5}\beta^2\gamma^3\right] - \frac{21}{5}k^3\gamma^2(1+\beta^2) \right\} , \qquad (63)$$

reducing in the case of Thomson scattering of low energy photons to the term linear in k (O'Dell 1981) and extending and correcting a higher order expansion (Calvani and Nobili 1982). To calculate the force on a relativistic plasma along the direction of the photon beam, a problem of interest in the study of relativistic jets (Cheng and O'Dell 1981), note that the momentum change along the direction of the photon momentum $\underset{\sim}{k}$ is $\Delta k = E\cos\chi - k$, where $\cos\chi = \cos\psi\cos\theta + \sin\psi\sin\theta\cos\phi$, with $\cos\theta = (\gamma k - x)/\beta\gamma k$ and $\cos\psi = (\gamma E - E^{*})/\beta\gamma E$. Calculating the rate of change of momentum in a manner similar to the earlier calculation for the rate of energy exchange gives

$$\left\langle \frac{\Delta k}{\Delta t} \right\rangle_{\text{ph-el}} = -k + \frac{\pi r_e^2}{x^2 \sigma_C(x)} \int_{\frac{x}{1+2x}}^{x} dE^{*} \cdot E^{*} \cdot [z \sin\theta \sin\theta' + \gamma \cos\theta (\beta + z\cos\theta')] \left(\frac{x}{E^{*}} + \frac{E^{*}}{x} - 1 + z^2 \right) , \tag{64}$$

and $\cos\theta' = (k - \gamma x)/\beta\gamma x$.

Higher order moments can be calculated from equation (54), although the algebra becomes increasingly tedious. An expansion in moments can be used to calculate approximate Compton scattered spectra. In Chapter V, we will use the approximation based on the average value of the photon energy after Compton scattering by a relativistic MB plasma to treat Comptonization.

III. APPLICATION TO PROCESSES IN A RELATIVISTIC PLASMA

A. Introduction

The principal use of this work is to calculate model spectra for astrophysical systems composed of relativistic plasmas. The most obvious example of such a system is a stable relativistic electron/ion gas. Because of pair and photon production mechanisms, a positron density will build to a steady-state value determined by the competition between pair production and pair annihilation. In addition to pair production from particle-particle collisions, photons will contribute to positron production through photon-particle and photon-photon pair creating processes.

In the absence of a magnetic field or an external photon source, the ambient photon density is a function of the optical depth $\tau = (n_+ + n_-)\sigma_{ph}(k)\, L \sim n_- \sigma_T L$, where L is a characteristic linear dimension of the system, so we should guess that the steady state positron density n_+ is a unique function of the temperature and the optical depth of the gas. The optical depth τ is technically a function of the sum of the electron and positron densities, but since positrons are produced conjointly with electrons, it is sufficient to identify $(n_+ + n_-)$ with $n = n_-$ for order-of-magnitude estimates of the various processes, as shown in Table 1. The characteristic linear dimension of the system is denoted by L, and the sum of all photon absorption or scattering cross sections $\sigma_{ph}(k)$, a function of the

Table 1. Principal Processes in a Relativistic Gas

Pair Producing Processes	Optically Thin ($\tau \ll 1$)	Optically Thick ($\tau \gg 1$) (Order of Process)
$ee \rightarrow eee^+e^-$	$\dot{n}_+ \sim \alpha^2 n t_C^{-1}$	α^2
$\gamma e \rightarrow ee^+e^-$	$\dot{n}_+ \sim \alpha^2 n \tau t_C^{-1}$	α
$\gamma\gamma \rightarrow e^+e^-$	$\dot{n}_+ \sim \alpha^2 n\tau^2 t_C^{-1}$	1
Photon Producing Processes		
$e^+e^- \rightarrow \gamma\gamma$	$n_{ph} \sim n_+\tau$	1
$ee \rightarrow ee\gamma$	$n_{ph} \sim \alpha n\tau$	α
$e\gamma \rightarrow e\gamma\gamma$	$n_{ph} \sim \alpha^2 n\tau^2$	α^2
Energy Changing Reactions		
$e\gamma \rightarrow e\gamma$	$n_{ph} \sim \alpha n\tau^2$	1
$\gamma\gamma \rightarrow \gamma\gamma$	$n_{ph} \sim \alpha^4 n\tau^3$	α^2
Thermalization Process		
$ee \rightarrow ee$	--	1

Note: The symbol "e" stands for particle, "γ" for photon, and $t_C^{-1} = n\sigma_T c$. The order of the process in the optically thick case is compared to $\sigma_T \sim r_e^2 = \alpha^2 \lambda\!\!\!^{-2}_C$, where $\lambda\!\!\!^{-}_C$ is the electron Compton wavelength.

photon energy k, is replaced by a value characteristic of the chief scattering process, namely the Thomson cross section for Compton scattering.

The dominance of the various processes depend on whether the gas is optically thick or thin, as indicated in Table 1. In the Table, all processes with four vertices or less in the Feynman diagram are included, excluding associated radiative processes which are in all cases of order α (= 1/137) smaller than the basic process (for example, $\gamma\gamma \rightarrow e^+e^-\gamma$ will always be dominated by $\gamma\gamma \rightarrow e^+e^-$, so may be neglected). However, the "double" Compton process $e\gamma \rightarrow e\gamma\gamma$ is retained, as it can be an important source of low energy photons.

In the extreme optically thick case, the plasma achieves its fully thermalized form with zero chemical potential for the photons, electrons, and positrons. In this event, the number densities of the three components are comparable in value, so that the dominant processes are determined by the lowest order Feynman diagram. Hence the most important processes are, beside the thermalization mechanisms, pair production through photon-photon interaction, electron-positron annihilation, and Compton scattering.

In the optically thin case, it is necessary to determine the relative importance of the various photon and positron production processes. As $\tau \rightarrow 0$, pair production through particle-particle

collisions is the dominant pair producing mechanism. The photon density $n_{ph} \sim n_1 n_2 R_{re} \langle t \rangle_{ph}$, where $R_{re}[cm^3/sec] \sim \alpha^i \sigma_T c$ is the reaction coefficient, i is the order of the process, and $\langle t \rangle_{ph} \sim L/c$ is the average photon residence time. Therefore the annihilation reaction $e^+ e^- \rightarrow \gamma\gamma$ and bremsstrahlung production of photons are of primary importance. If the optical depth is moderate ($\tau \geq \mathcal{O}(0.1)$), Compton scattering can also be significant, as can synchrotron emission, if a sufficiently strong magnetic field is present.

Thermalization processes are primary in both cases as they determine the character of the distribution. If they dominate all inelastic processes, the particles obtain a thermal form. The conditions under which a MB distribution can be assumed is treated in the last section of this chapter, and the remainder of the chapter is devoted to calculations of production rates and spectra on the basis of the formalism established in Chapter II, assuming that the particles achieve MB form. Also, opacities and absorption coefficients will be treated in Section D so that the proper photon density can be determined.

B. Electron-Positron Annihilation

The cross section for electron-positron annihilation in the frame of reference in which one of the particles is at rest and the other has Lorentz factor γ_r can be written as

$$\sigma_a(\gamma_r) = \frac{\pi r_e^2}{(\gamma_r+1)} \left[\left(\frac{\gamma_r^2 + 4\gamma_r + 1}{\gamma_r^2 - 1} \right) \ell n [\gamma_r + (\gamma_r^2 - 1)^{1/2}] - \frac{\gamma_r + 3}{(\gamma_r^2 - 1)^{1/2}} \right] \qquad (1)$$

(Jauch and Rohrlich 1976). The classical radius of the electron is denoted by r_e and the limiting forms of $\sigma_a(\gamma_r)$ are given by

$$\sigma_a(\gamma_r) \longrightarrow \pi r_e^2/\beta_r \quad , \quad \gamma_r - 1 \ll 1 \; ; \qquad (2a)$$

$$\sigma_a(\gamma_r) \longrightarrow \pi r_e^2 \left(\frac{\ell n\, 2\gamma_r - 1}{\gamma_r} \right) \quad , \quad \gamma_r \gg 1 \; . \qquad (2b)$$

As measured in the LS, the total energy released from a pair of particles with LS energies E_1 and E_2 before annihilation is, from equation (II-6),

$$\epsilon(\gamma_r, \gamma_c, u) = E_1 + E_2 = \gamma_c m_e [2(\gamma_r + 1)]^{1/2} \quad , \qquad (3)$$

where m_e is the electron mass. If the gas is at a temperature greater than about 10^6 K, annihilation proceeds primarily through the emission of two photons of equal energy in the CM of the annihilating particles (Crannell et al. 1976). Thus the energy liberated per photon as observed in the CM is

$$\epsilon^*(\gamma_r) = (m_e/2)[2(\gamma_r + 1)]^{1/2} \qquad (4)$$

since $s = 4m_e^2 \gamma^{*2} = 2m_e^2(\gamma_r + 1)$ and $E_0^* = m_e \gamma^*$, where γ^* is the electron (or positron) Lorentz factor in the CM.

Noting that the positron and electron masses are equal, though the particles are different, the reaction rate (II-16) becomes

$$r_a(\mu) = \frac{n_- n_+ \mu c}{K_2^2(\mu)} \int_1^\infty d\gamma_r (\gamma_r^2 - 1) \frac{K_1\{\mu[2(\gamma_r+1)]^{1/2}\}}{[2(\gamma_r+1)]^{1/2}} \sigma_a(\gamma_r) \quad , \tag{5}$$

defining $\mu = m_e/k_B T$ and letting $n_{-(+)}$ represent the electron (positron) density. Using equation (3) and the reasoning associated with equation (II-10), or equation (II-28) and (4), the luminosity is

$$\ell_a(\mu) = \frac{n_- n_+ \mu c}{K_2^2(\mu)} \int_1^\infty d\gamma_r (\gamma_r^2 - 1) K_2\{\mu[2(\gamma_r+1)]^{1/2}\} \sigma_a(\gamma_r) \quad . \tag{6}$$

The result for the production spectrum follows from equations (II-26) and (4), namely

$$S_a(k;\mu) = \frac{n_- n_+ \mu c}{K_2^2(\mu)} e^{-\mu\left(k + \frac{1}{2k}\right)} \int_1^\infty d\gamma_r (\gamma_r - 1) e^{-\mu\gamma_r/2k} \sigma_a(\gamma_r) \, , \tag{7}$$

where $k = E/m_e$, the dimensionless photon energy in units of the rest mass of the electron. (Equation [7] contains an additional factor of two because each annihilation yields two photons.)

The analytical expression (5) for the reaction rate is given in the work of Weaver (1976) and has been presented for the problem of the annihilation of electrons and positrons, together with the luminosity, in two papers by Svensson (1982, 1983). In the low temperature

($\mu > 1$) limit (though not so low that Coulomb corrections need be applied) and in the high temperature ($\mu < 1$) limit, agreement is found between approximations to the analytical results and the results of Zdziarski (1980) and the numerical work of Ramaty and Mészáros (1981) (though note a factor 2 error in Figures 2 and 3 of their paper).

An examination of the spectral emissivity (7) reveals that in the low temperature limit, the position of the peak of the emission as a function of temperature goes as $m_e(1 + 3/4\mu + 9/32\mu^2)$, retaining the quadratic term. A second order expansion gives $m_e(2/\mu)^{1/2} \cdot (1 + 3/4\mu)$ for the full width at half maximum (FWHM) in this limit. At high temperatures, equation (7) agrees with the expression derived by Svensson (1983) using detailed balance arguments. The spectral emissivity approaches

$$S_a(k;\mu) \longrightarrow n_- n_+ \mu^4 kc \left(\frac{\pi r_e^2}{2m}\right) e^{-\mu\left(k+\frac{1}{2k}\right)} \left[E_1\left(\frac{\mu}{2k}\right) - (1-\ell n\, 2)\, e^{-\mu/2k}\right] \tag{8}$$

for $\mu \ll 1$, where $E_1(y)$, the exponential integral function, is given by

$$E_1(y) = \int_y^\infty dt\; e^{-t} t^{-1} \longrightarrow -\gamma_E - \ell n\, y; \quad y \ll 1 \tag{9}$$

and $\gamma_E = 0.577...$ is Euler's constant. In the high temperature limit, the energy of the emission peak is also given by Svensson (1983) and the FWHM is given by $2\, u m_e/\mu\, (u^2 - u - 1)^{1/2}$, where

$u = 2 \ln (2/\mu) - \gamma_E$.

The behavior of the FWHM derived through second order expansions of the spectral emissivity about its peak reproduces the temperature dependence deduced in the numerical studies or in graphical representations of the approximations to the analytical results. It is, however, systematically 10-15% low in both limits, indicating that higher order terms are important. Thermal annihilation spectra at selected temperatures are shown in Figure 3. Note the broadening and blueshifting of the peak with increasing temperatures.

Equation (7) is used to describe the annihilation spectrum of a relativistic MB gas composed of electrons and positrons. In the extreme optically thick case, the proper distribution function is instead a Fermi-Dirac distribution, so equation (7) will not be appropriate for such a system. Ramaty and Mészáros, in the paper previously cited, also numerically calculate the production spectrum for a Fermi-Dirac distribution of electrons and positrons, and find that the reaction rates and peak positions are within 10% of the values for a MB distribution at temperatures less than 10^{10} K (≤ 0.85 MeV), with the greatest divergence of the spectral shape in the high frequency tail.

C. Bremsstrahlung

Bremsstrahlung is the principal photon producing mechanism in relativistic gases in the absence of a magnetic field. The object of this section is to present numerical calculations of the thermal

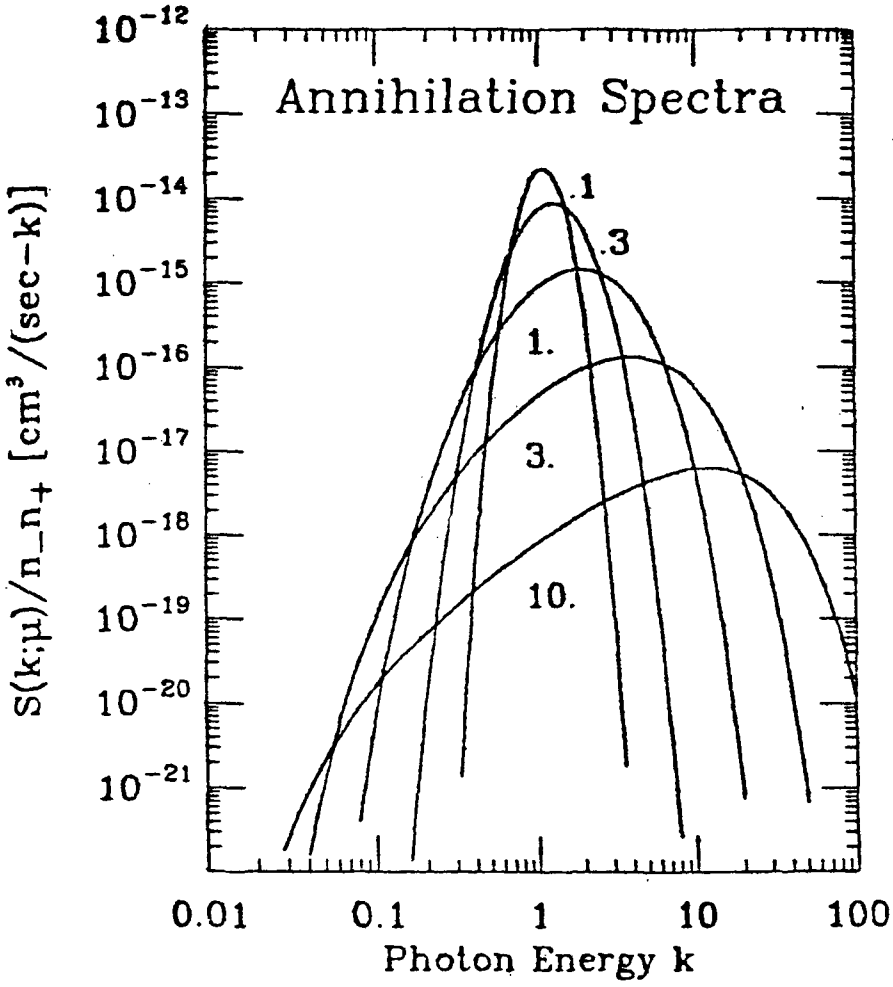

Figure 3. Thermal annihilation spectra. The thermal annihilation spectra from an electron-positron plasma are shown for temperatures $\mu^{-1} = k_B T/m_e = 0.1$, 0.3, 1, 3, and 10.

bremsstrahlung spectra for MB electron-ion (e-i), electron-electron (e-e), and electron-positron (e^+-e^-) gases. The positron-positron bremsstrahlung emission is equal to that of e-e bremsstrahlung, and the positron-ion bremsstrahlung is the same as e-i bremsstrahlung.

Except for the fact that the differential cross sections can be complicated, the calculation of thermal bremsstrahlung is straightforward. It is customary to present the results in terms of the thermal averaged Gaunt factor $g(k;\mu)$, where μ is the inverse temperature $m_e/k_B T$ and k, as before, is the dimensionless photon energy. The bremsstrahlung production spectrum $S(k)$, equation (II-26), is related to the Gaunt factor $g(k;\mu)$ through the relation

$$S(k) = \frac{2n_1 n_2 \alpha c \sigma_T}{k} \left(\frac{2\mu}{3\pi}\right)^{1/2} \exp(-\mu k)\, g(k;\mu) \quad . \tag{10}$$

For the case of e-i bremsstrahlung, the relevant differential cross section is the Bethe-Heitler (B-H) formula (Bethe and Heitler 1934; Jauch and Rohrlich 1976), which is the lowest order Born approximation result. Thermal e-i bremsstrahlung is of considerable astrophysical importance, and expressions for it at nonrelativistic temperatures (in terms of the Gaunt factor) can be found in the paper by Karzas and Latter (1961). Gould (1980, 1981a) calculates the high temperature, though subrelativistic, thermal e-i bremsstrahlung and Quigg (1967, 1968) calculates the same for extreme relativistic MB gases, both employing approximate forms of the B-H formula.

We calculate the thermal e-i bremsstrahlung using the exact B-H formula. It is interesting to note how the general formula, equation (II-26), reduces to a form that can be deduced through elementary considerations. The e-i thermal bremsstrahlung spectral emissivity is

$$S_{e\text{-}i}(k;\mu) = \frac{n_e n_i \mu \mu_i c}{2K_2(\mu)K_2(\mu_i)} \int_1^\infty \frac{d\gamma_r(\gamma_r^2 - 1)}{b[s(\gamma_r)]^{1/2}} \int_0^{\xi_{e\text{-}i}} \frac{dk'}{k'}$$

$$\cdot \frac{d\sigma_{B\text{-}H}(k', \gamma_r)}{dk'} \cdot e^{-b\gamma_c^-(k,k')[s(\gamma_r)]^{1/2}} , \qquad (11)$$

making some obvious notational changes. In equation (11), $s^{1/2}(\gamma_r) = (m_i^2 + m_e^2 + 2m_i m_e \gamma_r)^{1/2} \approx m_i + m_e \gamma_r$, $\xi_{e\text{-}i} = [s - (m_i + m_e)^2]/2s^{1/2} \approx m_e(\gamma_r - 1)$, $\gamma_c^- = (k'/k + k/k')/2$, and $d\sigma_{B\text{-}H}(k', \gamma_r)/dk'$ is the B-H formula (proportional to Z^2 for an ion of charge Z). Now $\mu_i = m_i/k_B T >> 1$ and $\mu = m_e/k_B T \sim \mathcal{O}(1)$, as the ion mass $m_i \gg m_e$ and $k_B T$. Thus $K_2(\mu_i) \to (\pi/2\mu_i)^{1/2} \exp(-\mu_i)$ and $bs^{1/2}(\gamma_r) \cong \mu_i + \mu\gamma_r$. Reversing the order of integration in equation (11) and noting, because of the large value of μ_i, that the exponential factor contributes to the value of the integral only in the immediate neighborhood of $k = k'$, we have

$$S_{e\text{-}i}(k;\mu) = \frac{n_e n_i \mu c}{K_2(\mu)} \int_{1+k}^\infty d\gamma_r(\gamma_r^2 - 1) e^{-\mu\gamma_r} \frac{d\sigma_{B\text{-}H}(k, \gamma_r)}{dk} . \qquad (12)$$

Equation (12) can be immediately derived by assuming that the protons are at rest in the LS, as advertised. Defining

$$\frac{\alpha r_e^2 Z^2}{k} f_{B-H}(k; \gamma_r) = \frac{d\sigma_{B-H}(k, \gamma_r)}{dk} \tag{13}$$

equations (10) and (12) give

$$g_{e-i}(k;\mu) = \frac{3}{16}\left(\frac{3\mu}{2\pi}\right)^{1/2} \frac{Z^2 c}{K_2(\mu)} e^{\mu k} \int_{1+k}^{\infty} d\gamma_r (\gamma_r^2 - 1) e^{-\mu\gamma_r} f_{B-H}(k, \gamma_r). \tag{14}$$

Values of the Gaunt factor for thermal e-i bremsstrahlung are shown in Figure 4a at selected temperatures.

The calculations of the production spectra for thermal e-e and e^+-e^- bremsstrahlung are much more difficult because of the extreme complexity of the cross sections. The e-e bremsstrahlung cross sections is given to lowest order by Haug (1975a) in terms of the cross section differential in the energy and the angle of the outgoing photon. He also (Haug 1975b) calculates thermal e-e bremsstrahlung at 100 keV. The cross section for electron-positron bremsstrahlung is evaluated by Swanson (1968), to lowest order. It requires two integrations over the angular distributions of the outgoing particles and an additional integration over the angular distribution of the produced photon to get it in a form suitable for equation (II-26).

Defining, in accordance with equation (13),

Figure 4. Gaunt factors for bremsstrahlung from relativistic thermal plasma. The Gaunt factors are given as a function of μk, where $\mu^{-1} = \Theta = k_B T/m_e$ is the dimensionless temperature and k is the photon energy in units of the electron rest mass energy, for values of the parameter $\Theta = 0.1, 0.3, 1, 3$, and 10. The Gaunt factors for thermal e-p bremsstrahlung, g_{e-p}, are shown in Figure 4a, and the Gaunt factors for thermal e-e bremsstrahlung, g_{e-e}, are shown in Figure 4b by the solid lines. The values of $g_{e^+-e^-}/2$, where $g_{e^+-e^-}$ is the Gaunt factor for thermal e^+e^- bremsstrahlung, are shown by the dashed lines in Figure 4b. At $\Theta \geq 1$, $g_{e^+-e^-} = 2g_{e-e}$ to the limit of accuracy of the integrations in the approximation used (see Appendix), over the range depicted.

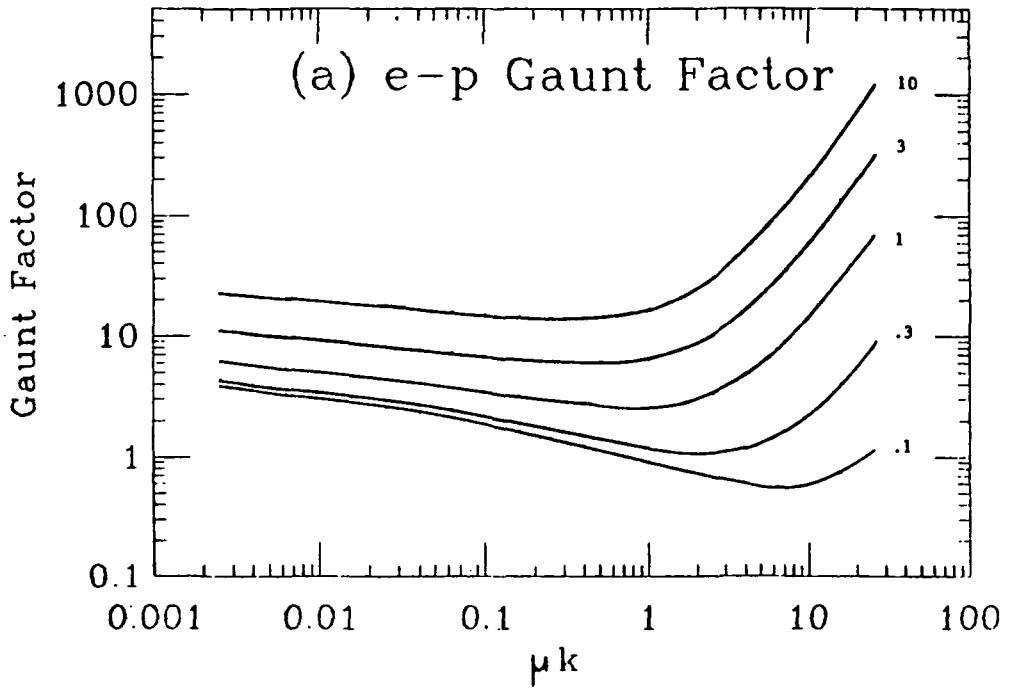
(a) e−p Gaunt Factor
Gaunt Factor
1000
100
10
1
0.1
0.001
0.01
0.1
1
10
100
μk
10
3
1
.3
.1

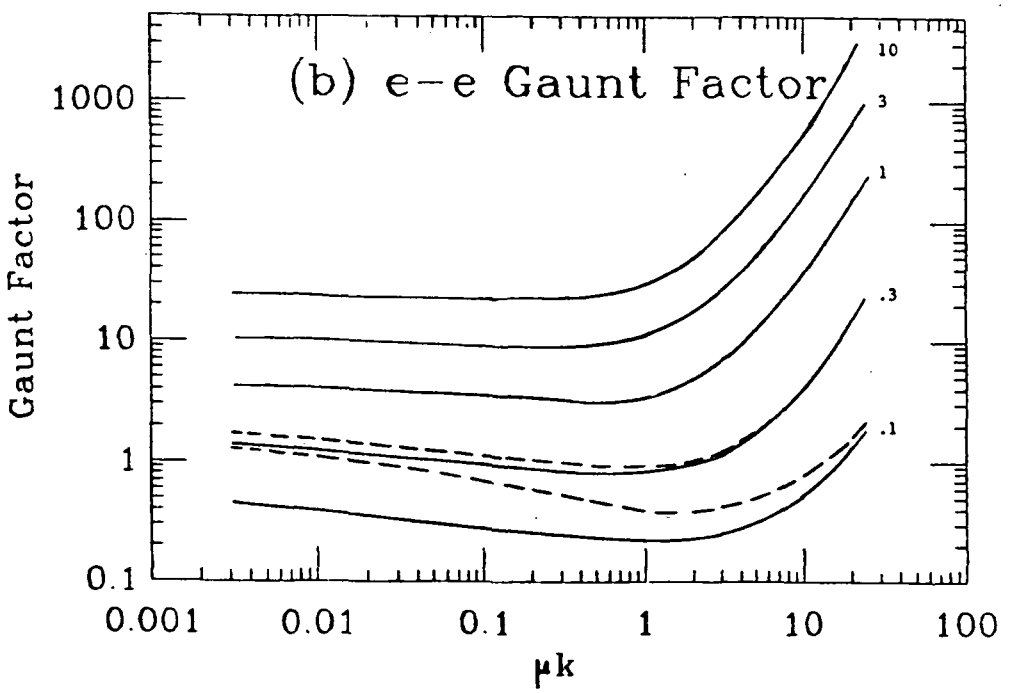
(b) e−e Gaunt Factor
Gaunt Factor
1000
100
10
1
0.1
0.001
0.01
0.1
1
10
100
μk
10
3
1
.3
.1

$$\frac{\alpha r_e^2}{k} f_{ee}(k, \gamma_r) = \frac{d\sigma_{ee}(k, \gamma_r)}{dk} , \tag{15}$$

equations (II-26), (10), and (15) give

$$g_{ee}(k; \mu) = \left(\frac{3\mu}{2\pi}\right)^{1/2} \cdot \frac{3k}{32(1+\delta_{12})} \cdot \frac{e^{\mu k}}{K_2^2(\mu)} \int_1^\infty d\gamma_r \frac{(\gamma_r^2 - 1)}{[2(\gamma_r + 1)]^{1/2}}$$

$$\times \int_0^{\xi_{ee}} \frac{dk'}{k'^2} f_{ee}(k', \gamma_r) \exp\left[-\mu \left(\frac{\gamma_r + 1}{2}\right)^{1/2} \left(\frac{k'}{k} + \frac{k}{k'}\right)\right] , \tag{16}$$

where $\xi_{ee} = (\gamma_r - 1)/[2(\gamma_r + 1]^{1/2}$ and δ_{12} equals 1 for e-e bremsstrahlung and 0 for e^+-e^- bremsstrahlung.

Thermal e-e bremsstrahlung has recently been calculated (Stepney and Guilbert 1983), and agreement is found with this calculation. The Gaunt factors are given, for various temperatures, by the solid line in Figure 4b. Thermal e^+-e^- bremsstrahlung has not been previously calculated. The calculation is performed in an approximate fashion, as described in the Appendix. The Gaunt factors for this process are shown in Figure 4b by the dashed lines.

In terms of the function $f(k, \gamma_r)$ defined for the three types of bremsstrahlung, the luminosity is given by equations (II-27) and (II-28) as

$$\ell = \frac{n_1 n_2 \mu_1 \mu_2 \alpha r_e^2 Z^2 c}{(1+\delta_{12}) K_2(\mu_1) K_2(\mu_2)} \int_1^\infty d\gamma_r \frac{(\gamma_r^2 - 1) K_2\{b[s(\gamma_r)]^{1/2}\}}{\{b[s(\gamma_r)]^{1/2}\}} \int_0^\xi dk' f(k', \gamma_r). \tag{17}$$

Alternately, it can be determined from an integration over the dimensionless energy k, weighted by k, in the production spectrum (10). Calculations of the luminosity are useful for the evaluation of energy loss timescales in Section F.

D. Absorption and Pair Production

In this section, the connection is drawn between the absorption coefficient and the reaction rate for a particle or photon traversing a relativistic particle/photon plasma. Application to sources of opacity such as Compton scattering and pair production are made. At sufficiently low photon energies, bremsstrahlung absorption can also be important, and is also considered.

The treatment will be brief, as much of the information can be found in other papers dealing with the subject, for example, Lightman and Band (1981), Lightman (1982), Gould (1982a), Svensson (1982), Zdziarski (1982), and Stepney and Guilbert (1983).

1. Opacity Considerations

The absorption coefficient for a particle or photon of momentum $\underset{\sim}{p}_2$ passing through an isotropic particle or photon gas described by the differential momentum distribution $dn_1(\underset{\sim}{p}_1)$ is just the probability for scattering (or absorption, as in a pair production process) per unit path length. Designate the absorption coefficient by $\kappa(\underset{\sim}{p}_2)$. Then

$$\kappa(\underset{\sim}{p}_2) = \iint dn_1(\underset{\sim}{p}_1)\, d\sigma \cdot \beta_r \cdot (1 - \underset{\sim}{\beta}_1 \cdot \underset{\sim}{\beta}_2) \quad . \tag{18}$$

This is related to the reaction rate r, equation (II-1), through

$$r = c(1 + \delta_{12})^{-1} \int dn_2(\underset{\sim}{p}_2)\, \kappa(\underset{\sim}{p}_2) \quad . \tag{19}$$

Now introduce the invariant quantity $q^2 = \pi_1 \cdot \pi_2 = E_1 E_2 - p_1 p_2 \cos\theta$, in analogy to the earlier use of γ_r, defined in equation (II-5). The utility of q^2 over γ_r is that problems associated with massless particles (i.e., photons) are thereby avoided. For a particle or photon of momentum p_2 traversing an isotropic gas of photons, electrons, positrons, and ions, each with distribution function described through equation (II-4), equation (18) becomes

$$\kappa(p_2) = \frac{2\pi A_1}{p_2 E_2} \int_{m_1}^{\infty} dE_1\, f_1(E_1) \int_{E_1E_2 - p_1p_2}^{E_1E_2 + p_1p_2} d(q^2)\, \sigma(q^2)(q^4 - m_1^2 m_2^2)^{1/2} \quad . \tag{20}$$

Equation (20) can also be written as an integral over E_1,

$$\kappa(p_2) = \frac{2\pi A_1}{p_2 E_2} \int_{m_1 m_2}^{\infty} d(q^2)\, \sigma(q^2)(q^4 - m_1^2 m_2^2)^{1/2} \int_{E_1^-}^{E_1^+} dE_1\, f_1(p_1(E_1)) \quad , \tag{21}$$

where

$$E_1^{\pm} = [E_2 q^2 \pm p_2 (q^4 - m_1^2 m_2^2)^{1/2}]/m_2^2 \quad . \tag{22}$$

As an illustration, consider the "absorption" coefficient in particle-particle scattering, when the particle of momentum p_2

traverses a relativistic MB distribution of particles described by equations (II-13) and (II-14). It is elementary to show that in this case, $\kappa(p_2) = c r_t(p_2)$, where $r_t(p_2)$ is the individual test particle reaction rate given in equation (II-33).

Evaluating equation (21) in the limit $m_2 \to 0$, that is, for a photon traversing a MB gas, one obtains, defining $k = p_2/m_e$,

$$\kappa_{\gamma\text{-par}}(k) = \frac{n_{par}}{2k^2 K_2(\mu)} \int_{k'_{thr}}^{\infty} dk'\, k'\, \sigma_{\gamma\text{-par}}(k') \exp\left[-\frac{\mu}{2}\left(\frac{k'}{k} + \frac{k}{k'}\right)\right] , \quad (23)$$

The quantity k' represents the photon energy in the rest frame of the particle, and k'_{thr} is the threshold energy of the process. For the Compton scattering opacity, $\sigma(k') \to \sigma_C(k')$ given by equation (II-56), and $k'_{thr} = 0$. For low photon energies ($k\mu \ll 1$), the opacity is

$$\kappa_C(k) = (n_+ + n_-)\sigma_T \left[1 - 2k \frac{K_3(\mu)}{K_2(\mu)} + \frac{26}{5} k^2 \frac{K_4(\mu)}{K_2(\mu)} + \cdots\right] . \quad (24a)$$

In the Klein-Nishina limit, that is, for $k/\mu \gg 1$, we find

$$\kappa_C(k) = \frac{(n_+ + n_-)\pi r_e^2}{k K_2(\mu)} \left\{K_1(\mu)\left[\ell n(2k) + \frac{1}{2}\right] + \int_0^{\infty} dx\, x\, \mathrm{sh}x \exp(-\mu \mathrm{ch}x)\right\} , \quad (24b)$$

reducing to the result of Gould (1982a) in the high temperature ($\mu \ll 1$) limit. The cross section for pair production through photon-particle reactions, which also contributes to the opacity, is given below.

For the process $\gamma\gamma \rightarrow e^+e^-$, the absorption coefficient for photon-photon scattering is

$$\kappa_{\gamma-\gamma}(k) = \frac{\pi r_e^2}{k^2} (4\pi A_\gamma) \int_{1/k}^{\infty} dk' \, f_\gamma(k') \, \bar{\varphi}(k' \cdot k) \ , \tag{25}$$

using equation (20). Equation (25) is written in terms of the function $\bar{\varphi}(k' \cdot k)$ defined by Gould and Schréder (1967). The number density of an isotropic photon source is, from equation (II-4)

$$n_\gamma = 4\pi A_\gamma \int_0^{\infty} dk' \, k'^2 \, f_\gamma(k') \ . \tag{26}$$

2. Particle-Particle Pair Production

The cross section for electron-positron pair production in particle collisions has been computed by the "equivalent-photon" method at extremely high energies (Bhabha 1935a, b; Williams 1935) and through the methods of quantum electrodynamics (Baier and Fadin 1971). The review of Budnev et al. (1975) summarizes the results of these and other calculations. For the process $ee \rightarrow eee^+e^-$ and $ei \rightarrow eie^+e^-$, the pair production cross section is given by

$$\sigma_{pp}(\gamma_r) = \frac{28}{27\pi} Z_1 Z_2 \alpha^2 r_e^2 \left[\ell n^3(2\gamma_r) - \left(\frac{178}{28}\right) \ell n^2(2\gamma_r) + B \, \ell n(2\gamma_r) + C \right] \ , \tag{27}$$

for $\gamma \geq 100$. The charges of the colliding particles are Z_1 and Z_2. For the ee reaction, the threshold Lorentz factor $\gamma_r^{thr} = 7$, $B = -11$, and $C \sim 100$. For the ep reaction, $\gamma_r^{thr} = 3$, $B = 2.6$, and

$C \sim 40$. Unfortunately there are no calculations or experimental data for pair production near threshold for these two reactions.

The cross section for pair production in the collision of two heavy charged particles is reduced by a factor of the order of the ratio of the electron and proton masses, so has insignificant effects in relativistic electron plasmas.

3. Photon-Particle Pair Production

The cross section for the process $\gamma e \rightarrow e e^+ e^-$, with threshold $k_{thr} = 4$, has been calculated by Haug (1975a). He provides the following fit, accurate to better than 0.3%, for the cross section (Haug 1981):

$$\frac{\sigma_{\gamma e}(k)}{\alpha r_e^2} = [5.6 + 20.4(k-4) - 10.9(k-4)^2 - 3.6(k-4)^3 + 7.4(k-4)^4] \times 10^{-3}(k-4)^2, \qquad 4 \le k \le 4.6;$$

$$= 0.582814 - 0.29842k + 0.04354k^2 - 0.0012977k^3, \qquad 4.6 \le k \le 6.0; \qquad (28)$$

$$= \frac{3.1247 - 1.3394k + 0.14612k^2}{1 + 0.4648k + 0.016683k^2}, \qquad 6 \le k \le 18;$$

$$= \frac{28}{9}\ln 2k - \frac{218}{27} + \frac{1}{k}\left[-\frac{4}{3}\ln^3 2k + 3.863\ln^2 2k - 11\ln 2k + 27.9\right], \qquad k \ge 14.$$

A fit to the cross section for pair production in photon-proton scattering is given by Stepney and Guilbert (1983), accurate to 0.1%.

Defining $\epsilon = (k^2 - 4)^{1/2}/k$, the fit is:

$$\frac{\sigma_{\gamma p}(k)}{\sigma_T} = \alpha \frac{\epsilon^6}{32} (1 + 0.875\epsilon^2 + 0.755\epsilon^4 + 0.661\epsilon^6 + 0.589\epsilon^8) ,$$

$$2 \le k \le 2.4 ;$$

$$= (7.620 - 8.0218k + 2.520k^2 - 0.2047k^3) \times 10^{-4} , \qquad (29)$$

$$2.4 \le k \le 4.0 ;$$

$$= \frac{7\alpha}{6\pi} (\ell n\, 2k - 109/42) + (473.65 + 241.26\, \ell n\, 2k - 81.151\, \ell n^2 2k$$

$$+ 5.3814\, \ell n^3 2k) \times 10^{-5}/k , \qquad k \ge 4.0$$

The threshold for the process is 2.

The rate of pair production due to photon-particle collisions in a relativistic MB gas can be found from equations (19) and (23). The rate is

$$r_{\gamma\text{-par}} = 4\pi A_\gamma c \int_0^\infty dk\, k^2 f_\gamma(k) \kappa_{\gamma\text{-par}}(k) \qquad (30)$$

(Gould 1971; Weaver 1976).

4. Photon-Photon Pair Production

The absorption coefficient for this process is given by equation (25). From equation (19), the pair production rate is

$$r_{\gamma\text{-}\gamma} = (c\pi r_e^2) \frac{16\pi^2 A_{\gamma_1} A_{\gamma_2}}{1 + \delta_{12}} \int_0^\infty dk\, f_{\gamma_2}(k) \int_{1/k}^\infty dk'\, f_{\gamma_1}(k') \bar{\varphi}(k \cdot k') . \qquad (31)$$

The Kronecker delta function corrects for double counting if self-interacting photon distributions are being considered.

5. Bremsstrahlung Absorption

Both bremsstrahlung (free-free) absorption and synchrotron self-absorption can be effective sources of photon opacity at sufficiently low photon energies and, for the latter case, high magnetic fields. From Kirchhoff's law, the bremsstrahlung absorption coefficient $\kappa_b(k;\mu)$ for a photon of energy k traversing an isotropic relativistic MB gas is

$$\kappa_b = \frac{\pi^2 \lambda_C^3}{ck^2} (e^{\mu k} - 1)\, S(k) \quad , \tag{32}$$

where λ_C is the electron Compton wavelength $\hbar/m_e c$ ($r_e = \alpha \lambda_C$). Equation (32) can be written in terms of the Gaunt factor through equation (10). Because of the slowly-varying logarithmic dependence of the Gaunt factor at low frequencies, the principle behavior of κ_b goes as k^{-2} as $k \to 0$.

Inserting numerical values for κ_b, it is readily seen that for an optically thin relativistic MB gas, bremsstrahlung absorption is only effective for extremely low photon energies ($k \lesssim \mathcal{O}[10^{-10}]$ for $n_p \sim 10^{10}$ cm^3)(Lightman and Band 1981). The synchrotron self-absorption coefficient $\kappa_s(k;\mu)$ for an extreme relativistic magnetoactive MB plasma has been treated by Jones and Hardee (1979), though note Gould's (1982a) correction.

E. Particle Production in Relativistic Nucleonic Plasmas

The inner region of an accretion disk surrounding a black hole has been proposed as a site of relativistic nucleonic plasmas, with temperatures in the range $0.01 \leq \Theta_p = k_B T/m_p \leq 1$ (Lightman, Shapiro, and Rees 1975). At these temperatures, pion-producing reactions from nucleon-nucleon collisions would be a source of energy loss and luminosity. Elements of such a system could only have a transient existence; otherwise pair production processes would conspire to transform the kinetic energy of the relativistic nuclei into an optically thick plasma of electron-positron pairs and photons (Bisnovatyi-Kogan, Zel'dovich, and Sunyaev 1971).

The object of this section is to compile the experimental data required to calculate the magnitude of secondary particle production in accretion phenomena. We consider only plasmas composed of protons. The effects of heavier nuclei can be accounted for in an approximate way by employing a multiplicative correction factor (Orth and Buffington 1976).

One might think that the cross section and production data would be readily available from cosmic ray studies. In fact most calculations of secondary production by cosmic rays in the past 10 years have depended upon high energy data, where scaling laws are supposed to apply. It is the cross section values near threshold and at intermediate energies (laboratory proton kinetic energies $E_k \approx$

1-10 GeV) that are most important for secondary particle production in accretion disks. Actually, these are also the most important energies for the production of the bulk of the secondary particles in cosmic ray interactions in the galaxy, but the scarcity of data and the promise of simple functional forms for the production cross sections at ISR energies have led workers to give more attention to the highest energy data.*

In addition, contrary to published assertions (Kolykhalov and Syunyaev 1979; Stephens and Badhwar (1981), some information on the momentum and energy distributions of secondary pions produced in proton-proton collisions at intermediate energies does exist. In Table 2 is tabulated all data between threshold and ISR energies which are concluded to have value as regards the production cross sections or the CM momentum or energy distributions of the produced pions in proton-proton collisions. Numerical fits are evaluated for the pion-producing processes and are given below. Secondary K mesons, and Λ and Σ baryons are neglected in this study, as they contribute at most 10% (by particle number) due to the small relative cross sections and large threshold energies.

Distinguish four channels of pion production: $pp \rightarrow \pi^+ d$, $pp \rightarrow \pi^+ X$, $pp \rightarrow \pi^o X$, and $pp \rightarrow \pi^- X$. The X refers to inclusive

---

*For example, Stephens and Badhwar (1981) show that 50% of all π^o's produced in the galaxy come from cosmic rays with $E_k \leq 2.5$ GeV.

production (Section II. C) except in the case $pp \rightarrow \pi^+ X$, where it is understood that the contribution from the channel $pp \rightarrow \pi^+ d$ is excluded, d standing for a deuteron. For energies near threshold, the cross section for pion production is described by the Mandelstam model (for a general reference, see Lock and Measday 1970). At the highest energies, the inclusive cross section, denoted by $\sigma_{\pi X}$ for the process $pp \rightarrow \pi X$, can be shown to have the form $\sigma_{\pi X} = A + C \ln s$ as $s \rightarrow \infty$, from elementary considerations of the scaling hypothesis. In this expression, s, defined earlier, is the sum of the four-momenta of the two colliding particles: $s = 2m_p(E_k + 2m_p)$, where E_k is the kinetic energy of one proton when the other is at rest. Based on considerations of the fragmentation model of the production process, it is proposed in reference 25 to add the term $Bs^{-1/2}$. Since $s \sim 2m_p p_\ell$ at these energies, where p_ℓ is the momentum of one of the colliding particles in the frame of reference in which the other is at rest, the high energy functional form is taken to be $\sigma_{\pi X}(\text{mb}) = A + Bp_\ell^{-1/2} + C \ln p_\ell$. The coefficients A, B, and C are determined by minimizing the vertical variance of the fit with respect to the experimental cross sections. All momenta and energies have units of GeV, and the fits intermediate to the threshold and high energy regimes have no theoretical basis.

Threshold laboratory kinetic energies for the four processes are $E_{k,thr}^{\pi^+ d} = 0.288$, $E_{k,thr}^{\pi^+ X} = 0.292$, $E_{k,thr}^{\pi^o X} = 0.280$, and $E_{k,thr}^{\pi^- X} =$

0.600. The respective values of $\overline{m}_X$ (Section II.C) are m_d, $m_p + m_n$, $2m_p$, and $2m_p + m_{\pi^+}$. The quantity η is defined as

$$\eta = \frac{p^*_{max}}{m_\pi} = \frac{[(s - m_\pi^2 - \overline{m}_x^2) - 4m_\pi^2 \overline{m}_x^2]^{1/2}}{2m_\pi s^{1/2}} , \qquad (34)$$

where m_π is the mass of the produced pion for the channel under consideration ($m_{\pi^\pm} = 0.1396$, $m_{\pi^0} = 0.135$), and p^*_{max} is the maximum pion CM momentum. Then the following fits are valid from threshold to the highest accelerator energies, within the accuracy of the experimental data:

$$\sigma_{\pi^+ d}(\text{mb}) = \begin{cases} 0.18\eta + 0.95\eta^3 - 0.016\eta^9 , & E^{\pi^+ d}_{k,\,thr} \le E_k < 0.65 \\ 0.56\, E_k^{-3.9} , & 0.65 \le E_k < 1.43 \\ 0.34\, E_k^{-2.5} , & 1.43 \le E_k ; \end{cases} \qquad (35)$$

$$\sigma_{\pi^+ X}(\text{mb}) = \begin{cases} 0.95\eta^4 + 0.099\eta^6 + 0.204\eta^8, & p^{\pi^+ X}_{1,\,thr} \le p_1 < 0.954 \\ 0.67\,\eta^{4.7} + 0.3 , & 0.954 \le p_1 < 1.29 \\ 22.0(p_1 - 1.27)^{0.15} , & 1.29 \le p_1 < 2.81 \\ -40.9 + 57.9\, p_1^{-1/2} + 27.0 \ln p_1, & 2.81 \le p_1 ; \end{cases} \qquad (36)$$

$$\sigma_{\pi^o X}(\text{mb}) = \begin{cases} 0.032\eta^2 + 0.040\eta^6 + 0.047\eta^8, & p_{1,\text{thr}}^{\pi^o X} \le p_1 < 0.954 \\ 32.6(p_1 - 0.8)^{3.21}, & 0.954 \le p_1 < 1.29 \\ 5.4(p_1 - 0.8)^{0.81}, & 1.29 \le p_1 < 5.32 \\ -59.5 + 48.5\, p_1^{-1/2} + 32.0 \ln p_1, & 5.52 \le p_1 ; \end{cases} \tag{37}$$

$$\sigma_{\pi^- X}(\text{mb}) = \begin{cases} 2.33(p_1 - 1.65)^{1.2}, & 1.65 \le p_1 < 2.81 \\ 0.32\, p_1^{2.1}, & 2.81 \le p_1 < 5.52 \\ -69.3 + 74.2\, p_1^{-1/2} + 28.2 \ln p_1, & 5.52 \le p_1 . \end{cases} \tag{38}$$

The experimental data for the latter three channels of pion production, together with the fits, are shown in Figure 5.

From the fits (35) - (38), we can calculate the reaction coefficient $R = r/n_p^2$, where n_p is the proton density and r is the relativistic reaction rate (II-16). The results are shown in Figure 6 as a function of the dimensionless temperature Θ_p. For $\Theta_p \ll 1$, the reaction coefficient is a factor of two smaller than found in two previous calculations (Weaver 1976; Kolykhalov and Syunyaev 1979). The correctness of the present calculation was verified by using the cross section for π^o production given in the latter paper, confirming their factor-of-two error.

To evaluate the luminosity and production spectrum from a relativistic MB plasma of protons, it is only necessary to have the

Table 2. Compilation of Pion Production Cross Sections in Proton-Proton Collisions

Ref.	1	2	3	4′	5	5	6	7′	8
p_L	0.800-1.30	0.897-1.01	1.06-1.29	1.17	1.16	1.29	1.29	1.28	1.38
σ_0	*	*		0.91 ± 0.15	1.2 ± 0.3	3.4 ± 0.4		3.0 ± 0.3	3.46 ± 0.25
σ_+		*	*	5.21 ± 0.44	5.0 ± 1.0	10.2 ± 1.2	13.1 ± 1.2	10.8 ± 0.5	
σ_-									

Ref.	9′	10′†	11′	12′†	13′†	14′†	16′	17	18′
p_L	1.475	1.66	1.66	2.23	2.81	3.68	3.68	5.52	12.0
σ_0		3.7 ± 0.3	4.3 ± 0.1	7.74 ± 0.4	9.35 ± 0.4			19.2 ± 1	35.2 ± 2.4
σ_+	17 ± 3	18.3 ± 0.7	16.4 ± 1.5	22.2 ± 0.8	23.4 ± 0.6		24.6 ± 1	29.9 ± 1.5	42.7 ± 0.7
σ		0.01 ± 0.01		1.275 ± 0.2	2.99 ± 0.2	4.64 ± 0.2		11.5 ± 1	21.1 ± 0.4

Ref.	19	20	18′	21**	21**	21**	21**	22**	22**
p_L	12.4	19.0	24.0	69	100	205	303	69	102
σ_0	31.6 ± 2.6	41.6 ± 3	53.5 ± 5.1					80.5 ± 3	85 ± 8
σ_+		47.5 ± 3	56.8 ± 0.9	78.5 ± 1.3	91.8 ± 9.2	108 ± 11	125 ± 13		
σ_-		29.7 ± 3	33.8 ± 0.6	57.5 ± 0.6	66.9 ± 1.3	86 ± 2	99.5 ± 3		

Ref.	22**	22**	22**	22**	23	24	25′′	25′′	25′′	25′′
p_L	205	500	1100	1500	303	405	270	500	1100	1500
σ_0	107 ± 7	139 ± 11	158 ± 24	169 ± 24	138 ± 10	159.3±16.8				
σ_+							114	129	148	158
σ_-							95.4	110	129	138

*Reference gives several cross section values.

′Contains CM energy or momentum distribution data of produced pions.

† Values given include renormalization of cross section from Ref. 15.

**Values taken from compilation of cross sections.

′′Assessed errors for cross sections: ±10%.

References for Table 2:

1. Dunaitsev, A. F. and Pokoshkin, Iu. D. 1959, JETP, 9, 1179.

2. Fields, T. H., Fox, J. G., Kane, J. A., Stallwood, R. A., and Sutton, R. B. 1958, Phys. Rev., 109, 1713; Stallwood, R. A., Sutton, R. B., Fields, T. H., Fox, J. G., and Kane, J. A. 1958, Phys. Rev., 109, 1716.

3. Neganov, B. S. and Savchenko, O. V. 1957, JETP, 5, 1033.

4. Baldoni, B. et al. 1962, Il Nuovo Cimento, XXVI, 1376.

5. Mescheriakov, M. G., Zrelov, V. P., Neganov, B. S., Vzorov, I. K., and Shabudin, A. F. 1957, JETP, 4, 60.

6. Meshkovskii, A. G., Pligin, Iu. S., Shalamov, Ia. Ia., and Shebanov, V. A. 1957, JETP, 4, 60.

7. Guzhavin, V. M. et al. 1964, JETP, 19, 847.

8. Cence, R. J., Lind, D. L., Mead, G. D., and Moyer, B. J. 1963, Phys. Rev., B1, 2713.

9. Morris, T. W., Fowler, E. C., Garrison, J. D. 1956, Phys. Rev., 103, 1472.

10. Bugg, D. V. et al. 1964, Phys. Rev., 133, B1017.

11. Batson, A. P., Culwick, B. D., Hill, J. G., and Riddiford, L. 1958, Proc. Roy. Soc. London, A251, 218.

12. Eisner, A. M., Hart, E. L., Louttit, R. I., and Morris, T. W. 1965, Phys. Rev., 138, B670.

13. Fickinger, W. J., Pickup, E., Robinson, D. K., and Salant, E. O. 1962, Phys. Rev., 125, 2082; Pickup, E., Robinson, D. K., and Salant, E. O. 1962, Phys. Rev., 125, 2091.

14. Smith, G. A., Courant, H., Fowler, E. C., Kraybill, H., Sandweiss, J., and Taft, H. 1961, Phys. Rev., 123, 2160; Hart, E. L., Louttit, R. J., Luers, D., Morris, T. W., Willis, W. J., and Yamamoto, S. S. 1962, Phys. Rev., 126, 747.

15. Bugg, D. V., Salter, D. C., Stafford, G. H., George, R. F., Riley, K. F., and Tapper, A. J. 1966, Phys. Rev., 146, 980.

16. Melissinos, A. C., Yanamouchi, T., Fazio, G. G., Lindenbaum, S. J., and Yuan, L. C. L. 1962, Phys. Rev., 128, 2372; Melissinos, A. C., Fazio, G. G., Yamanouchi, T., Lindenbaum, S. J., and Yuan, L. C. L. 1961, Phys. Rev. Letters, 7, 454.

17. Alexander, G. et al. 1967, Phys. Rev., 154, 1284.

18. Blobel, V. et al. 1974, Nuclear Phys., B69, 454.

19. Jaeger, K. et al. 1976, Phys. Rev., D7, 1756.

20. Boggild, H. et al. 1971, Nuclear Phys., B27, 285.

21. Likhoded, A. K. and Shlyapnikov, P. V. 1978, Sov. Phys. Usp., 21, 1.

22. Whitmore, J. 1974, Phys. Rpts., 10C, 273.

23. Dao, F. T. et al. 1973, Phys. Rev. Letters, 30, 1151.

24. Seidl, A. A. et al. 1974, Bull. APS, 19, 467.

25. Antinucci, M. et al. 1973, Lett. al Nuovo Cimento, 6, 121.

Figure 5. Inclusive pion production cross sections in proton-proton collisions. The experimental data of Table 2 for the inclusive cross sections, in millibarns, for the production of pions in proton-proton collisions are shown with numerical fits to the data given in the text. The data is plotted as a function of the momentum of one of the photons, p_1, when the other is at rest in the LS. Figure 5a: inclusive cross section for the production of π^o-mesons. Figure 5b: inclusive cross section for the production of π^+-mesons, excluding the channel $pp \rightarrow \pi^+ d$. Figure 5c: inclusive cross section for the production of π^--mesons.

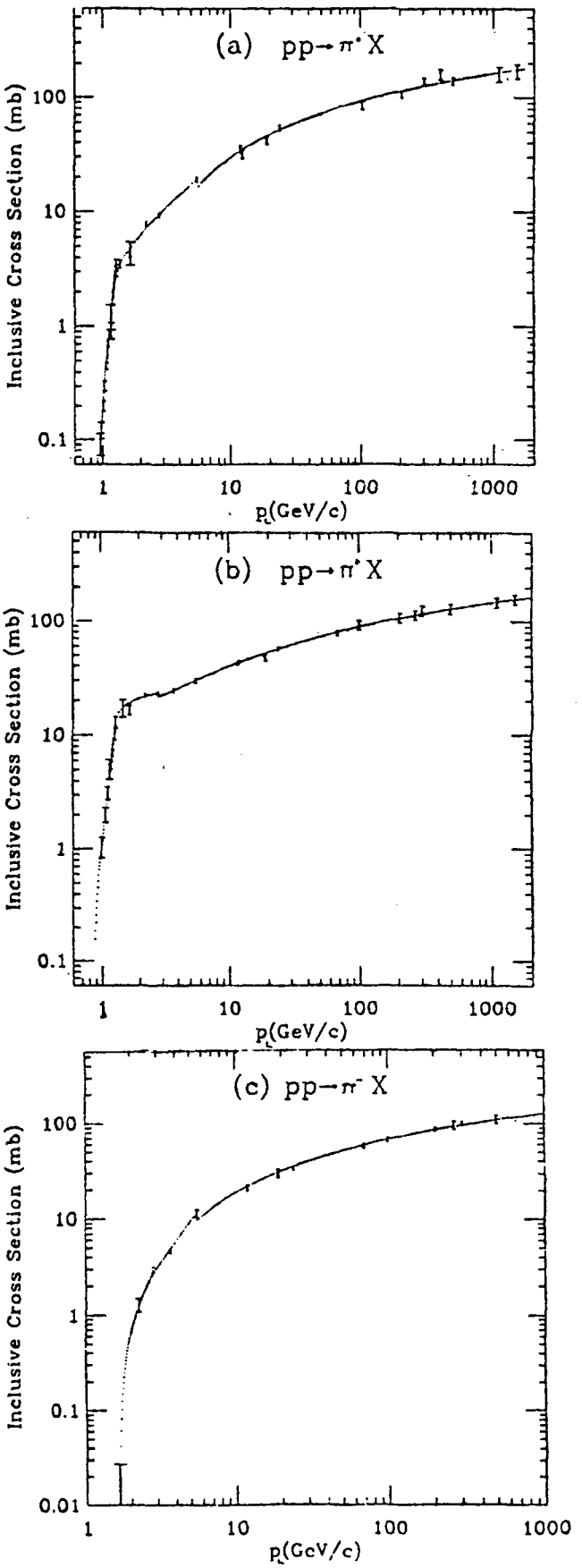
(a) pp→π⁺X
(b) pp→π⁻X
(c) pp→π⁻ X
Inclusive Cross Section (mb)
p_t(GeV/c)
100
10
1
0.1
0.01
1
10
100
1000

Figure 6. Reaction coefficient vs. Θ_p in a relativistic MB plasma of protons. The reaction coefficient R for the production of π-mesons in a relativistic MB plasma of protons is shown as a function of temperature $\Theta_p = k_B T/m_p$. The reaction coefficients for the channels $pp \rightarrow \pi^+ d$ (solid light line), $pp \rightarrow \pi^o X$ (dotted line), $pp \rightarrow \pi^+ X$ (dashed line), and $pp \rightarrow \pi^- X$ (dot-dashed line) are shown separately, along with the total reaction coefficient (solid heavy line) for all channels of pion production.

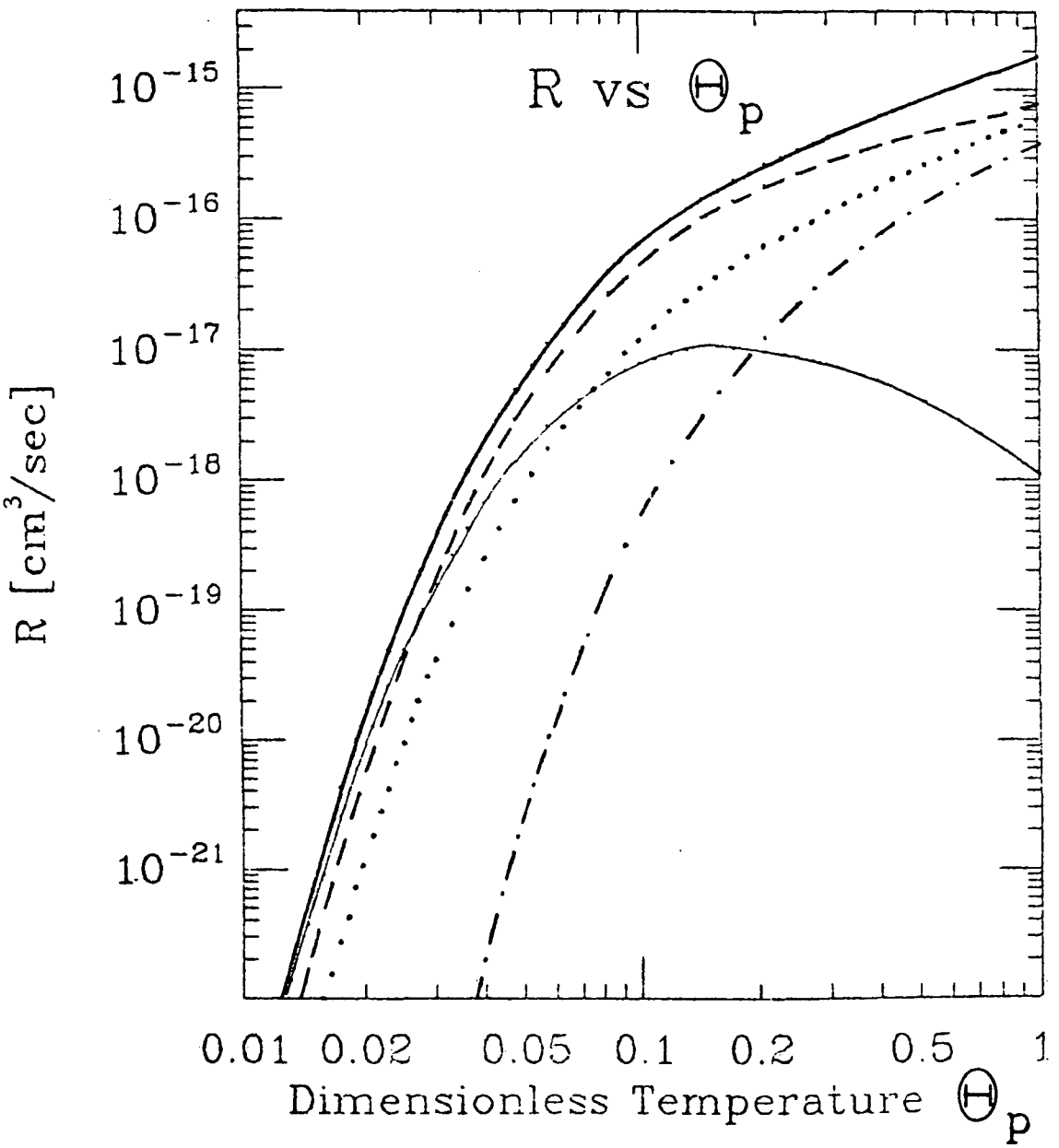
R vs Θp
R [cm³/sec]
10⁻¹⁵
10⁻¹⁶
10⁻¹⁷
10⁻¹⁸
10⁻¹⁹
10⁻²⁰
10⁻²¹
0.01
0.02
0.05
0.1
0.2
0.5
1
Dimensionless Temperature Θp

angle-averaged energy spectra of the produced pions in the CM. For the process $pp \rightarrow \pi^+ d$, this information is automatically determined from two-body kinematics. Essentially complete information for the CM spectra of π^+ and π^o are given in Refs. 4, 10, and 13 of Table 2. Reference 13 also gives the CM energy distribution of π^-. To determine the luminosity, only the cross section weighted by the energy in particles produced, equation (II-27), is needed. These numbers were calculated from the previously mentioned references. At higher energies, the values were derived from expressions for the Lorentz invariant production cross sections used in cosmic ray studies (Bahdwar and Stephens 1977; Bahdwar, Stephens and Golden 1977). The average energy $\langle E \rangle^{\pi}$ for the three types of produced pions can be fitted to the expression

$$\langle E \rangle^{\pi} = K(E_k - E_{k,thr})^{\alpha} , \qquad (39)$$

where $K = 0.276$, 0.285, and 0.275, and $\alpha = 0.22$, 0.185, and 0.187, for π^+, π^o, and π^-, respectively. The luminosity coefficients $L = \ell / n_p^2$ for the various channels and the total luminosity coefficient, calculated from equation (II-28), are shown in Figure 7 vs. Θ_p. Also shown is the energy loss timescale, used to determine if a MB distribution of particle energies can be established in a relativistic plasma of protons. Its significance will be discussed in the next section.

Figure 7. Luminosity coefficient and energy loss timescale vs. Θ_p in a relativistic MB plasma of protons. The luminosity coefficient L for the production of π-mesons in a relativistic MB plasma of protons is shown as a function of temperature $\Theta_p = k_B T/m_p$. Key for the graph is the same as in Figure 6, except that the curve labelled "T_{EL}" refers to the energy loss timescale due to pion production. The values on the right side refer to the energy loss timescale in units of seconds, and the values on the left side refer to the luminosity coefficient in units of GeV-cm^3/sec.

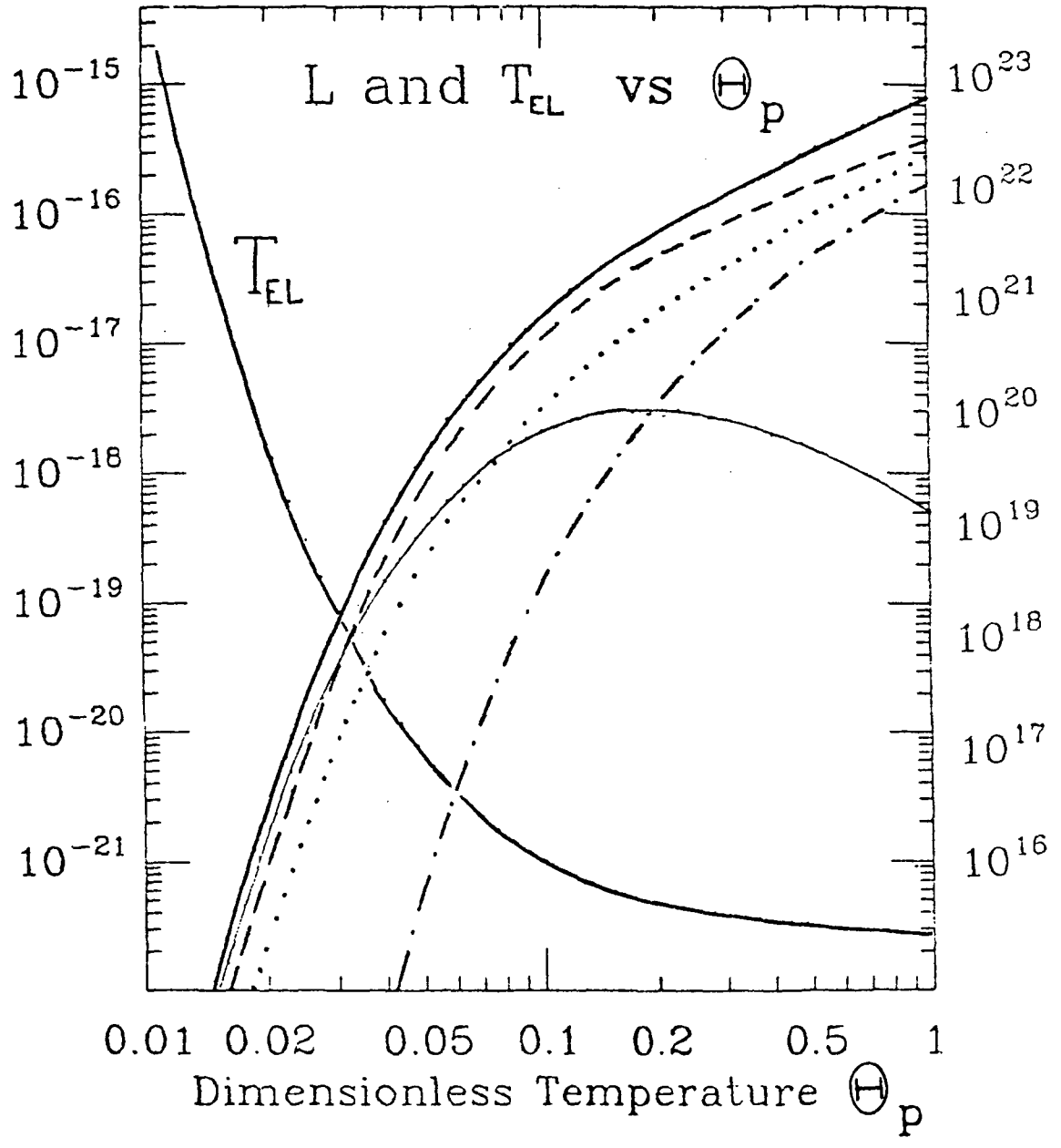
L and T_{EL} vs Θ_p
T_{EL}
10^{-15}
10^{-16}
10^{-17}
10^{-18}
10^{-19}
10^{-20}
10^{-21}
10^{23}
10^{22}
10^{21}
10^{20}
10^{19}
10^{18}
10^{17}
10^{16}
0.01 0.02 0.05 0.1 0.2 0.5 1
Dimensionless Temperature Θ_p

F. Thermalization, Reaction, and Energy Loss Timescales

We now treat the problem of the establishment of a MB distribution in particle energies using the results of Section II.D. Consider first the case of a highly relativistic electron of Lorentz factor γ_2 traversing a MB electron gas at temperature (in units of the electron mass energy) $\Theta = \mu^{-1}$. Assuming $\gamma_2 \gg \Theta$, the test electron will be in the high energy portion of the distribution, which is the last to thermalize because of the reduction of the value of the elastic scattering cross section at high energies. The test particle will be thermalized if the characteristic time for elastic scattering is shorter than the timescales for energy loss or annihilation.

The timescale for annihilation can be found from equations (II-33) and (2b). If the gas is subrelativistic, the annihilation time approaches

$$T_{a,t} \xrightarrow{\Theta << 1} \frac{\gamma_2}{n_-(c\pi r_e^2)\,[\ell n(2\gamma_2) + 1/2]}\,, \tag{40}$$

since $\gamma_2 \gg 1$, and $\gamma_2\gamma_r(1+\beta_2\beta_r) \to 2\gamma_2\gamma_r$ and $\gamma_2\gamma_r(1-\beta_2\beta_r) \to 1/2(\gamma_2/\gamma_r + \gamma_r/\gamma_2)$ in the limit $\Theta \ll 1$ in equation (II-33). For an extreme relativistic gas, the annihilation time is, in the approximation $\gamma_2 \gg \Theta \gg 1$,

$$T_{a,t} \xrightarrow{\Theta \gg 1} \frac{2\gamma_2\Theta}{n_-(c\pi r_e^2)\,[\ell n\,(2\gamma_2) + 1/2]}\,. \tag{41}$$

Compare this last result with the annihilation time computed for a MB gas composed of electrons and positrons at extreme relativistic temperatures. Defining $T_{a,MB} = n_+/r_a$, with r_a given by equation (5), we obtain

$$T_{a,MB} \xrightarrow{\Theta \gg 1} \frac{2\Theta^2}{n_-(c\pi r_e^2)\,\ell n\,\Theta} \quad . \tag{42}$$

(The approximation requires the information that $\int_1^\infty dx\, x^{3/2} \cdot \exp(-x) = 1.13$ and $\int_1^\infty dx\, \ell n\, x \cdot x^{3/2} \cdot \exp(-x) = 1.03$.) Comparing equation (41) with (42), we see that (for this case at least) it is permissible to identify γ_2 with Θ to get reliable estimates for the timescales from the test particle approximations. (Note the order of magnitude error for the result (41) cited by Lightman (1983).)

Thermalization in a pure electron gas occurs through Møller scattering. The cross section for this process is given by Jauch and Rohrlich (1976). In the test particle approximation, the thermalization timescale can be evaluated through equation (II-41). Assuming $\gamma_2 \gg \Theta \gg 1$, one can approximate $\Omega^+ \approx \Omega^-$, $\gamma_r \gg 1$, and retain only the leading terms in the Møller scattering cross section to get

$$T_{t,M\phi} \xrightarrow{\Theta \gg 1} \frac{\gamma_2 \Theta}{n_-(c\pi r_e^2)\left(\frac{9}{8} - \ell n\, 2 - \ell n\, \psi_m^*\right)} \quad . \tag{43}$$

In this expression, the minimum scattering angle ψ_m^* is the ratio between the maximum and minimum momentum transfers, $\psi_m^* =$

$h\omega_p/\gamma_2 m_e \sim 4\times10^{-17}\,[\mu n(cm^{-3})]^{1/2}/\gamma_2$, where $\omega_p^2 = 4\pi r_e \mu c^2 n_e/3$, the square of the plasma frequency (Gould 1981).

A similar calculation can be performed for a positron slowing in a pure electron gas through Bhabha (e^+-e^- elastic) scattering. The characteristic time in this case is

$$T_{t,\,Bha} \xrightarrow[\Theta \gg 1]{} \frac{\gamma_2 \Theta}{n_-(c\pi r_e^2)\left(\ell n\, 2 - \frac{11}{12} - \ell n\, \psi_m^*\right)} \,. \qquad (44)$$

Equations (43) and (44) may be contrasted with the results of Gould (1982a, b) by the inclusion of the Coulomb logarithm, $-\ell n\, \psi_m^*$. Identifying γ_2 with μ^{-1} in these equations according to the argument following equation (42), and assigning for $-\ell n\, \psi_m^*$ the canonical value 30 for astrophysical problems, it can be seen that both annihilation and thermalization timescales possess the same dominant behavior, proportional to Θ^2. Considering the numerical coefficients, one finds that the thermalization time is always considerably shorter, by an order of magnitude, than the annihilation time, for $\Theta \gg 1$. Thus, a positron should be able to thermalize before annihilating in an extreme relativistic MB gas of electrons.

Whether the electron gas obtains the MB form depends on the timescales for energy loss of the electron gas. For the extreme relativistic case, Alexanian (1968) has calculated the electron-electron bremsstrahlung luminosity $\ell_{e\text{-}e}$. It is

$$\ell_{e\text{-}e} \xrightarrow[\Theta \gg 1]{} 24 n_-^2 m_e \alpha r_e^2 c\Theta \left[\ell n(2\Theta) - \gamma_E + \frac{5}{4}\right] \quad . \tag{45}$$

For $\Theta \gg 1$, the kinetic energy density e_k approaches $3m_e n\Theta$. Comparing the energy loss timescale $T_{e\text{-}e} = e_k/\ell_{e\text{-}e}$ with the thermalization time $T_{t,M\phi}$, equation (43), we find that for temperatures greater than about 10 MeV, energy loss through bremsstrahlung emission dominates the thermalization process, so the establishment of a MB distribution cannot be assumed.

The thermalization of a gas containing electrons and ions depends on the energy exchange rate between the electron and ion component of the gas. Gould (1981) considers the energy exchange between electrons and ions through Mott scattering. For a neutral electron-proton extreme relativistic gas, he obtains

$$T_{e\text{-}p} \xrightarrow[\Theta \gg 1]{} \frac{3\Theta}{4\pi} \frac{1}{(n_- c r_e^2)} \frac{m_p}{m_e} (\ell n\, 2 + 1 - \gamma_E - \ell n\, \psi_m^*)^{-1} \tag{46}$$

where the temperatures of the electron and ion components of the gas are assumed to be of the same order of magnitude. Quigg (1968) derives the $\Theta \gg 1$ electron-proton bremsstrahlung luminosity

$$\ell_{e\text{-}p} \xrightarrow[\Theta \gg 1]{} 12 n_- n_p m_e \alpha r_e^2 c\Theta \left[\ell n\, 2\Theta - \gamma_E + \frac{3}{2}\right] \quad . \tag{47}$$

Note that it is almost exactly one-half the electron-electron bremsstrahlung luminosity, equation (45), in this limit. The total energy radiated in an extreme relativistic e-p gas will be the sum of

equations (45) and (47). Proceeding as for the pure electron gas case, it can be determined that the characteristic time for energy loss by bremsstrahlung is always less than the thermalization time, equation (46). Thus an extreme relativistic MB electron-proton gas cannot be assumed to exist in nature. The timescales become equal at $\mu \sim 1$, that is, near 0.5 MeV, but the relativistic approximations are no longer valid in this regime. However, numerical evaluation of equation (II-46), generally valid, yields a similar temperature (Stepney 1983).

Elastic scattering between protons, including Coulomb and nuclear effects, has been treated by Gould (1982c) and Stepney (1983). The timescale for energy loss must be compared with the thermalization time by elastic scattering to determine if a MB distribution in particle energies for a relativistic plasma of protons can be established. The energy loss timescale is plotted in Figure 7. It was evaluated according to the relation

$$T_{EL}^{-1} = n_p(R_{\pi^+ d} + L_\pi n_p/e_k) \qquad (48)$$

where $R_{\pi^+ d}$ is the temperature-dependent reaction coefficient for the process $pp \rightarrow \pi^+ d$ (Fig. 6), and L_π is the total luminosity coefficient in pions excepting the $pp \rightarrow \pi^+ d$ channel. The kinetic energy density e_k of the relativistic proton plasma has been given in equation (II-48).

To the accuracy of the experimental data (10-20%) and to the extent that pion production is the dominant energy loss mechanism, the calculated energy loss time is exact. Comparing the inelastic timescale to the elastic scattering time calculated in the previously cited papers, we find equality of timescales at 60 MeV. Thus, for temperatures less than 60 MeV, the establishment of a relativistic MB plasma of protons can in principle take place.

If there were a magnetic field present, synchrotron energy losses could prevent the formation of a MB distribution. The ratio of the electron thermalization time, equation (43), and the characteristic synchrotron energy loss timescale for a relativistic MB distribution of electrons (Gould 1982a), is

$$\frac{T_{M\phi}}{T_{syn}} \xrightarrow[\Theta \gg 1]{} \frac{128\Theta^4}{3}\left(\frac{9}{8} - \ell n\, 2 - \ell n\, \psi_m^*\right)^{-1}\left(\frac{e_B}{e_k}\right) , \qquad (49)$$

where $e_B = B^2/8\pi$ is the magnetic field energy density. Therefore at equipartition field strengths, the synchrotron cooling is able to dominate thermalization mechanisms and prevent the formation of a MB distribution.

The ratio of the characteristic time for annihilation, equation (42), and the energy loss timescale for synchrotron cooling, as computed above, gives

$$\frac{T_a}{T_{syn}} \xrightarrow{\Theta \gg 1} 100 \frac{(n_+ + n_-)}{n_-} \Theta^4 \left[\ln \Theta + \frac{1}{2}\right]^{-1} \frac{e_B}{e_k}, \qquad (50)$$

for $\Theta \gg 1$. Hence a magnetic field two to three orders of magnitude less than the equipartition value can cool electrons from extreme relativistic temperatures before annihilation. This ratio is important for interpreting annihilation line features in gamma ray burst spectra.

IV. PHYSICAL APPLICATIONS

A. Boltzmann and Pair Balance Equations

In this section, we examine the properties of static, non-magnetic, relativistic thermal plasmas. The appearance of such systems in nature could conceivably come about in several ways: through dissipation of energy in shocks moving at relativistic speeds; mechanical heating of a neutron star crust due to, for example, a phase transition in the interior (Ramaty, Lingenfelter, and Bussard 1981); the heating of a diffusive coronal plasma by an intense source of energetic photons (Guilbert, Fabian, and Rees 1983); accretion flow (either disk or spherical) near a collapsed object; etc. In what follows, a number of approximations will be made in order to model an ideal type of system, namely a steady spherical plasma cloud of radius L with uniform density and temperature. This is the sort of object that Lightman and Band (1981) and Lightman (1982) have considered at extreme relativistic temperatures $\Theta \gg 1$, and Svensson (1982) for all temperatures, but at small optical depth. In a recent preprint, Svensson (1984) examines the properties of this system for all optical depths and throughout the entire relativistic range of temperatures.

Even the strongest gravitational fields, as on the surface of a neutron star, are inadequate to confine such a system (Colgate and Petschek 1981). A sufficiently strong magnetic field can, but the

production of photons through the synchrotron process changes the properties of the system, a circumstance beyond the scope of this work. In the absence of a confinement mechanism, the relativistic plasma will expand adiabatically, and a uniform density and temperature cannot be assumed. Thus, the adopted model must be considered artificial, serving only to suggest properties of a more realistic and more complicated system. (Discussion of plasma confinement and trapping are found in Lightman (1982) and Svensson (1984).)

Nevertheless, the assumption of homogeneity throughout a spherical region permits a quantitative analysis. Beyond this, we assume that the particles are described by a thermal distribution, which, as we showed in Section III. F, is not strictly true for $\Theta \gg 1$. Qualitative behavior of solutions should however be expected to be correct, as only the magnitude of particle production and annihilation rates are affected, not the character of these rates. Also, photons that Compton scatter with energies $k \sim \Theta(\Theta)$ are assumed to obtain a Wien form, as we examine in more detail below. External photon sources are not considered, and double Compton scattering is treated in an approximate fashion, as this process can be important for the calculation of the steady state positron density in the low temperature, large optical depth regime (Svensson 1984).

In general, Svensson's (1982, 1984) notation is used. The density of protons is denoted by n_p, of positrons by $n_+ = zn_p$, and

two optical depths are distinguished, the proton Thomson optical depth $\tau_p = n_p \sigma_T L$, and the Compton optical depth $\tau_C(k; \theta) = \kappa_C(k; \theta) L$, where $\kappa_C(k; \theta)$ is the frequency-averaged Compton opacity, Eqs. (III-23) and (III-24), and is shown in Figure 8a for selected temperatures. All mechanisms associated with scatterings, absorption, or loss from the system are treated on the same footing, in terms of an associated absorption coefficient, or opacity. Thus we can write a differential equation for the photon number spectrum, $n_\gamma(k,t)$, namely

$$\frac{\partial n_\gamma(k)}{\partial t} = -c \{ \kappa_L(k) + \kappa_C(k) + \kappa_{\gamma\text{-par}}(k) + \kappa_{\gamma-\gamma}[k, n_\gamma(k)] + \kappa_b(k) \} n_\gamma(k) + S_\gamma(k) + Q_C(k,k') . \quad (1)$$

$S_\gamma(k)$ is the photon source term associated with bremsstrahlung processes, electron-positron annihilation, and double Compton scattering, and $Q_C(k,k')$ represents a photon source term due to Compton scattering of a photon from energy k' to energy k. The absorption coefficients in the brackets in Equation (1) are associated with loss from the system, Compton scattering, photon-particle and photon-photon pair production, and bremsstrahlung absorption, respectively. The temporal and temperature variables, as well as dependences on various system parameters, are implicit in the terms of the equation.

The form of $\kappa_L(k)$ can be established by examining the behavior in the optically thick and thin limits. As τ_p (and τ_C) $\to 0$, the average photon path length is about L; therefore $\kappa_L(k) \to 1/L$ in this limit. For large optical depth, $L^2 = N\ell_{mfp}^2$, where $\ell_{mfp}^{-1} = \kappa_C(k;\Theta)$ and N is the average number of "steps" required for a photon to go a distance L. Thus $N = \tau_C^2$ and the average total distance travelled by a photon is given by $\xi N \ell_{mfp} = \xi \tau_C L$, where ξ is a geometrical factor equal to about 1/3 for diffusive escape from a uniform spherical distribution of sources (Sunyaev and Titarchuk 1980). We take $\kappa_L(k) = n_p \sigma_T / \tau_p (1 + \tau_C/3)$, bridging the two limits. The other absorption coefficients are given in Chapter III, but note that because the bremsstrahlung absorption coefficient $\kappa_b \propto n_p^2$, whereas the rest of the coefficients are proportional to n_p, the number of variables required to completely specify the system are 3: Θ, L (or τ_p), and n_p. The steady state positron density is then $z = z(\Theta, \tau_p, n_p) \to z(\Theta, \tau_p)$ for $\tau_p \leq 1$, because only when Comptonization of extremely low energy photons is important should the effects of free-free absorption be felt on the rate of pair production.

Previous studies of relativistic gases of photon and particles have proceeded by introducing characteristic photon energies which define regimes where the free-free absorption coefficient κ_b dominates κ_C, and where it dominates κ_L. A third photon energy is introduced which characterizes those photons suffering significant

changes in energy due to Compton scattering; i.e., where the so-called Compton y parameter exceeds unity (Shapiro, Lightman, and Eardley 1976; Rybicki and Lightman 1979). Semi-quantitative spectra are determined for the various photon energy regimes on the basis of the relative importance of scattering and absorption.

Instead, we solve equation (1) directly by assigning to $Q_C(k, k')$ an approximate form. Even so, it will prove easier to determine the spectra and properties of the system in various temperature and optical depth regimes by considering dominant mechanisms and solving equation (1) in an approximate fashion.

Recall from Chapter II.E the expression derived for the average energy change of a photon that is Compton scattered by an electron (or positron) in a reaction characterized by the reaction parameters γ, x, k. Averaging over a MB distribution of electrons, the exact average energy increase per scattering by a MB distribution of electrons and positrons is, from equations (II-56, 57, 58),

$$A(k;\Theta) - 1 = \frac{\int_0^\infty dx\, e^{-\mu\phi}\, \sigma_C(x)[\Gamma(x) - 1]\cdot[2\mu k^2 x + \mu k^2 - \mu x^2 - 2xk]}{2\mu k^2 \int_0^\infty dx\, x\, \sigma_C(x)\, e^{-\mu\phi}}, \quad (2)$$

where $\phi = \frac{1}{2}\left(\frac{x}{k} + \frac{k}{x}\right)$. In Figure 8b, the function $A(k;\Theta)$ is plotted for $\mu^{-1} = \Theta = 0.1, 0.3, 1, 3, 10$. A photon with energy k before scattering emerges with energy $A(k)\cdot k$ after scattering. The exact

Figure 8. Compton scattering opacity and average Compton energy increase. In Figure 8a is shown the opacity of a photon with energy k due to Compton scattering by a MB distribution of electrons at various temperatures in the transrelativistic regime. The average energy increase of a photon that initially had energy k, due to Compton scattering by a MB distribution of electrons at different temperatures, is shown in Figure 8b.

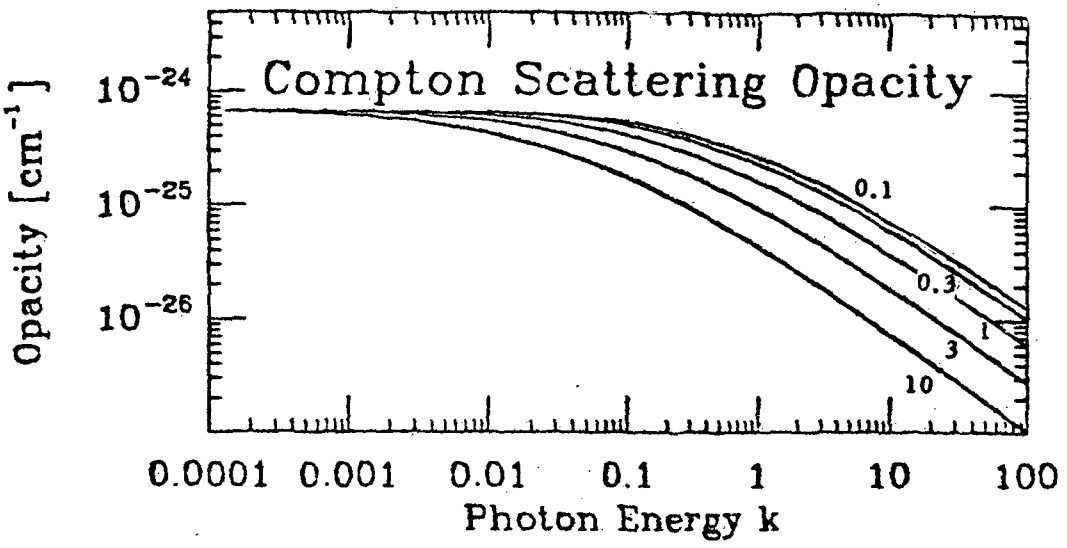

Figure 8a.

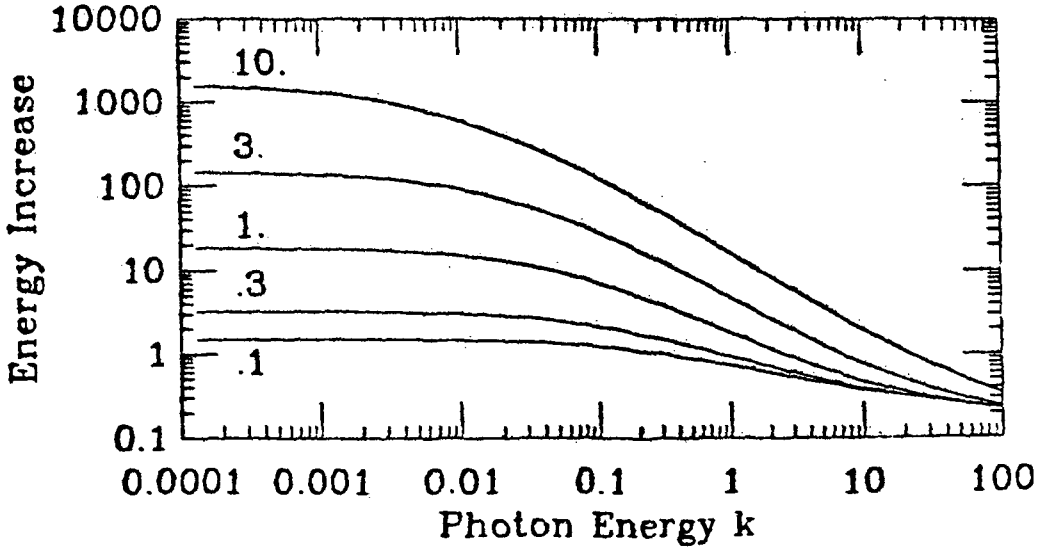

Figure 8b.

average increase in photon energy in the limit $k \to 0$ is, from equation (2),

$$A(k \to 0;\ \Theta) = 1 + \frac{4K_3(\mu)}{\mu K_2(\mu)} \quad . \tag{3}$$

For $\Theta \ll 1$, $A \to 1 + 4\Theta$, and for $\Theta \gg 1$, $A \to 16\Theta^2$. These limiting forms can also be determined from simpler considerations (Rybicki and Lightman 1979). In addition, $A(k, \Theta) = 1$ for $k \cong 3\Theta$, as expected since the average photon energy in a Wien distribution is 3Θ.

The approximation we employ for Compton scattering is to assume that each photon of energy k scatters at a rate defined by the exact Compton opacity averaged over a MB distribution of particles, $\kappa_C(k; \Theta)$, and is promoted in energy by the factor $A(k; \Theta)$, equation (2). Then the source function of equation (1) is given by

$$Q_C(k, k') = c\kappa_C(k')(k'/k)\, n_\gamma(k') \quad , \tag{4}$$

where k and k' are related through $k = A(k') \cdot k'$, and the phase space factor k'/k is required to preserve total photon number. Alternately, introduce the factor $\rho(k)$ that tells the energy k' that a photon of energy k had prior to being Compton scattered: $\rho(k) \cdot k = k'$. The static solution to equation (1) is

$$n_\gamma(k) = \frac{S_\gamma(k)}{c\,\kappa_{TOT}(k)} + \frac{\kappa_C(k')}{\kappa_{TOT}(k)} \cdot n_\gamma(k') \quad , \tag{5}$$

where the term in braces in equation (1) is denoted $\kappa_{TOT}(k)$. On the LHS of equation (5), $n_\gamma(k')$ is given again by equation (5), but with $k \to k'$ and $k' \to k''$, so

$$n_\gamma(k) = [c\kappa_{TOT}(k)]^{-1} \sum_{i=0}^{\infty} \left[\prod_{j=0}^{i} \chi^j(k) \right] S_\gamma[\rho^i(k)] \quad , \tag{6}$$

where

$$\chi^j(k) = \left(\frac{\rho^j(k)}{k} \right) \cdot \frac{\kappa_C[\rho^j(k)]}{\kappa_{TOT}[\rho^j(k)]} \quad . \tag{7}$$

The argument $\rho^i(k)$ is an i^{th} order operator on k: $\rho^1(k) = \rho(k) \cdot k = k'$; $\rho^2(k) = \rho(k') \cdot \rho^1(k) = \rho(k') \cdot k'$; and so on. At large optical depths, it is only the presence of free-free absorption that shuts off higher order scattering and provides convergence, as $S_\gamma(k) \sim 1/k$ for bremsstrahlung photons in the limit $k \to 0$. Hence the importance of low frequency absorption and production processes in the limit of large optical depths. Equation (6) can be numerically evaluated to determine $n_\gamma(k)$ and z.

Because $\kappa_\gamma = \kappa_{\gamma\gamma}[k, n_\gamma(k)]$, equation (5) must be solved in an iterative sequence. A steady state solution requires the equality between the pair production and pair annihilation rates:

$$r_a(\Theta) = r_{par-par}(\Theta) + r_{\gamma-par}(\Theta) + r_{\gamma-\gamma}(\Theta) \quad . \tag{8}$$

Expressions for these quantities in terms of integrals over cross sections and photon distribution functions are given in the preceding

chapter. Joint satisfaction of equations (6) and (8) yields the photon number spectrum and the allowable steady state positron density z. Numerical solutions near $\Theta \cong \mathcal{O}(1)$, where simple approximation techniques are not possible, will be shown later. We will first consider features of the results that do not require extensive numerical simulation.

B. Ultrarelativistic Regime: Approximate Treatment of Comptonization

The first systematic study of the physics of relativistic thermal plasmas is given in the paper by Bisnovatyi-Kogan, Zel'dovich, and Sunyaev (1971). Their principal conclusion is that a stable, optically thin, relativistic plasma cannot exist above a certain critical temperature Θ_{cr}. Even in the limit of zero proton optical depth in which the photon density goes to zero (Table 1), pair production through particle-particle collisions overwhelms pair annihilation, and any increase in energy goes into pair production rather than thermal energy (Stepney 1983). The existence of the critical temperature is due to the decrease with energy of the annihilation cross section σ_a, equation (III-2b), and the corresponding increase in the pair production cross sections σ_{pp}, equation (III-27).

We can summarize the argument as follows: in the limit of zero optical depth, the pair balance relation (8) gives

$$n_+ n_- \sigma_a(\bar{\gamma}_r) \approx (n_+ + n_-)^2 \sigma_{pp}(\bar{\gamma}_r) , \qquad (9)$$

where $\bar{\gamma}_r$ is a characteristic electron Lorentz-function at temperature Θ. The less important proton-electron pair production cross section is neglected (see Figure 9). Solving the quadratic equation (9) for n_+, and finding that the determinant $\sigma_a^2 - 4\sigma_a\sigma_{pp}$ vanishes when $\bar{\gamma}_r \cong 850$ gives $\Theta_{cr} \cong 17$, since $\bar{\gamma}_r \approx 3\Theta^2$.

The original paper of Bisnovatyi-Kogan et al. gives $\Theta_C \approx 40$, as does Lightman (1982). Zdziarski (1982) points out that the thermal averaged pair production rate from particle collisions used in these studies is a factor of four too low. He calculates $\Theta_{cr} \cong 25$, so this crude estimate is not far off. Calculating the thermally averaged pair production rates from particle collisions through equations (II-16) and (III-27), along with the pair annihilation rate (III-5), gives an accurate determination of Θ_{cr}. A linear increase in the cross section, as suggested by Svensson (1982), from threshold to $\gamma_r = 50$ for the electron-proton rate, and from threshold to $\gamma_r = 100$ for the electron-positron rate, gives the rate coefficients R_{ee} and R_{ep} shown in Figure 9. The pair balance equation (8) becomes

$$z(z+1)R_a = (2z+1)R_{ep} + [(z^2/2) + (z+1)^2/2 + z(z+1)]R_{ee}, \qquad (10)$$

dropping all photon-related pair production rates in the limit $\tau_p \to 0$. Equation (10) has no positive real solutions for $\Theta > \Theta_{cr} \cong 24$, using the values shown in Figure 9, thus agreeing with Zdziarski's result.

Physically, at temperatures above Θ_{cr}, any incremental

Figure 9. Reaction coefficients vs. temperature Θ in relativistic plasma. Numerically calculated rate coefficients are plotted as a function of temperature, including pair production from particle-particle, photon-particle, and photon-photon interactions, in addition to the annihilation rate coefficient. For pair production from bremsstrahlung photons, only the rates associated with the electron-proton bremsstrahlung spectrum are shown. Symbols for rate coefficients are related to rates explained in text.

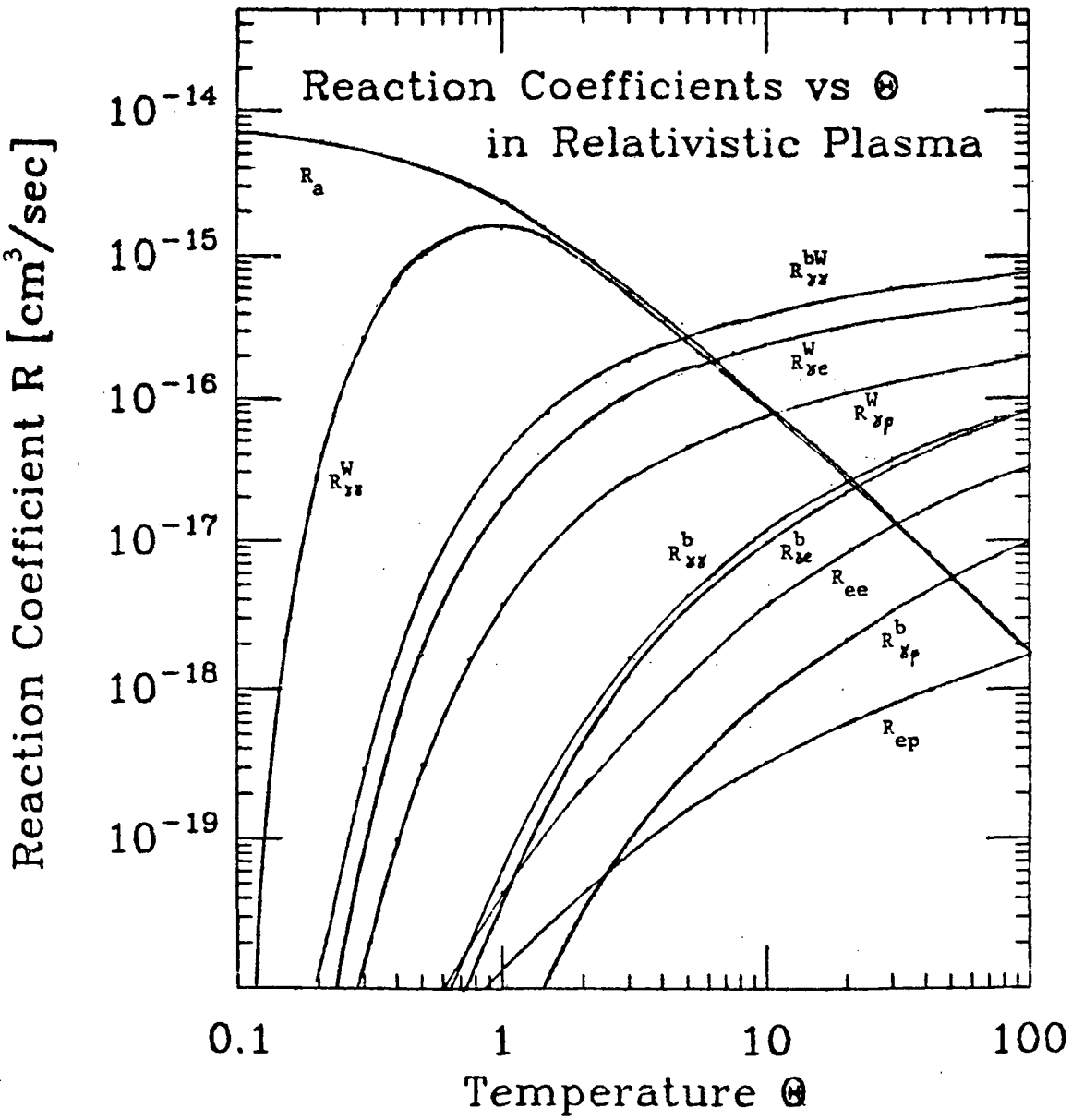
Reaction Coefficients vs Θ
in Relativistic Plasma
Reaction Coefficient R [cm³/sec]
10⁻¹⁴
10⁻¹⁵
10⁻¹⁶
10⁻¹⁷
10⁻¹⁸
10⁻¹⁹
0.1
1
10
100
Temperature Θ
R_a
R^bW_γγ
R^W_γe
R^W_γp
R^W_γγ
R^b_γγ
R^b_γe
R_ee
R^b_γp
R_ep

increase in the pair density will be accompanied by an increase in the rate of pair production through particle-particle collision that is always greater than the corresponding increase in the rate of pair annihilation. Therefore no pair balance is possible at these temperatures. If the optical depth of the system is non-negligible, internally produced photons will also contribute to pair production. One should think that the effect of this would be to lower Θ_{cr} and give a critical temperature $\Theta_{cr}(\tau_p)$. This is indeed the case, as investigated by Lightman (1982) at extreme relativistic (ER) temperatures. In fact, $\Theta_{cr} = \Theta_{cr}(\tau_p, n_p)$, from preceding considerations. In what follows, we calculate Θ_{cr}, or equivalently $\tau_p^{cr}(\Theta, n_p)$, in the limit $\Theta \gg 1$, in addition to the steady state positron density z, on the basis of approximations to equation (6).

At temperatures greater than about 2 MeV, that is, for $\Theta \geq 4$, asymptotic expressions for the rate functions in equation (8) can be evaluated analytically. For those rates depending on the photon distribution, it is necessary to determine an approximate form for the photon number spectrum. This we do by assuming that the photon distribution is composed of two components in the pair production region: the internally produced bremsstrahlung photons and the Compton scattered photons. We further assume that those photons Compton scattering into the regime of photon energies $k \sim \mathcal{O}(\Theta)$ obtain the Wien form

$$dn_\gamma^W(k) = \frac{n_\gamma^W}{2\Theta^3} \exp(-\mu k)\, k^2\, dk \ , \qquad (11)$$

or $f_\gamma(k) = \exp(-\mu k)$, with $A_\gamma = n_\gamma^W/8\pi\Theta^3$ from equation (III-26). The volume density of photons in the Wien distribution is then just n_γ^W.

The Wien spectrum is the most probable distribution that a gas of photons will obtain after Compton scattering with a thermal distribution of electrons (Synge 1957). It corresponds to the Bose distribution with negative chemical potential, reflecting conservation of photon number. One can formally show on the basis of the formalism developed in Section II. E that the time scale for energy exchange through photon-electron (Compton) scattering is always much shorter than the time scale for energy loss through bremsstrahlung due to the different orders of the two processes; thus, the model is consistent. However, it would be necessary to solve a time-dependent Boltzmann equation using the exact Compton scattering function, equation (II-52), to characterize the establishment of a Wien distribution after one, or a succession, of scatterings of a photon in the region $k \sim \mathcal{O}(\Theta)$. The assumption adopted, namely that this occurs after a single scattering into this regime of photon energy, remains uncertain.

In the high temperature limit the spectrum of annihilation photons gives only a small contribution to the total photon number spectrum; for this reason it is neglected. This is because

annihilation photons are produced conjointly with bremsstrahlung photons, which always dominate at ER temperatures. For example, at temperature $\Theta = 3$, the value of the e^+-e^- bremsstrahlung spectrum is a factor of 3 greater than the e^+-e^- annihilation spectrum at the peak of the annihilation spectrum, as can be seen from a comparison of equations (II-8) and (II-10) and the values shown in Figure 3b. Adding in the accompanying e^+p, e^-p, and e^--e^- bremsstrahlung-produced photons, this represents a 15% contribution at most, and decreases on either side of the annihilation peak (note the k^2 dependence of the Gaunt factor for $k \gg \Theta$, $\Theta \gg 1$ in Figure 3). For temperatures Θ greater than 3, the annihilation spectrum is relatively even weaker.

A corollary to this observation is that no annihilation line should be visible from a stable ER thermal plasma (Lightman 1982). Indeed, because of the decline of the pair density at subrelativistic temperatures, except when the optical depth is so great than the annihilation line then suffers severe Compton broadening, Svensson (1984) concludes that an annihilation feature cannot be observed from a stable relativistic plasma in pair balance.

In order to calculate the number of photons being scattered into the Wien regime per second, $S^W(\Theta)$, an asymptotic form for the electron-proton bremsstrahlung Gaunt factor is useful. At $\Theta \gg 1$ and $k \ll \Theta$, one obtains

$$g(k;\Theta) = \left(\frac{3\Theta}{2\pi}\right)^{1/2}\left[\ell n\left(\frac{2\Theta^2}{k}\right)+\frac{5}{2}-2\gamma_E\right] , \tag{12}$$

using the approximate form for the electron-proton bremsstrahlung cross section,

$$d\sigma = \left(\frac{2\alpha}{\pi}\right)\sigma_T\, k^{-1}\, dk\left[\ell n\left(\frac{2\gamma_r^2}{k}\right)-\frac{1}{2}\right] , \tag{13}$$

valid for soft photon production at relativistic ($\gamma_r \gg 1$) electron energies. At ER temperatures, the various thermal bremsstrahlung production spectra have identical form. Incorporating appropriate multiplicative factors, the total bremsstrahlung production spectrum becomes

$$S_\gamma^b(k;\Theta) = (8z^2+10z+3)\left(\frac{2n_p^2\,\alpha c\sigma_T}{\pi}\right)\cdot k^{-1}\cdot\exp(-\mu k)\,\ell n\left(\frac{\eta_E\Theta^2}{k}\right) , \tag{14}$$

for $k \ll \Theta$ and $\Theta \gg 1$, where $\eta_E = 2\exp(5/2 - 2\gamma_E)$.

The value of $S^W(\Theta)$ is determined from the relation

$$S^W(\Theta) = \int_0^\infty dk\; p(k;y)\, S_X^b(k;\Theta) , \tag{15}$$

where $p(k;y)$ is the probability of a photon with energy k being scattered into the Wien regime, and y represents those parameters (Θ, n_p, ...) upon which p may depend. In the Compton scattering approximation we use,

$$p(k;\, y) = X(k)^{\alpha(k)} \quad , \tag{16}$$

where $\alpha(k) = \ell n(3\Theta/k)/\ell n\, A(k;\, \Theta)$ characterizes the average number of scatterings required for a photon of energy k to reach the Wien ($k \approx 3\Theta$) regime, and X represents an averaged probability that the photon will be Compton scattered rather than absorbed or lost from the system. Its meaning will become clear as specific regimes of photon energy are treated.

We require a photon to scatter at least one time to enter the Wien regime. It is therefore appropriate to divide the bremsstrahlung generated photons into two regimes depending on whether the energy k of the photon is less than or greater than $3\Theta/A$, where A denotes the asymptotic value $A(k \to 0;\, \Theta)$, equation (3). This is because A is sufficiently large that $A(k = 3\Theta/A;\, \Theta) \approx A$ for $\Theta \gg 1$. In the former regime, a photon has a probability of scattering into the Wien regime given by the multiple scattering form of p, equation (16). In the latter regime p becomes $X(k)$, the probability of a single Compton scattering at photon energy k. In addition, photons below a characteristic energy k_b defined through the relation $\kappa_b(k_b) = \kappa_L(k_b)$ will more likely be absorbed through the inverse bremsstrahlung process than lost from the system because of the rapid increase in the free-free absorption coefficient as $k_b \to 0$ (equation (III-32)). (In any event, the value of k_b is not critical at low to moderate optical depths because these low energy photons

will only rarely saturate to the Wien regime.) Equation (15) becomes

$$S^W(\Theta) = S_1^W(\Theta) + S_2^W(\Theta) = \int_{k_b}^{3\Theta/A} dk\ X^{\alpha(k)}(k)\, S_\gamma^b(k;\Theta)$$

$$+ \int_{3\Theta/A}^{\infty} dk\ X(k)\, S_\gamma^b(k;\Theta) \quad . \tag{17}$$

An examination of the absorption coefficients in Figures 8 and 10 shows that the only significant sources of photon opacity at photon energies $k_b \leq k \leq 3\Theta/A$ are loss from the system and Compton scattering. The Compton scattering opacity for these energies takes place almost entirely in the Thomson limit. This is because the separation between the Thomson and Klein-Nishina (KN) regimes is at photon energy k_s determined by the condition $\bar{\gamma}_r (k_s \approx 1)$, where $\bar{\gamma}_r$ is again the Lorentz factor typical of thermal electrons. For $\Theta \gg 1$, we have $k_s \approx (3\Theta)^{-1}$. This may be compared to the value $k = (3\Theta/A) \cong (5\Theta)^{-1}$ separating the two scattering regimes in the ER limit.

Therefore, when $k_b < k < 3\Theta/A$, we can calculate $X(k)$ by assuming that the scattering is described in the Thomson approximation to the Compton cross section. Hence $X(k) \cong \kappa_C \cdot (\kappa_C + \kappa_L)^{-1} \cong [1 + (\tau_C^o + \tau_C^{o2}/3)^{-1}] = X_0$ in $S_1^W(\Theta)$, where $\tau_C^o = \tau_C(k \to 0) = (2z+1)\tau_p$. The limits of X_0 are $X_0 \to \tau_C^o$ for $\tau_C^o \ll 1$, and

$X_0 \to 1 - (3\tau_C^o)^{-2}$ for $\tau_C^o \gg 1$. Integrating S_1^W, using equation (14), one obtains

$$S_1^W(\Theta) = \Sigma_b \cdot \int_{k_B}^{3\Theta/A} dk\, k^{-1}\, X_0^{\ell n(3\Theta/k)/\ell n\, A}\; \ell n(\eta_E \Theta^2/k) \tag{18}$$

$$= \Sigma_b \cdot \Omega \cdot \left\{ \Omega \left[X_0^{u_b}(u_b \ell n\, X_0 - 1) - X_0(\ell n\, X_0 - 1) \right] + \ell n\left(\frac{\eta_E \Theta}{3}\right) (X_0^{u_b} - X_0) \right\} ,$$

where $\Omega = \ell n\, A/\ell n\, X_0$, $u_B = \ell n(3\Theta/k_B)/\ell n\, A$, and $\Sigma_b = (8z^2 + 10z + 3) \cdot (2n_p^2 \alpha c \sigma_T/\pi)$. In the case of unsaturated Comptonization of the low energy photons $k \geq k_b$, that is, when $X_0^{u_b} \ll 1$,

$$S_1^W(\Theta) \approx \Sigma_b \cdot \Omega \cdot X_0 \left[\Omega(1 - \ell n\, X_0) - X_0\, \ell n\, (\eta_E \Theta/3 \right] . \tag{19}$$

We now turn to the second integral of equation (17), $S_2^W(\Theta)$, representing those photons produced with $k > 3\Theta/A$ which scatter one time before entering the Wien distribution. It is necessary to incorporate the effects of the KN decline in the Compton cross section on the Compton opacity in order to calculate this rate. At ER temperatures, the Compton opacity is given by Gould (1982a) or from equation (III-24b), namely

$$\kappa_C(k; \Theta) = (2z+1)\, n_p \sigma_T\, (3/16\, k\Theta) \cdot \ell n(\eta_C\, k\Theta) , \tag{20}$$

where $\eta_C = 4 \exp(1/2 - \gamma_E)$. This expression is valid for $k > 1/\Theta$, so we need an interpolation formula between the Thomson

and KN regimes to account for photon energies in the range $3\Theta/A \leq k \leq 1/\Theta$. Take $k = 30\,\Theta/A$ for the upper photon energy of the intermediate regime, which is well within the KN regime of the Compton opacity. One finds that $\kappa_C\,(k = 30\Theta/A) \cong 0.19\,(2z+1)\,n_p\sigma_T$ for $\Theta \gg 1$. An accurate (10-20%) interpolation formula at $3\Theta/A \leq k \leq 30\Theta/A$ is given by the formula

$$\kappa_C(k;\Theta) = (2z+1)\,n_p\sigma_T\,(1 - 0.43\,k\Theta)\ , \tag{21}$$

which reduces to the known values at $k = 30\Theta/A$ and for $k \to 0$.

Inserting equations (20) and (21) into the second integral of equation (17) gives

$$S_2^W \cong \Sigma_b(2z+1)\tau_p\left[(1+\tau_C^o/3)\int_{3\Theta/A}^{30\Theta/A} dk\,k^{-1}(1 - 0.43\,k\Theta)\,\ell n\left(\frac{\eta_E\Theta^2}{k}\right)\right.$$

$$\left. + \left(\frac{3}{16\Theta}\right)\int_{30\Theta/A}^{3\Theta} dk\,k^{-2}\,\ell n(\eta_C k\Theta)\,\ell n\left(\frac{\eta_E\Theta^2}{k}\right)\right] \tag{22}$$

in the approximation $\tau_C^o < 1$. The exponential factor from equation (14) is taken equal to unity in the first integral above, a good approximation considering the photon energies of the intermediate regime, and is used to impose an artificial cutoff at $k = 3\Theta$ in the second integral. This is a crude approximation, not to mention the fact that the Gaunt factor (12) is no longer valid at these photon energies. But the contribution of the second integral in equation

(22) is at any rate small compared to both S_1^W and the first integral in equation (22) at ER temperatures because of the secular decrease in the Compton opacity (20).

Evaluating the integrals in equation (22), retaining only the dominant terms from the second integral, gives

$$S_2^W \cong \Sigma_b(2z+1)\tau_p[(1+\tau_C^o/3)\cdot 4.7\,\ell n(2.5\Theta) + 0.1\,\ell n(\eta_C\Theta)\ell n(\eta_E\Theta^2)]\,, \quad (23)$$

using $A = 16\Theta^2$ in the limit $\Theta \gg 1$. This equation, in conjunction with equation (18) or (19), provides an approximate analytic treatment for the rate at which bremsstrahlung photons are Compton scattered into the Wien component of the photon number spectrum per unit volume. Though equation (23) is only valid under the assumption $\tau_p(2z+1) < 1$, numerical comparisons of equations (18) and (23) show that when $\tau_C^o \geq 0.1$, that is, for low to moderate optical depths, equation (23) gives a small contribution to equation (17). This simply reflects the cascade of low energy photons into the Wien distribution as the optical depth for Compton scattering begins to be significant. Since equation (18) does not suffer from the low optical depth approximation, this analysis permits a treatment of Comptonization in an ultra-relativistic plasma at all optical depths. For an alternate treatment of Comptonization in a thermal plasma at ER temperatures, the reader is referred to the paper of Lightman and Band (1981).

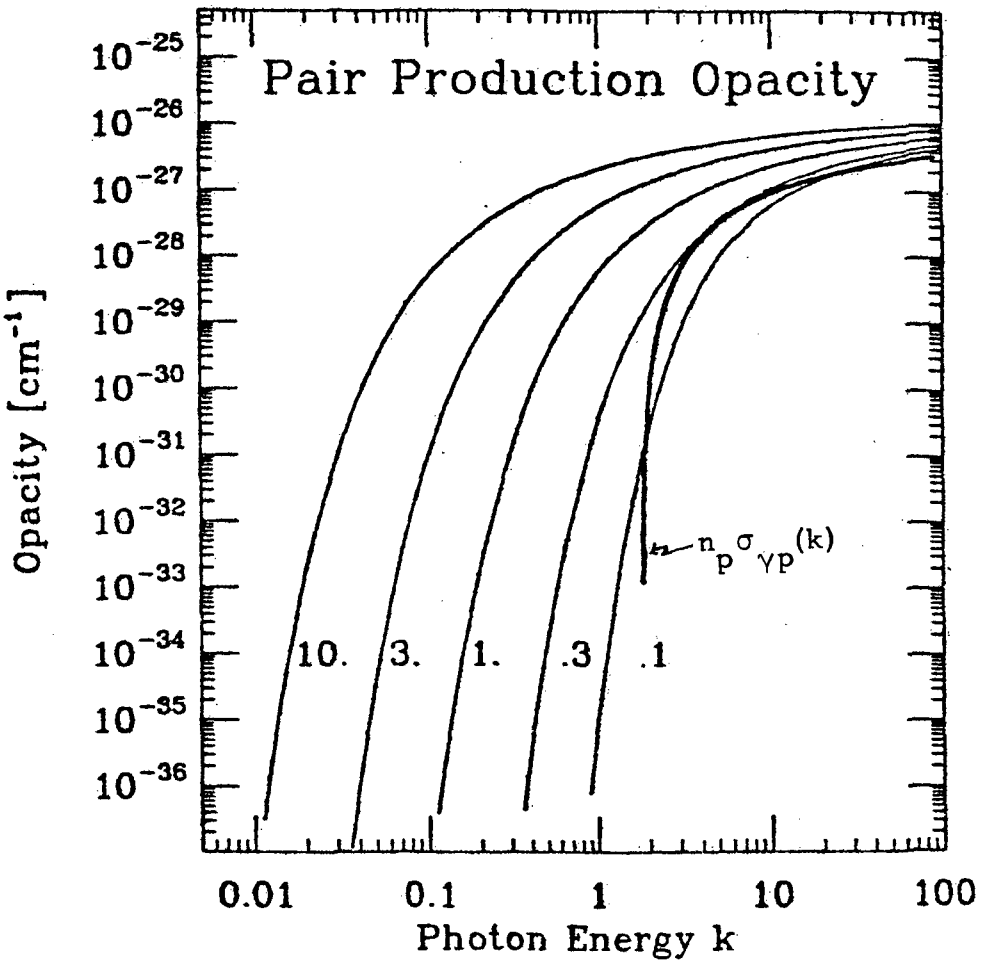

Figure 10. Photon-particle pair production opacity. The opacity of a photon with energy k due to photon-particle pair production from a MB distribution of electrons or protons is shown at various temperatures. For photon-photon pair production at these temperatures, the opacity is given by $n_p \sigma_{\gamma p}(k)$, where n_p is the proton number density and $\sigma_{\gamma p}(k)$ is the cross section (II-29).

C. Untrarelativistic Regime: Asymptotic Forms for the Rate Processes

Having described a method for calculating the rate at which photons populate the Wien component, it is now necessary to give expressions for the rates associated with pair production and annihilation from the various photon and particle processes. At ER temperatures, asymptotic forms can be derived so that the pair balance equation (8) can be solved directly. This ultimately gives the steady state positron density $z(\tau_p, \Theta, n_p)$ and the critical proton optical depths $\tau_p^{cr}(n_p, \Theta)$, when equations (8) and (15) are jointly satisfied.

The asymptotic expressions given below for rates of pair production through different processes are accurate to roughly 10-20%, with the accuracy typically increasing with temperature. This is adequate since, as mentioned earlier, the basic assumption that the particles obtain a thermal form is not correct at these temperatures (Section III. F), though an effective temperature could be assigned on the basis of the average particle energy. The annihilation rate r_a at ultrarelativistic temperatures has already been derived. It is proportional to the reciprocal of equation (III-42):

$$r_a = z(z+1)\, n_p^2 (c\pi r_e^2)\, \ell n\, \Theta / (2\Theta^2) \quad , \tag{24}$$

valid for $\Theta \gg 1$. The associated rate coefficient is shown in Figure 9.

For the production of pairs in e^+-e^- collisions, the reaction rate

$$r_{+-} = z(z+1)\, n_p^2\, 28\, \alpha^2 \sigma_T c\, \ell n^3 \Theta / 9\pi^2 \qquad (25)$$

is used (Zdziarski 1982). Since pair production from e^--e^- and e^+-e^+ collisions have similar form, the total pair production rate r_{ee} for the three mechanisms is equal to r_{+-}, but with $z(z+1)$ changed to $(2z^2 + 2z + 1/2)$. An adequate representation for the pair production rate from collisions of protons with electrons and positrons is, fitting the numerical results shown in Figure 9,

$$r_{ep} = (2z+1)\, n_p^2\, \alpha^2 \sigma_T c\, \ell n^2 \Theta / 16 . \qquad (26)$$

The rate of pair production through photon-particle and photon-photon interactions depends on the steady state photon spectral density. For the internally produced bremsstrahlung photons, the spectral density is given by

$$n_\gamma^b(k) = \tau_p\, t_C\, S_\gamma^b(k) \qquad (27)$$

where $t_C = (c\, n_p \sigma_T)^{-1}$ and $S_\gamma^b(k)$ is the source function of bremsstrahlung photons. This relation assumes that the magnitudes of the absorption coefficients κ_C, $\kappa_{\gamma\text{-par}}^b$, and $\kappa_{\gamma-\gamma}^b$ are small compared to κ_L at photon energies important for pair production, that is, for $k > 1/\Theta$ (cf. equations (1) and (5)).

In other words, the use of equation (27) to calculate rates

from a bremsstrahlung-type spectrum of photons does not require the system to be optically thin except at photon energies $k > 1/\Theta$. Otherwise there is a frequency-dependent distortion, and the use of equation (27) will not provide valid estimates for the pair production rate processes. In terms of the Compton opacity, this requirement translates into $\tau_C(k)/3 = \kappa_C(k) \cdot L/3$ at $k = 1/\Theta$, where the Compton opacity is largest. At ER temperatures, this value of k is in the KN regime and one gets the condition $\tau_C^o = (2z+1)\tau_p < 12$, using equation (20) to evaluate $\tau_C(k)$.

Absorption of energetic photons through pair producing mechanisms can also distort the spectrum (27). From equation (23) and the high energy form of the cross section (III-28), $\sigma_{\gamma e}(k) \rightarrow (7\alpha/6\pi)\sigma_T(\ell n\, 2k - 109/42)$, one obtains

$$\kappa_{\gamma e}(k) = (2z+1)(\alpha n_p \sigma_T)\left(\frac{7}{6\pi}\right) e^{-\mu\delta}\left\{1 + \left(1+\frac{\mu\delta}{2}\right)\left[\ell n(2\delta) - \frac{109}{42}\right] + e^{\mu\delta/2} E_1(\mu\delta/2)\right\} , \qquad (28)$$

where $\delta = \max[\delta_+, \mu/2]$ and $\delta_+ \cong 4/k$. For $4 \ll k \ll 8\Theta$, equation (28) reduces to

$$\kappa_{\gamma e}(k) = (2z+1)(7/6\pi)(\alpha n_p \sigma_T)\,\ell n(4\eta_p k\Theta) , \qquad (29)$$

with $\eta_p = \exp(1 - \gamma_E - 109/42)$. Requiring $\kappa_{\gamma e} < n_p\sigma_T/\tau_p$ at photon energies where $\kappa_{\gamma e}(k)$ is largest in the pair producing

regime, namely for $k \sim 3\Theta$, one obtains the requirement $(2z+1)\,\tau_p < 6\pi\alpha^{-1}/7\,\ell n(4\eta_p k\Theta)$, a much weaker condition than that imposed by the Compton opacity. The contribution to absorption due to pair production in photon-proton collisions is even smaller than $\kappa_{\gamma e}(k)$, though the asymptotic forms of the cross sections (II-28) and (III-29) are the same in the limit $k \to \infty$. The argument resembles the one presented in the Appendix contrasting reaction rates for a nonrelativistic and ER system of particles.

To determine whether the bremsstrahlung spectrum is distorted from photon-photon absorption of one bremsstrahlung photon by another, one must calculate the absorption coefficient $\kappa^b_{\gamma\gamma}$ of a photon traversing a photon gas having a bremsstrahlung-type distribution. Using the spectrum (14) for the bremsstrahlung photons with equation (III-25) gives

$$\kappa^b_{\gamma\gamma}(k) = \tau_p(8z^2+10z+3)(2n_p \alpha r_e^2) \int_1^\infty du\, u^{-3}\, \ell n\left(\frac{\eta_E \Theta^2 k}{u}\right) \bar{\varphi}(u)\,. \qquad (30)$$

The values of the definite integrals defined by equation (30) are 1.55 and 3.40 from numerical calculation, the latter number referring to the integral containing the $\ell n\, u$ term. From equation (30), one obtains the condition

$$(8z^2 + 10z + 3)\,\tau_p^2 < \alpha^{-1}/1.2\,\ell n(\eta_W k\Theta^2)\,, \qquad (31)$$

where $\eta_W = 0.86$, requiring that $\kappa_{\gamma\gamma}(k) < n_p \sigma_T / \tau_p$. This estimate is accurate because pair production in photon-photon collisions occurs chiefly for photons k and k' related by $k \cdot k' \sim \mathcal{O}(1)$ due to the threshold and high energy behavior of the photon-photon pair production cross section. When $k \sim \mathcal{O}(\Theta)$, the bremsstrahlung photons $k' \sim \mathcal{O}(\Theta^{-1})$ primarily responsible for pair production are well described by the Gaunt factor (12) at ER temperatures.

From the preceding considerations, we see that the severest restriction to the use of the spectrum (27) for calculating rates comes from the Compton opacity condition, $\tau_C^o < 12$. Therefore, at optical depths as great as one or two, the calculated pair production rates will be accurate. In fact, when optical depths approach this value, the greater portion of pair production proceeds through the photons Comptonized to the Wien form, so that the rates calculated from equation (27) are least accurate when the net contribution of the bremsstrahlung spectrum (27) to pair production is smallest.

Numerical techniques were used to evaluate pair production rates from a bremsstrahlung spectrum containing the exact B-H formula as a check to analytical estimates. The formula derived by Lightman (1982) for the pair production rate from photon-electron collisions accurately describes the numerical results for this process. The rate is

$$r^b_{\gamma e} = \tau_p (2z+1)(8z^2+10z+3) \left(\frac{16}{9\pi}\right) (\alpha^2 n_p^2 c\sigma_T) \ell n^2 \Theta \, \ell n \, 4\Theta \, (1 - \Theta^{-1}) , \qquad (32)$$

adding the term $(1 - \Theta^{-1})$ to the equation of Zdziarski (1982). The expression

$$r^{b}_{\gamma p} = \tau_p (8z^2 + 10z + 3)(0.014)(\alpha^2 n_p^2 c\sigma_T) \ell n^2 \Theta \ \ell n^3 \ 3\Theta \qquad (33)$$

is valid for the pair production rate due to bremsstrahlung photons interacting with protons at ER temperatures. The pair production rate due to self-interacting bremsstrahlung photons is described by the formula

$$r^{b}_{\gamma\gamma} = \tau_p^2 (8z^2 + 10z + 3)^2 (0.91)(\alpha^2 n_p^2 c\sigma_T) \ell n^3 \Theta \ (1 + 2/\Theta^2) \ . \qquad (34)$$

The numerical calculations for the associated rate coefficients are shown in Figure 9.

The values calculated for $r^{b}_{\gamma\gamma}$ are in poor agreement with Zdziarski's numerical calculation. Moreover, the rates given by Svensson (1982) for these processes are seriously in error, so the results of the calculations of this paper are suspect.

Turning now to the Wien component of the photon spectrum, considerations based on equation (1) give

$$n^{W}_{\gamma} = [\, c(\kappa_L + \kappa_{\gamma\text{-par}} + \kappa_{\gamma\gamma})]^{-1} S^{W}_{\gamma} \qquad (35)$$

for the number density of photons in the Wien distribution. The production rate of Wien photons was calculated in the preceding section, and the term in brackets represents an average residence time

$\overline{T}^{W}(\Theta)$ for a photon in the Wien distribution (κ_C, of course, is absent, since Comptonization merely sustains a Wien photon in the distribution). Letting

$$\overline{T}^{W}(\Theta) = [T_L^{-1}(\Theta) + T^{-1}_{\gamma\text{-par}}(\Theta) + T^{-1}_{\gamma\gamma}(\Theta)]^{-1}, \tag{36}$$

it is a simple matter to calculate the individual average timescales of equation (36) by considering averages over the Wien spectrum (11). Recalling the form of $\kappa_L(k)$, we have

$$T_L(\Theta) = (2\Theta^3)^{-1} \int_0^\infty dk\, k^2 (c\,\kappa_L)^{-1} \exp(-\mu k)$$

$$= t_C\, \tau_p (2\Theta^3)^{-1} \int_0^\infty dk\, k^2 (1 + \tau_C/3) \exp(-\mu k). \tag{37}$$

For $\Theta \gg 1$, an insignificant fraction $\sim (6\Theta^6)^{-1}$ of the Wien photons are scattering outside the KN regime $k > \Theta^{-1}$. Thus, it is an excellent approximation to use equation (20) in equation (37), giving

$$T_L(\Theta) = t_C \tau_p \left[1 + \frac{\tau_C^o \ln(\eta_L \Theta^2)}{32\Theta^2}\right], \tag{38}$$

where $\eta_L = 4 \exp(3/2 - 2\gamma_E)$.

There are four other average residence times in equation (34) associated with photon-electron, photon-proton, and photon-photon absorption of the Wien photons, the last depending on whether the

opacity results from photons in the Wien or bremsstrahlung component of the photon spectrum. These timescales may be estimated as proportional to the inverse of the reaction rates, according to the relation $T^{W}_{\gamma e} = n^{W}_{\gamma}/r^{W}_{\gamma e}(\Theta)$, with analogous expressions for $T^{W}_{\gamma p}$, $T^{W}_{\gamma\gamma}$, and $T^{Wb}_{\gamma\gamma}$, employing obvious notation.

The particle production rates from photon-particle collisions can be derived from the asymptotic forms of the cross sections (III-28) and (III-29) at high energies. One obtains for the pair production rate from ER thermal electrons and positrons interacting with photons in the Wien distribution, using equations (III-30) and (29),

$$r^{W}_{\gamma e}(\Theta) = (2z+1)\,\alpha c \sigma_T\, n_p\, n^{W}_{\gamma} \left(\frac{7}{16\pi}\right) \ell n(\eta_u \Theta^2) , \qquad (39)$$

where $\eta_u = 4 \exp(5/2 - 2\gamma_E - 109/42)$. The pair production rate from Wien photons interacting with protons can also be determined from equation (III-30), though now with $\mu >> 1$. The result is

$$r^{W}_{\gamma p}(\Theta) = \alpha c \sigma_T\, n_p\, n^{W}_{\gamma} \left(\frac{7}{16\pi}\right) (\ell n \Theta - 0.98 + 1.2/\Theta) . \qquad (40)$$

The term in Θ^{-1} was added in order to more accurately fit the numerically calculated rate near $\Theta \cong 3$.

The pair production rate from a self-interacting Wien distribution of photons can be derived from equations (III-31) and the asymptotic form of $\bar{\varphi}(k \cdot k')$ given by Gould and Schréder (1967). One obtains

$$r^{W}_{\gamma\gamma}(\Theta) = c\pi r_e^2 n_\gamma^{W\,2} [\ln\Theta + (\ln 4 - 2\gamma_E)]/2\Theta^2 \qquad (41)$$

at ER temperatures. The pair production rate from the Wien component interacting with the bremsstrahlung component of photons is calculated from equations (III-30) and (30). One finds that at ER temperatures,

$$r^{Wb}_{\gamma\gamma}(\Theta) = \tau_p(8z^2 + 10z + 3)\ 3.1\ \alpha c r_e^2 n_p n_\gamma^{W} \ln(\eta_{Wb}\Theta^3), \qquad (42)$$

where $\eta_{Wb} = \eta_W \exp(3/2 - \gamma_E)$. This expression is accurate to 5% for temperatures $\Theta \geq 3$, as verified by the numerical calculations plotted in Figure 9.

The preceding rates were used to model a stable ER thermal plasma. The results are shown in Figure 11. In the Figure, the positron density is plotted as a function of temperature for various values of the proton optical depth τ_p, at proton density $n_p = 10^{10}\ cm^{-3}$. Either zero, one, or two roots exist for each value of Θ and τ_p, because the pair balance equation (8) is a polynomial equation in z. The annihilation term, proportional to $z(z+1)$, vanishes at zero, whereas the pair production term is a higher order polynomial with positive coefficients multiplying the powers of z, so the maximum number of roots is two.

The physical conditions corresponding to the absence of a stable solution to the pair balance equation were discussed above.

Figure 11. Equilibrium pair density and maximum proton optical depth at extreme relativistic temperatures. The steady state pair density z of a nonmagnetic relativistic thermal plasma is shown in Figure 11a as a function of temperature Θ for $\Theta \gg 1$ at different values of the proton optical depth τ_p. The proton number density $n_p = 10^{10}$ cm^{-3}. The maximum τ_p of a steady thermal relativistic plasma is shown in Figure 11b as a function of critical temperature Θ_{cr}. For proton optical depths greater than the values indicated, a stable system must be in a condition of complete thermodynamic equilibrium. The dependence on proton number density at these temperatures is shown for $n_p = 1.0$ cm^{-3} and $n_p = 10^{25}$ cm^{-3}.

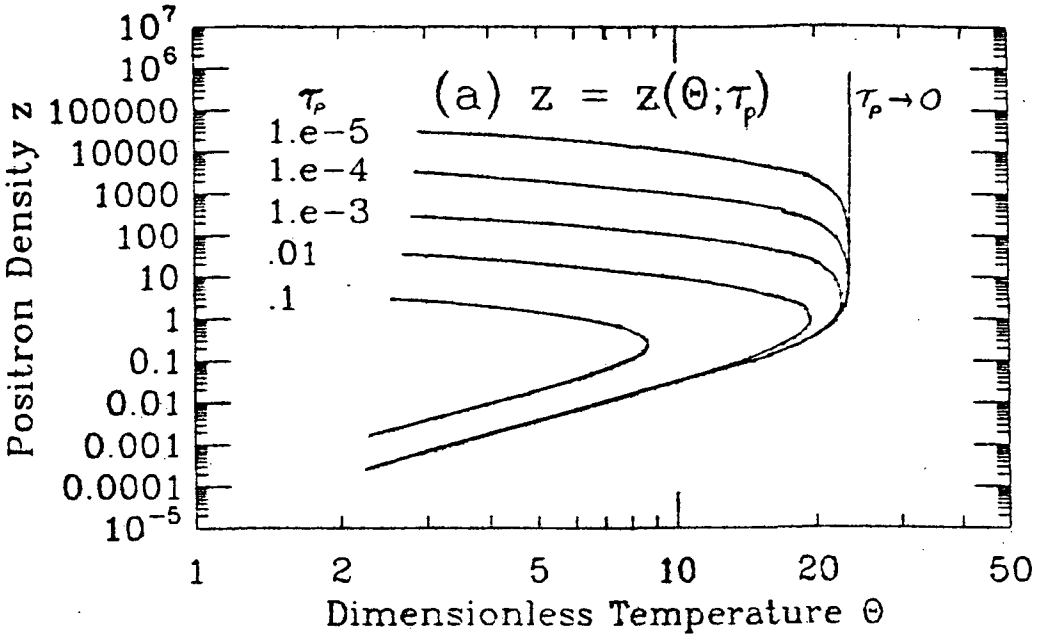
Positron Density z
10^7
10^6
100000
10000
1000
100
10
1
0.1
0.01
0.001
0.0001
10^{-5}
τ_p
1.e-5
1.e-4
1.e-3
.01
.1
(a) z = z(Θ;τ_p)
$\tau_p \to 0$
1
2
5
10
20
50
Dimensionless Temperature Θ

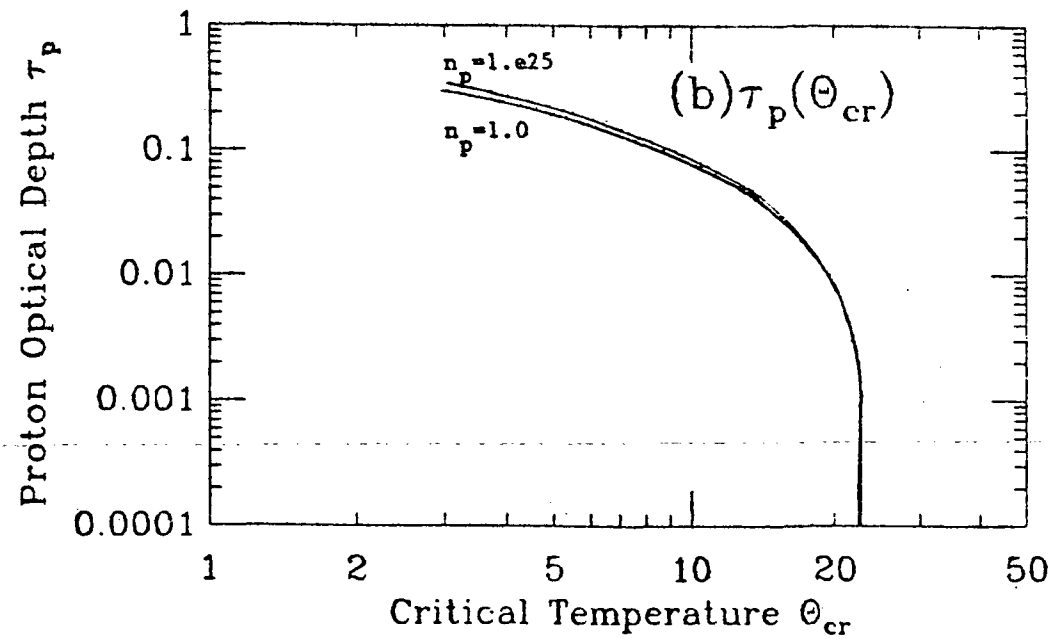
Proton Optical Depth τ_p
1
0.1
0.01
0.001
0.0001
n_p=1.e25
n_p=1.0
(b)$\tau_p(\Theta_{cr})$
1
2
5
10
20
50
Critical Temperature Θ_{cr}

The temperature at which a single root exists represents the maximum critical temperature for a given proton optical depth. Values of $\tau_p(\Theta_{cr})$ at ER temperatures are shown in Figure 11b. The maximum critical temperature is approximately equal to 24 in the limit of zero optical depth, as calculated earlier. A weak dependence of the critical temperature on n_p is observed at densities of astrophysical interests, which becomes more pronounced as τ_p increases, reflecting the increasing importance of Comptonization and the value of the bremsstrahlung absorption cutoff. The model breaks down at temperatures $\Theta \sim 2\text{-}4$ where the asymptotic forms for the rate factors begin to fail. Discussion of the double roots below the critical temperature at a given optical depth will follow a treatment of the system at subrelativistic temperatures, where the same behavior is observed.

D. Subrelativistic Regime: Large Optical Depths

For temperatures $\Theta \ll 1$, the steady state positron density decreases exponentially with temperature at low optical depth due to the threshold behavior of the cross section and the Boltzmann factor $\exp(-E/\Theta)$ governing the distribution of particles or photons with energy E. This behavior is suggested by the variation of the rate coefficients in Figure 9 at low temperatures. One sees that a significant positron density will be produced only if there is a large Wien component of the photon spectrum, that is, when the system

has large optical depth and Comptonization is important. The large value of $R^{W}_{\gamma\gamma}$ compared to the other pair production coefficients obtains because the average photon energy in the Wien distribution is relatively large.

The phase diagram corresponding to Figure 11a can be completed at subrelativistic temperatures and large optical depths by applying the method of the last two sections to this regime. Comptonization will be treated as before, though now with the appropriate production spectra. The most important photon sources are annihilation, bremsstrahlung, and double Compton production. The double Compton mechanism if of the same order as bremsstrahlung in the fine structure constant, so is significant when the density of photons approaches the particle density.

We employ the nonrelativistic Born approximation for the bremsstrahlung production cross section in the soft photon limit at subrelativistic temperatures, giving

$$S^{b}_{\gamma}(k;\Theta) = \Sigma_{b}\, k^{-1}\, \ell n\left(\frac{\eta_{g}\Theta}{k}\right) , \tag{43}$$

where $\Sigma_{b} = 2[z(z+1) + 2^{1/2}(1+2z)]\, n_{p}^{2}\, \alpha c \sigma_{T} (\pi\Theta)^{-1/2}$ and $\eta_{g} = 4\exp(-\gamma_{E})$. The term proportional to $z(z+1)$ accounts for the contribution from e^{+}-e^{-} bremsstrahlung, and follows from the considerations of Joseph and Rohrlich (1958; cf. Appendix). The other term is for e-p bremsstrahlung. The e^{-}-e^{-} and e^{+}-e^{+} thermal

bremsstrahlung spectra are much smaller at these temperatures since there is no dipole moment in the scattering system of two identical particles, so is neglected. In the same soft photon low temperature regime, the double Compton spectrum

$$S_{\gamma}^{d}(k;\Theta) = (2z+1)\, n_p\, n_{\gamma}^{W}\, \alpha c r_e^2 \left(\frac{16}{9}\right) \Theta^2 k^{-1} \qquad (44)$$

is used (Svensson 1984).

Since $\Theta \ll 1$, all Compton scattering takes place in the Thomson limit. Solving the integral (15) for the rate of population of the Wien regime by Comptonization, noting that for $\tau_C^o \gtrsim 1$ most photons originate in the soft photon portion of the production spectra, one obtains

$$S^{W}(\Theta) = \left(\frac{2\kappa_C}{\kappa_{TOT}^{a}}\right) r_a(\Theta) + \left[\Sigma_{dC} + \ell n\left(\frac{\eta_g}{3}\right)\Sigma_b\right] \Omega\left(X_0^{u_b} - X_0^{u_0}\right)$$

$$+ \Sigma_b\, \Omega^2 \left[X_0^{u_b}(u_b \ell n\, X_0 - 1) - X_0^{u_0}(u_0 \ell n\, X_0 - 1\right] . \qquad (45)$$

The terms X_0, Ω, and u_b are defined as before, and $u_0 = \ell n\, 3/\ell n\, A$, though now $A \to 1 + 4\Theta$ in the definitions of u_b and u_0. The value of k_b is found by identifying $\kappa_b(k)$ and $\kappa_C(k)$, since $\kappa_L \ll \kappa_C$ at large optical depths. The analytic result (30) was evaluated by imposing a cutoff at $k = \Theta$ which, from our previous discussion, should not be a bad approximation in an optically thick system.

The first term in equation (45) is due to the Comptonized

annihilation photons, the factor of two accounting for the two photons produced per annihilation event. At temperatures $\Theta \leq 0.4$, the annihilation rate is given approximately by

$$r_a(\Theta) = z(z+1)n_p^2 R_a(\Theta) = z(z+1)n_p^2 c\pi r_e^2 (1 - 0.9\Theta) \quad . \tag{46}$$

The probability that an annihilation photon will be Comptonized rather than ultimately absorbed or lost from the system is given by the ratio of the absorption coefficients

$$\frac{\kappa_C}{\kappa_{TOT}^a} \cong \left[1 + \frac{\left(\kappa_L + \kappa_{\gamma\gamma}^a + \kappa_{\gamma\gamma}^{Wa} \right)}{\kappa_C} \right]^{-1} \tag{47}$$

neglecting the opacity that an annihilation photon might suffer due to pair production from a proton, positron, or electron, which are exponentially small at these temperatures. The absorption coefficients $\kappa_{\gamma\gamma}^{Wa}$ and $\kappa_{\gamma\gamma}^{a}$ represent the opacity of an annihilation photon to pair production from interactions with other photons in the Wien or annihilation component, respectively. At these low temperatures most annihilation photons have energies near $k = 1$, so we can approximate the coefficients by the frequency-independent relations $c\kappa_{\gamma\gamma}^{Wa} = r_{\gamma\gamma}^{Wa}(\Theta)/n_\gamma^a$ and $c\kappa_{\gamma\gamma}^{a} = r_{\gamma\gamma}^{a}(\Theta)/n_\gamma^a$, where n_γ^a is the number density of annihilation photons. Numerical expressions for the rate coefficients $r_{\gamma\gamma}^{Wa}(\Theta)$ and $r_{\gamma\gamma}^{a}(\Theta)$ to photon-photon pair production are given below.

The number density of Wien photons n_γ^W is computed as in the earlier section, by introducing an average residence time $\overline{T}^W(\Theta)$ during which a Wien photon survives before being lost from the distribution. It is given by

$$\overline{T}^W(\Theta) \cong \left[cK_L + r_{\gamma\gamma}^W(\Theta)/n_\gamma^W + r_{\gamma\gamma}^{Wa}(\Theta)/n_\gamma^W \right]^{-1} , \qquad (48)$$

retaining only the important absorption processes. Thus $n_\gamma^W = \overline{T}^W(\Theta) S^W(\Theta)$, with the expression for Wien photon/annihilation photon reaction rate $r_{\gamma\gamma}^{Wa}$ given below.

The reaction coefficient for the production of pairs due to a self-interacting Wien distribution was numerically calculated and is shown in Figure 9. Weaver (1976) gives a numerical fit to the low temperature rate. Noting the errors in his equation (33), it is

$$r_{\gamma\gamma}^W = \frac{c\pi^2 r_e^2 e^{-2/\Theta}}{8\Theta^3} (1.042) [1 + 0.728\Theta]^{7/2} n_\gamma^{W2} , \qquad (49)$$

good to 5% for $\Theta \leq 0.4$. A numerical fit to the rate coefficient $R_{\gamma\gamma}^{Wa}(\Theta)$ describing pair production from annihilation photons interacting with Wien photons is given by

$$R_{\gamma\gamma}^{Wa}(\Theta) = 0.80\, c r_e^2\, \Theta^{-1.9} e^{-1/\Theta} . \qquad (50)$$

The associated reaction coefficient is given by the expression

$$r_{\gamma\gamma}^{Wa}(\Theta) = z(z+1) n_p^2 n_\gamma^W R_{\gamma\gamma}^{Wa}(\Theta) t_C^{-1} \overline{T}^a(\Theta) , \qquad (51)$$

employing the value t_C for the average lifetime $\bar{T}^a(\Theta)$ of an annihilation photon in the calculation of equation (51). Likewise characterizing the average spectral density of annihilation photons through the use of the residence time t_C, one obtains

$$r^a_{\gamma\gamma}(\Theta) = z^2(z+1)^2 n_p^4 [2.06\, c\, r_e^2\, \Theta \exp(-4\Theta)]\, t_C^{-2} [\bar{T}^a(\Theta)]^2 \qquad (52)$$

for the rate at which pairs are produced by self-interacting annihilation photons, from a fit to the numerical results. The rate coefficient $R^a_{\gamma\gamma}$ is the term in brackets in equation (52). Equations (50) and (52) are accurate to 10% for $0.075 \leqslant \Theta \leqslant 0.4$.

The mean lifetime of an annihilation photon is given by $\bar{T}^a = (c\kappa^a_{TOT})^{-1}$. Using the definition (47) of κ^a_{TOT} and the rates (46), (51), and (52), one finds that

$$t_C^{-1}\bar{T}^a(\Theta) = \left\{(2z+1) + [\tau_p(1+\tau_C^o/3)]^{-1} + \frac{[z(z+1)n_p^2 R^a_{\gamma\gamma} + n^W_\gamma R^{Wa}_{\gamma\gamma}]}{2R_a}\right\}^{-1}. \qquad (53)$$

Given n_p, τ_p, and z, equation (48) and (53) are iterated until the two are jointly satisfied. Then z is incremented until the pair balance equation

$$r^a(\Theta) = r^W_{\gamma\gamma}(\Theta) + r^a_{\gamma\gamma}(\Theta) + r^{Wa}_{\gamma\gamma}(\Theta) \qquad (54)$$

is additionally satisfied.

The numerical simulation was performed throughout the temperature regime $\Theta \leq 0.4$, not only where the expressions for the rates associated with annihilation photons were accurate. This was because these rates proved small at the temperatures and optical depths used, relative to the pair production rate (49) associated with self-interacting Wien photons, which is valid down to the lowest temperatures.

The results are plotted in Figure 12 for a background proton density $n_p = 10^{10}\ cm^{-3}$, along with the ER temperature results for comparison. Proton optical depths $\tau_p = 0.5$, 1.0, 3.0, and 5.0 were used. Although the approximations (such as the calculation of k_b) applied to the optically thick regime, it appears that one could smoothly extend the curve $z(\Theta, \tau_p = 0.5)$ to the expected values at ER temperatures. Additional pair production due to internally produced bremsstrahlung photons would serve to increase the value of z in the low z branch of the curve for $\tau_p = 0.5$, improving the agreement. Thus we can be confident that the results for the model at ER temperatures and at subrelativistic temperatures, large optical depths are consistent.

E. Discussion

Above a critical temperature, a steady optically thin non-magnetic plasma cannot exist. The efficiency of particle producing mechanisms will ensure that excess energy is transformed into

Figure 12. Equilibrium pair density at subrelativistic temperatures. The steady state pair density z of a nonmagnetic relativistic thermal plasma is shown as a function of Θ for $\Theta \ll 1$ at different values of the proton optical depth τ_p. The proton number density $n_p = 10^{10}$ cm^{-3}. The results at extreme relativistic temperatures, from Figure 11a, are shown for comparison.

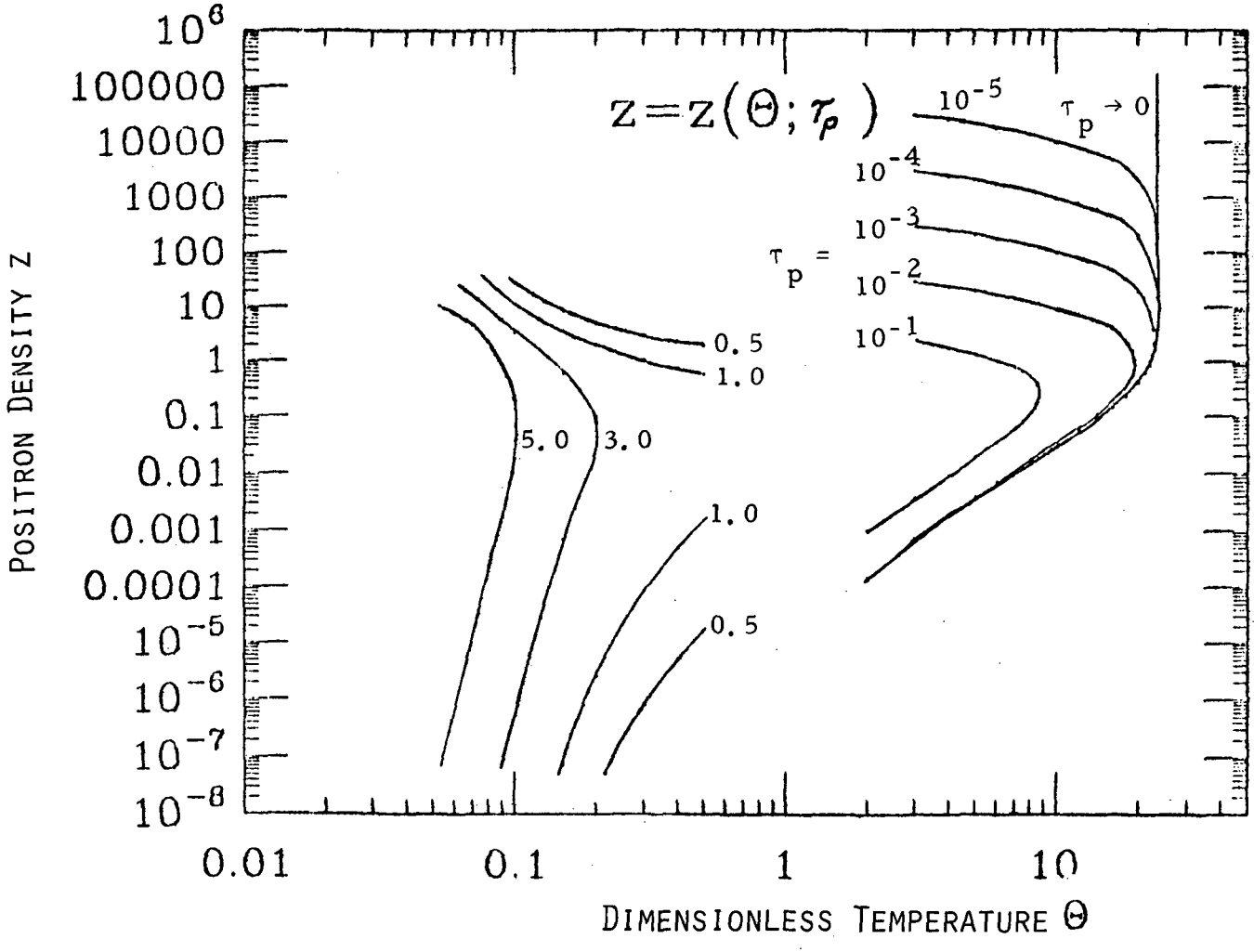
$Z = Z(\Theta; \tau_p)$
$\tau_p \to 0$
10^{-5}
10^{-4}
10^{-3}
10^{-2}
10^{-1}
$\tau_p =$
0.5
1.0
5.0
3.0
1.0
0.5
POSITRON DENSITY Z
10^6
100000
10000
1000
100
10
1
0.1
0.01
0.001
0.0001
10^{-5}
10^{-6}
10^{-7}
10^{-8}
0.01
0.1
1
10
DIMENSIONLESS TEMPERATURE Θ

particles and photons until conditions of complete thermodynamic equilibrium obtain. To produce a system in thermodynamic equilibrium at relativistic temperatures would require a tremendous energy source, as the energy density goes as Θ^4.

This conclusion does not invalidate the existence of relativistic nucleonic gases and the calculations of Section III.E, provided that the system has a transient lifetime. For a consistent characterization, the system lifetime would have to be bracketed between the timescale for thermalization and the timescale for particle production. The most obvious candidate for such a configuration would be accretion into a massive compact object or black hole. Zdziarski (1982) has considered these timescale in the context of spherical accretion, and a great deal of effort is being devoted to the task of calculating spectra resulting from disk and spherical accretion (Eilek 1980; Eilek and Kafatos 1983; Mészáros and Ostriker 1983; Mészáros 1983).

The existence of two roots for the positron density below the critical temperature at a given set of values of the system parameters follows from the assumptions adopted for the thermal plasma. The numerical results show that except near the critical temperature and when optical depths $\tau_p \geq 0.1$, the lower branch is dominated by pair production from particle-particle collisions, and the upper branch is dominated by pair production through photon processes. When

$\tau_p \geq 0.1$, it is the Comptonized Wien photons that make the largest contribution to pair production in both branches.

Both solutions are valid for a uniform system. Lightman (1982) interprets the upper branch as being physically unstable to density and temperature perturbations. He arrives at this conclusion because the upper branch has a negative specific heat, that is, a differential increase in the energy of the system will lead to a reduction in temperature, because most of the added energy will be transformed into particle mass energy which in turn must be thermalized. The physical result will be clumping in the system.

Comparing the results of the positron density phase diagrams, Figures 11 and 12, with the work of other investigators, one finds acceptable agreement with only one other study, that of Svensson (1984). At the highest temperatures the phase portrait differs from that of Lightman (1982) due to his error in the pair production rate from particle-particle collisions. At temperatures near $\Theta = 3$ and optical depths at which this mechanism is no longer important, general agreement is found. Disagreement with the paper of Svensson (1982) was traced to numerical errors in his calculations of pair production rates arising from internally produced bremsstrahlung photons. Evidently these errors are corrected in his 1984 paper, as a different phase portrait is presented. Even though different methods were used, the numerical values of $z(\Theta, \tau_p, n_p)$ between this work

and Svensson's latest results are in agreement (20-40% difference at worst).

A complete numerical simulation of the system was also undertaken with the Compton scattering process performed by means of numerical calculation of equations (6) and (7). It was found necessary to broaden the Comptonized spectra over one decade in energy consistent with conservation of energy and photon number in order to reduce numerical artifacts originating from the discrete nature of the Compton scattering approximation. At any rate, this broadening probably more closely simulates actual Comptonization by relativistic thermal electrons, judging from the Monte Carlo calculations of Pozdnyakov, Sobol', and Syunyaev (1978).

Calculation of the emergent spectra from relativistic thermal plasma at temperatures $\Theta = 1$ and $\Theta = 3$ is shown in Figure 13 for arbitrary values of the proton optical depth. The system is in a condition of pair equilibrium with $n_p = 10^{10}$ cm^3. The lower curves of Figure 13 labeled "1" represent the production spectra due to bremsstrahlung and annihilation processes. The upper curves labeled "2" represent the production spectra after suffering effects of absorption, and the curves labeled "3" are the emergent spectra after accounting for Comptonization of the produced photons, calculated in a self-consistent manner. One observes moderate Comptonization in Figure 13a, and the formation of a Wien peak in Figure 13b. In Figure

13c, a distorted Wien hump is seen in the emergent spectrum. This is because the temperature used is very close to the critical temperature at this optical depth, where photon-photon absorption becomes important for photons with energies near $k = 1$. The features of the emergent spectrum at low photon energies in Figure 13c are not to be considered as artifacts of the Comptonization method. Comparing the Monte Carlo results of Pozdnyakov et al. just cited, one finds that low energy spectral variations can propagate over many decades of photon energy, even after multiple Compton scatterings.

A recent preprint (Zdziarski 1984) gives spectra from a full Monte Carlo simulation of a nonmagnetic relativistic thermal plasma, even treating changes in photon density over the spherical region. Though the parameters used are not the same, one can compare the features of the spectra in Figure 13 with those of this paper. The agreement is good. One must note, however, that Zdziarski artificially imposes a pair density in his model, so his system is not in pair balance.

The fully numerical treatment gives general agreement with results for the equilibrium pair density calculated in the approximate analytic fashion. It was not pursued because the analytic method proved more fruitful, and convergence problems arose in the numerical method at large optical depths. In both cases, though, no annihilation feature was determined to be expected from a stable, relativistic plasma in pair balance, agreeing with the conclusion of Svensson (1984).

Figure 13. Numerical simulation of nonmagnetic relativistic thermal plasma. Production and emergent spectra of a uniform nonmagnetic relativistic plasma are shown for temperatures and optical depths indicated. Calculated equilibrium positron densities are also shown. Label "1" refers to the photon production spectrum from bremsstrahlung and annihilation processes, label "2" refers to the steady photon spectrum after suffering effects of absorption, and label "3" refers to the emergent spectrum after Comptonization.

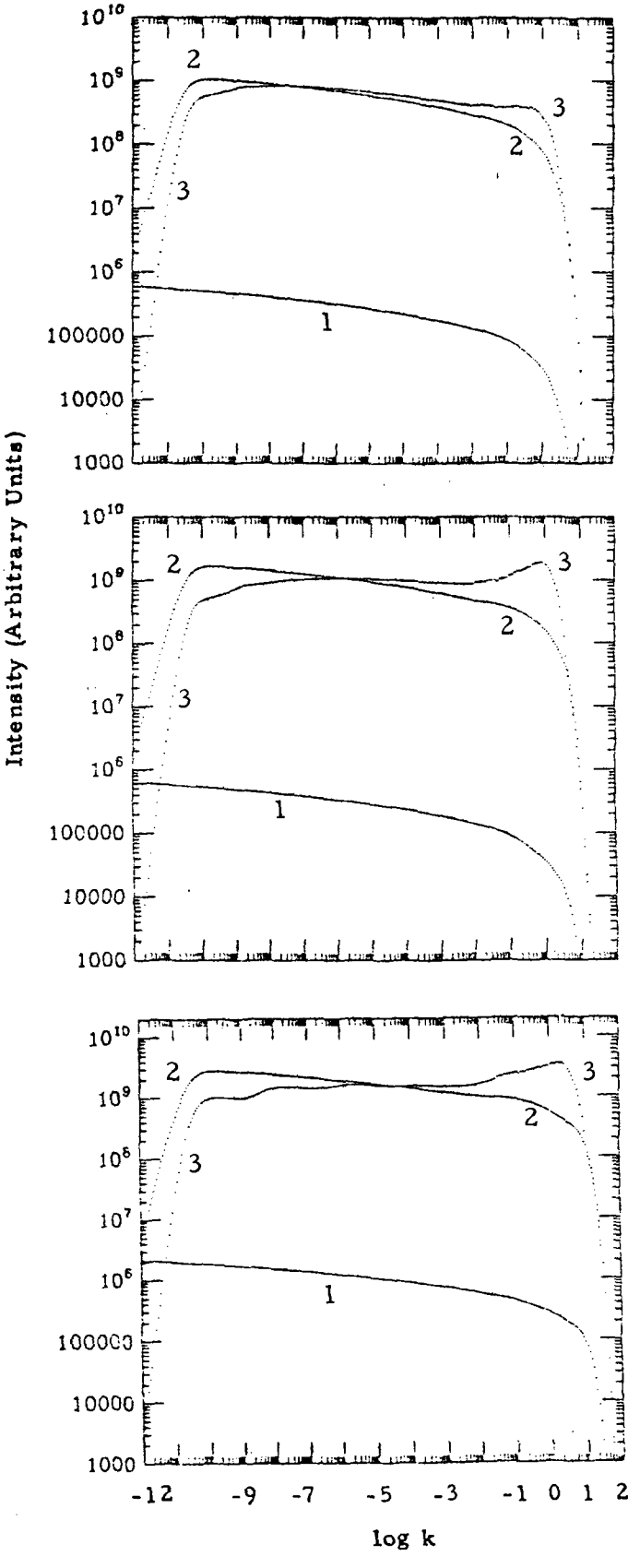

(a) $\Theta = 1.0$
$\tau_p = 0.5$
$z = 3.2 \cdot 10^{-4}$

(b) $\Theta = 1.0$
$\tau_p = 1.0$
$z = 1.6 \cdot 10^{-2}$

(c) $\Theta = 3$
$\tau_p = 0.4$
$z = 2.8 \cdot 10^{-2}$

V. SUMMARY AND CONCLUSIONS

This preliminary investigation into the physics of nonmagnetic, relativistic thermal plasmas was motivated by astrophysical observations showing that the existence of plasmas at relativistic temperatures may not be an uncommon feature of the universe. Most models suggest that relativistic plasmas originate from the dissipation of kinetic or elastic energy in the intense gravitational field of a compact massive object. Other speculations, such as bulk matter-antimatter annihilation, must however not be excluded.

In order to frame quantitative analyses of models relating to such observations, the elementary physics must be properly performed. It was the object of this study to help contribute to this goal. The principal results of this work are as follows:

(1) A relativistically correct description of the kinematics of particle and photon gases was performed, giving exact expressions for reaction rates and opacities of an isotropic gas consisting of photons and/or particles, and luminosities and production spectra from an isotropic particle plasma.

(2) Specializing to an isotropic Maxwell-Boltzmann particle gas consisting generally of different mass particles led to expressions for the reaction rate and luminosity in terms of a single integral over the invariant cross section, and to the production spectra (yielding either photons or material particles) in terms of a double

integral over the center-of-momentum cross section differential in the energy of the produced particles or photons.

(3) These results were used to analytically calculate the reaction rate, luminosity, and production spectra of annihilation photons from a Maxwell-Boltzmann electron-positron plasma, and to numerically calculate thermal electron-electron bremsstrahlung. Thermal electron-positron bremsstrahlung was calculated by interpolating between the modified Bethe-Heitler formula at nonrelativistic energies and the lowest order electron-electron bremsstrahlung cross section at relativistic energies.

(4) A treatment of the Compton power and moments of the Compton scattered spectrum was used to provide an approximate description of Comptonization in a relativistic plasma of photons and particles.

(5) Single particle reaction rates and energy loss timescales were examined in a relativistically correct manner. An expression for the luminosity (energy loss or energy exchange rate per unit volume) from the interaction of two different temperatures, different mass Maxwell-Boltzmann gases of particles was derived. This has potential application to two-temperature accretion disk models.

(6) Calculation of energy loss timescales led to the conclusion that an optically thin relativistic electron-proton plasma cannot obtain the Maxwell-Boltzmann form at temperatures greater than about 1 MeV, agreeing with the results of other workers.

(7) A compilation of pion production data from proton-proton collisions was made from threshold to ISR energies. The reaction rates and luminosities for different modes of pion production were calculated for a Maxwell-Boltzmann gas of protons at temperatures between 1 MeV and 1 GeV. It was concluded that above temperatures greater than about 60 MeV protons in the gas cannot obtain the Maxwell-Boltzmann form because of the energy loss due to pion production.

(8) A consideration of dominant processes was used to model a steady, uniform, nonmagnetic, relativistic thermal plasma. An approximate treatment of Comptonization was developed at subrelativistic temperatures $\Theta \leq 0.4$ and extreme relativistic temperatures $\Theta \geq 3$, where Θ is the temperature measured in units of the rest mass energy of the electron. Asymptotic expressions for rate processes were calculated, permitting quantitative analysis of the system.

(9) The equilibrium pair density was calculated as a function of temperature, proton optical depth, and proton number density. Either zero, one, or two roots were found for each set of values. Above a critical temperature dependent on the proton optical depth and proton number density, only a system in full thermodynamic equilibrium could exist under conditions of steady state.

(10) No annihilation feature should be observed from a non-magnetic relativistic thermal plasma in pair equilibrium, in agreement with other studies.

Further work must concern the properties of relativistic thermal plasmas in the presence of magnetic fields. The first steps in this direction have been taken at extreme relativistic temperatures (Araki and Suguru 1983; Kusunose and Takahara 1983). Having characterized the static properties of these systems, a dynamic treatment will be possible, permitting a better understanding of such interesting systems as gamma ray bursts, active galaxies, extragalactic jets, and quasi-stellar objects.

APPENDIX: NUMERICAL CALCULATION OF THERMAL BREMSSTRAHLUNG

Calculation of the Gaunt factors associated with thermal e-p, e-e, and e^+-e^- bremsstrahlung was performed numerically on a VAX/VMS. For e-p bremsstrahlung, only a single integral had to be evaluated (equation (III-14)). The integration was performed using Gauss-Laguerre quadrature after making the variable change $y = (\gamma_r - 1 - k)$. A 20-point routine proved sufficient.

The three-fold integral for the calculation of thermal e-e bremsstrahlung, equation (III-16), was more difficult due to the peaking of the angle-dependent differential cross section in the forward and backward directions. The small angle regime was magnified through the transformation $\cos\Theta = 1 - \exp(-z)$, extending the range of the integral from 0 to ∞ Also, double precision was required in the angular integration because of the presence of large, nearly cancelling factors.

For photon energies that were not small, that is, for $k \geq \Theta_e/10$, the transformation $x = \xi_{ee}/(k'+1)$ served to broaden the range of the k' integration. In both cases, the 20-point Gauss-Laguerre quadrature formula was employed for the integration. A Simpson algorithm, written to evaluate an integral to any desired degree of accuracy, was used to perform the integration over γ_r. Because of the slow variation of the integrand in the variable γ_r, 8 or 16 iterations were usually enough to calculate the integral over

an interval in γ_r to 1% accuracy, and typically 5 to 10 intervals of γ_r were needed to calculate the Gaunt factor to the same accuracy. This method exhibited which relative Lorentz factors are chiefly responsible for bremsstrahlung emission at a given temperature and photon energy.

For extremely low photon energies, the Gauss-Laguerre technique was not sufficiently accurate in the integration over k' due to the effects of the exponential in equation (III-18). This caused the value of the integral to be due largely from contributions in the immediate neighborhood of $k' = k$. In this case, the integral over k' was evaluated with Simpson's approximation to either side of $k' = k$, after determining in the program the range of the exponential factor for each iteration.

The Gaunt factors for thermal e^+-e^- bremsstrahlung were evaluated as for the e-e case, with a cross section appropriate to the problem. At relativistic energies, the spectra of e^+-e^- and e-e bremsstrahlung are the same except at the hard ends of the spectra (Baier, Fadin, and Khoze 1968), which are not supposed to contribute appreciably after averaging over a thermal distribution (Svensson 1982). Thus the Gaunt factor for e^+-e^- bremsstrahlung is a factor of 2 grester than e-e bremsstrahlung at relativistic temperatures as the electron and positon are distinct.

At nonrelativistic (NR) energies, the bremsstrahlung emission in e^+-e^- scattering is larger than the e-e emission since the

e^+-e^- system possesses a dipole moment. Joseph and Rohrlich (1958) argue that the CM bremsstrahlung spectrum from e^+-e^- scattering in a collision characterized by the relative velocity β_r is equivalent to the emission from a charged particle of reduced mass $m_e/2$ scattering with an infinitely heavy proton, again at relative velocity β_r. This is simply the NR B-H formula with $m_e \to m_e/2$:

$$f_{e^+e^-}(k;\gamma_r) = \frac{1}{\alpha r_e^2}\, k\, \frac{d\sigma_{B\text{-}H}(k;\gamma_r)}{dk}\bigg|_{m_e \to m_e/2} \xrightarrow{\gamma_r - 1 \ll 1} \frac{16}{3\beta_r^2}\, \ell n \left(\frac{\beta_r + \beta'}{\beta_r - \beta'}\right) . \qquad \text{(A1)}$$

The value of β' is defined through $\gamma' = \gamma_r - 2k$. Hence $\beta'^2 = \beta^2 - 4k$ in the NR limit (whereas $\gamma' = \gamma_r - k$ for e-p bremsstrahlung).

On this basis, the low energy ($\gamma_r < 2$) e^+-e^- bremsstrahlung was taken to be the B-H formula, with reduced mass $m_e/2$. In the transrelativistic regime, as shown in Figure A, the B-H spectrum (solid line) and the e-e bremsstrahlung spectrum (dotted line), given there as a function of $\omega = m_e k$, are found to be agreeably similar. For $2 \le \gamma_r \le 4$, the e^+-e^- bremsstrahlung spectrum is taken to be $1/2(\gamma_r - 2) f_{e\text{-}e} + 1/2(4 - \gamma_r) f_{B\text{-}H}$, as shown explicitly for the case $\gamma_r = 3$ by the dot-dashed line. At the two extremes, the appropriate spectra are used as discussed above. Also, the exact value $\xi_{e\text{-}e} =$

$(\gamma_r - 1)/[2(\gamma_r + 1)]^{1/2}$ for the maximum CM photon energy is used in the interpolation region. At NR energies, $1/2(\gamma_r - 1) \rightarrow \xi_{e\text{-}e}$, as required.

At this point, I wish to correct a mistake made by Svensson (1982). He claims that the NR e^+-e^- bremsstrahlung luminosity evaluated through the NR cross section (A1) is $2^{3/2}$ greater than the NR e-p bremsstrahlung luminosity. Actually, this ratio is $2^{-1/2}$. First note that in the limit $\gamma_r - 1 \ll 1$, the integral

$$\frac{\epsilon^*(\gamma_r)\sigma(\gamma_r)}{\alpha r_e^2} = \frac{1}{\alpha r_e^2}\int_0^{\xi_{e\text{-}e}} dk\, k\, \frac{d\sigma_{B\text{-}H}(k;\gamma_r)}{dk} \xrightarrow{\gamma_r - 1 \ll 1}$$

$$\frac{16}{3}\int_0^{\beta_r^2/4} dk\, \frac{k}{\beta_r^2}\, \ell n\left(\frac{\beta_r + \beta'}{\beta_r - \beta'}\right) \qquad \text{(A2)}$$

can be performed exactly and is independent of β_r. Its value is 1 (in units of the electron rest mass energy) for e-p scattering and 1/2 for e^+-e^- scattering. Therefore, the ratio of luminosities, other than this factor of 2, simply reflects the relative number of scatterings per unit volume per unit time (the reaction rate) in the following two systems: (i) NR electrons scattering with NR protons, and (ii) NR electrons scattering with NR positrons, all scatterings defined by the same energy-independent cross section. The ratio of the reaction rates of (ii) to (i) is just $2^{1/2}$, as can be seen either

through equations (II-16) or (II-28), or simple considerations of the NR reaction rates. Since each e^+-e^- scattering yields, on average, one-half the energy as an e-p scattering, but occurs at a rate greater by a factor of $2^{1/2}$, the conclusion follows.

Figure A. Single particle bremsstrahlung spectra. Frequency-dependent bremsstrahlung spectra as a function of the relative Lorentz factor γ_r are shown for different values of γ_r in the interpolation regime for the approximate calculation of thermal e^+-e^- bremsstrahlung. The solid line refers to the modified Bethe-Heitler formula, employing the reduced mass $m_e/2$. The dotted line refers to the exact, lowest order e^--e^- bremsstrahlung spectrum, and the interpolation spectrum, shown only for $\gamma_r = 3$, is given by the dot-dashed line. The formula for the interpolation spectrum is given in the text.

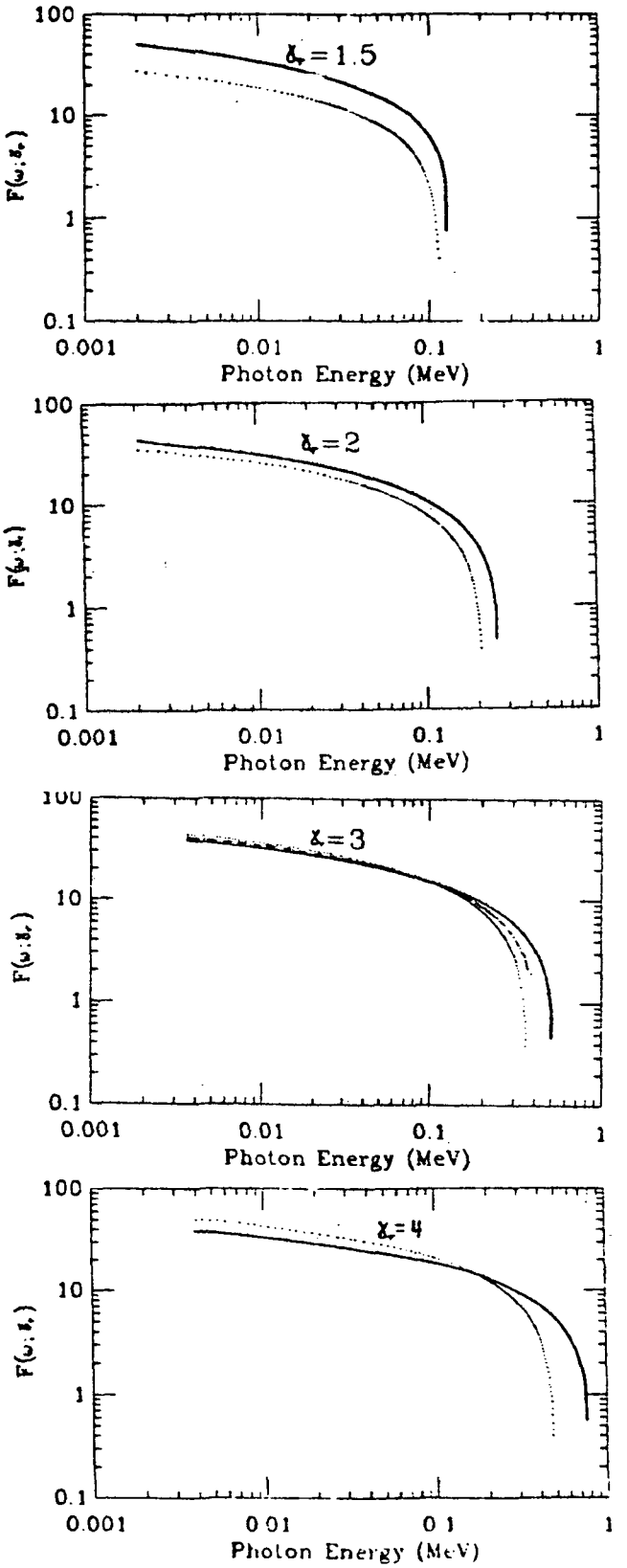
100
10
1
0.1
0.001
0.01
0.1
1
Photon Energy (MeV)
F(ω;γ)
γ=1.5
γ=2
γ=3
γ=4

REFERENCES

Abramowitz, M., and Stegun, I. 1965, Handbook of Mathematical Functions (New York: Dover).

Alexanian, M. 1968, Phys. Rev., 165, 253.

Araki, S., and Lightman, A. P. 1983, Ap. J., 269, 49.

Badhwar, G. D., Stephens, S. A., and Golden, R. L. 1977, Phys. Rev. D15, 820.

Badhwar, G. D. and Stephens, S. A. 1977, XVth International Conf. on Cosmic Ray Physics, 1, 398.

Baier, V. N., and Fadin, V. S. 1971, Zh. ETF 61, 476, JETP, 34, 253 (1972).

Baier, V. N., Fadin, V. S., and Khoze, V. A. 1968, Soviet Phys. JETP, 26, 1238.

Berger, E. L. 1975, in Laws of Hadronic Matter, A. Zichichi, ed. (New York: Academic Press), p. 557.

Bethe, H. A., and Heitler, W. 1934, Proc. Roy. Soc. A146, 83.

Bhabha, H. S. 1935a. Proc. Roy. Soc., A152, 559.

Bhabha, H. S. 1935b. Proc. Camb. Phil. Soc., 31, 394.

Bisnovatyi-Kogan, G. S., Zel'dovich, Ya. B., and Sunyaev, R. A. 1971, Soviet Astr.-AJ, 15, 17.

Blumenthal, G. R., and Gould, R. J. 1970, Rev. Mod. Phys., 42, 237.

Budnev, V. M., Ginsburg, I. F., Meledin, G. V., and Servo, V. G. 1975, Phys. Rept., 15C, 181.

Calvani, M., and Nobili, L. 1982, Lettere al Nuovo Cimento, 35, 7.

Cheng, A. Y. S., and O'Dell, S. L. 1981, Ap. J., 251, L49.

Colgate, S. A. and Petschek, A. G. 1981, Ap. J., 248, 771.

Crannell, C. J., Joyce, G., Ramaty, R., and Werntz, C. 1976, Ap. J., 210, 582.

de Groot, S. R., van Leeuwen, W. A., and van Weert, Ch. G. 1980, Relativistic Kinetic Theory (Amsterdam: North-Holland).

Eilek, J. A. 1980, Ap. J., 236, 664.

Eilek, J. A. and Kafatos, M. 1983, Ap. J., 271, 804.

Felten, J. E., and Morrison, P. 1966, Ap. J., 146, 686.

Gould, R. J. 1982a, Ap. J., 254, 755.

Gould, R. J. 1982b, in Gamma Ray Transients and Related Astrophysical Phenomena, R. E. Lingenfelter, H. S. Hudson, and P. M. Worrall, eds. (New York: AIP), p. 169.

Gould, R. J. 1982c, Ap. J., 263, 879.

Gould, R. J. 1981a, Ap. J., 243, 677.

Gould, R. J. 1981b, Phys. Fluids, 24, 102.

Gould, R. J. 1980, Ap. J., 238, 1026.

Gould, R. J. 1971, Am. J. Phys., 39, 911.

Gould, R. J. and Schréder, G. 1967, Phys. Rev., 155, 1404.

Guilbert, P. W., Fabian, A. C., and Rees, M. J. 1983, MNRAS, 205, 593.

Haug, E. 1981. Z. Naturforsch., 36a, 413.

Haug, E. 1975a. Z. Naturforsch., 30a, 1099.

Haug, E. 1975b. Z. Naturforsch., 30a, 1546.

Heitler, W. 1954, The Quantum Theory of Radiation (Oxford: Clavendon Press).

Jauch, J. M., and Rohrlich, R. 1976, The Theory of Photons and Electrons (New York: Springer-Verlag).

Jones, F. C. 1968, Phys. Rev., 167, 1159.

Jones, F. C. 1965, Phys. Rev., 137, B1306.

Jones, T. W., and Hardee, P. F. 1979, Ap. J., 228, 268.

Joseph, J., and Rohrlich, F. 1958, Rev. Mod. Phys., 30, 354.

Jüttner, F. 1928, Z. Physik, 47, 542.

Jüttner, F. 1911a, Ann. d. Phys., 34, 856.

Jüttner, F. 1911b, Ann. d. Phys., 35, 145.

Karzas, W., and Latter, R. 1961, Astrophys. Journal Supple., 6, 167.

Kolykhalov, P. I., and Syunyaev, R. A. 1979, Sov. Astr., 23, 189.

Kusunose, M., and Takahara, F. 1983, Prog. Theor. Phys., 69, 1443.

Landau, L. D., and Lifshitz, E. M. 1962, The Classical Theory of Fields (Reading, MA: Addison-Wesley).

Lightman, A. P. 1982, Ap. J., 253, 842.

Lightman, A. P. 1983, in Positron-Electron Pairs in Astrophysics, ed. M. L. Burns, A. K. Hardy, and R. Ramaty (New York: American Institute of Physics), p. 387.

Lightman, A. P., and Band, D. L. 1981, Ap. J., 251, 713.

Lightman, A. P., Shapiro, S. L., and Rees, M. J. 1975, Proc. Inter. School of Physics, Course LXV.

Likhoded, A. K., and Shlyapnikov, P. V. 1978, Usp. Fiz. Nauk 124, 3 (English Trans.: Sov. Phys. Usp., 21, 1).

Lock, W., and Measday, D. F. 1970, Intermediate Energy Nuclear Physics (London: Methuen and Co.).

Mészarós, P. 1983, Ap. J., 274, L13.

Mészarós, P., and Ostriker, J. P. 1983, Ap. J., 273, L59.

O'Dell, S. L. 1981, Ap. J., 243, L147.

Orth, C. D., and Buffington, A. 1976, Ap. J., 206, 312.

Pozdnyakov, L. A., Sobol', I. M., and Syunyaev, R. A. 1977, Astron. Zh., 54, 1246 (English Transl.: Sov. Astr., 21, 708).

Quigg, C. 1968, Ap. J., 151, 1187.

Quigg, C. 1967, Phys. Fluids, 11, 461.

Ramaty, R., and Mészáros, P. 1981, Ap. J., 250, 384.

Ramaty, R., Lingenfelter, R. E., and Bussard, R. W. 1981, Ap. and Space Sci., 75, 193.

Rybicki, G. B., and Lightman, A. P. 1979, Radiative Properties in Astrophysics (New York: Wiley).

Shapiro, S. L., Lightman, A. P., and Eardley, D. M. 1976, Ap. J., 204, 187.

Spitzer, L. 1962, Physics of Fully Ionized Gases (New York: Wiley).

Stephens, S. A., and Badhwar, G. D. 1981, Ap. Space Sci., 76, 213.

Stepney, S., 1983, MNRAS, 202, 467.

Stepney, S., and Guilbert, P. W. 1983, MNRAS, 204, 1269.

Sunyaev, R. A., and Titarchuk, L. G. 1980, Astron. and Astrophys., 86, 121.

Svensson, R. 1984, preprint.

Svensson, R. 1983, Ap. J., 270, 300.

Svensson, R. 1982, Ap. J., 258, 321.

Swanson, S. M. 1967, Phys. Rev., 154, 1601.

Synge, J. L. 1957, The Relativistic Gas (Amsterdam: North Holland).

Tan, L. C., and Ng, L. K. 1981, J. Phys. G., 7, 1135.

Taylor, F. E. et al. 1976, Phys. Rev., D14, 1217.

Weaver, T. A. 1976, Phys. Rev., A13, 1563.

Williams, E. J. 1935, Kgl. Danske Vid. Sel., 13, 4.

Zdziarski, A. A. 1984, preprint.

Zdziarski, A. A. 1982, Astron. Astrophys., 110, L7.

Zdziarski, A. A. 1980, Acta Astr., 30, 371.

BIBLIOGRAPHIC DATA SHEET

1. Report No.	2. Government Accession No.	3. Recipient's Catalog No.
TM-86154		

4. Title and Subtitle	5. Report Date
PHYSICS OF NONMAGNETIC RELATIVISTIC THERMAL PLASMAS	July 1984
	6. Performing Organization Code 665
7. Author(s) Charles Dermer	8. Performing Organization Report No.
9. Performing Organization Name and Address NASA/GSFC Greenbelt, MD 20771	10. Work Unit No.
	11. Contract or Grant No.
	13. Type of Report and Period Covered
12. Sponsoring Agency Name and Address Goddard Space Flight Center Greenbelt, MD 20771	14. Sponsoring Agency Code

15. Supplementary Notes

16. Abstract A detailed treatment of the kinematics of relativistic systems of particles and photons is presented. In the case of a relativistic Maxwell-Boltzmann distribution of particles, the reaction rate and luminosity are written as single intergrals over the invariant cross section, and the production spectrum is written as a double integral over the cross section differential in the energy of the produced particles (or photons) in the center-of-momentum system of two colliding particles.

The results are applied to the calculation of the annihilation spectrum of a thermal electron-positron plasma, confirming previous numerical and analytic results. Relativistic thermal electron-ion and electron-electron bremsstrahlung are calculated exactly to lowest order, and relativistic thermal electron-positron bremsstrahlung is calculated in an approximate fashion. An approximate treatment of relativistic Comptonization is developed.

The question of thermalization of a relativistic plasma is considered. A furmula for the energy loss or exchange rate from the interaction of two relativistic Maxwell-Boltzmann plasmas at different temperatures is derived.

Application to a stable, uniform, nonmagnetic relativistic thermal plasma is made. Comparison is made with other studies.

17. Key Words (Selected by Author(s))	18. Distribution Statement
hydronamics, relativity, atomic processes, plasmas	

19. Security Classif. (of this report)	20. Security Classif. (of this page)	21. No. of Pages	22. Price*
UN	UN	161	

*For sale by the National Technical Information Service, Springfield, Virginia 22161